WT-1725

UNCLASSIFIED

WT-1725

This document consists of 94 pages.

No. 164 of 240 copies, Series A

Operation

HARDTACK

April - October 1958

Program 39 (Projects 39.1 and 39.2)

ATTENUATION OF WEAPONS RADIATION: APPLICATION TO JAPANESE HOUSES

Issuance Date: March 15, 1961

CIVIL EFFECTS TEST OPERATIONS

Defense Nuclear Agency
6801 Telegraph Road
Alexandria, Virginia 22310-3398

ISST

26 January 1996

MEMORANDUM FOR DEFENSE TECHNICAL INFORMATION CENTER
ATTENTION: OCD/Mr. Bill Bush

SUBJECT: Declassification of WT-1725

The Defense Nuclear Agency Security Office (OPSSI) **has declassified** the following report:

WT-1725
Operation HARDTACK, April-October 1958,
Program 39 (Projects 39.1 and 39.2),
Attenuation of Weapons Radiation:
Application to Japanese Houses.

Distribution statement **"A"** applies.

Since this office has no record of DTIC receiving a copy of the report, a copy is enclosed. We would appreciate notification of your accession number once it is asigned.

Enclosure:
A/S

FOR JOSEPHINE B. WOOD
Chief, Technical Support Branch

DISCLAIMER NOTICE

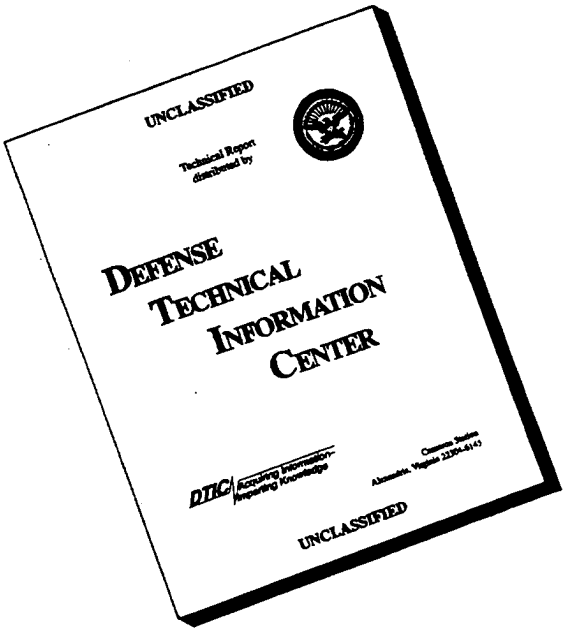

THIS DOCUMENT IS BEST QUALITY AVAILABLE. THE COPY FURNISHED TO DTIC CONTAINED A SIGNIFICANT NUMBER OF PAGES WHICH DO NOT REPRODUCE LEGIBLY.

When no longer required, this document may be destroyed in accordance with applicable security regulations.

DO NOT RETURN THIS DOCUMENT

USAEC Office of Technical Information Extension
Oak Ridge, Tennessee

[redacted]

UNCLASSIFIED

Report to the Scientific Director

ATTENUATION OF WEAPONS RADIATION: APPLICATION TO JAPANESE HOUSES

By

J. A. Auxier
J. S. Cheka
F. W. Sanders

Approved by: R. L. CORSBIE
Director
Civil Effects Test Operations

Health Physics Division
Oak Ridge National Laboratory
Oak Ridge, Tennessee
September 1960

[redacted]

RESTRICTED DATA

This [redacted] contains restricted data as
def[redacted] the Atomic Energy Act of [redacted].
Its [redacted] disclosure of its
co[redacted] in any manner to an unauthorized
pers[redacted] prohibited.

UNCLASSIFIED

[redacted]

PARTICIPANTS

OAK RIDGE NATIONAL LABORATORY

J. A. Auxier
T. V. Blosser
T. J. Burnett
C. W. Caldwell
J. S. Cheka
R. E. Coleman
M. J. Cook
D. M. Davis
F. J. Davis
L. C. Emerson
F. M. Empson
M. F. Fair
C. E. Haynes
P. N. Hensley
G. S. Hurst
W. W. Ogg
P. W. Reinhardt
R. H. Ritchie
F. W. Sanders
R. M. Simmons
E. B. Wagner
H. P. Yockey

EDGERTON, GERMESHAUSEN & GRIER, INC.

H. M. Borella
J. Brashears
L. Burpee
Eve Craft
J. D. Hoffman
W. R. Mitchell
P. C. Murphy
W. M. Quam
S. C. Sigoloff

U. S. ATOMIC ENERGY COMMISSION

N. A. Meador

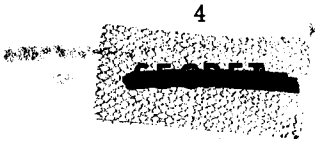

ABSTRACT

Measurements were made of the radiation-dose distributions in facsimiles of Japanese dwellings as a function of house size, orientation, and mutual shielding. Collimators were used in determining the angular distribution of neutrons and gamma rays incident on the point of measurement relative to a line between the point and the detonation. The relaxation length for fast neutrons measured for three nuclear detonations was 210, 218, and 205 yards, reduced to standard temperature and pressure. Criteria have been established to calculate the fast-neutron-dose distribution in Japanese houses for a given geometrical configuration and free-space dose.

ACKNOWLEDGMENTS

The authors wish to express their appreciation to the participants, whose diligence made possible the completion of the experiments, and, in particular, to G. S. Hurst and R. H. Ritchie of the Health Physics Division, Oak Ridge National Laboratory, who guided the development of the study and contributed in many ways to the analysis of the data.

They also gratefully acknowledge the over-all support of the program by R. L. Corsbie and members of the Civil Effects Test Operations staff. Because of the limited time for building the houses before the first participation and for repairing them between detonations, the program could not have been a success without the tremendous efforts of the staffs of Reynolds Electrical and Engineering Company and Holmes & Narver, Inc., Atomic Energy Commission support contractors.

CONTENTS

CONTENTS (Continued)

ILLUSTRATIONS

CHAPTER 3 DESCRIPTION OF FACILITIES AND PROCEDURES

CHAPTER 4 PRESENTATION OF DATA

ILLUSTRATIONS (Continued)

TABLES

TABLES (Continued)

Chapter 1

INTRODUCTION AND OBJECTIVES

1.1 INTRODUCTION

Early in 1956 a program was initiated to determine the radiation doses received by survivors of the nuclear bombings of Hiroshima and Nagasaki, Japan. The feasibility of such a program had been indicated by the successful dosimetry experiments during Operation Teapot[1] in 1955 and by examination of the records accumulated and maintained over a period of years by the Atomic Bomb Casualty Commission. A series of field experiments was completed at the Nevada Test Site (NTS) during Operation Plumbbob in 1957 to provide basic information concerning weapons radiation.[2] This information included air-dose measurements, angular distribution of radiation incident on the point of measurement relative to the point-to-burst axis, and slab-penetration measurements as a function of these angles. The effects of distance from the point of burst and of type of nuclear device were investigated for each type measurement. The angular distribution was found to be an insensitive function of type of device and distance from the burst. In addition, dose distributions were measured in two replicas of typical Japanese dwellings. These experiments indicated that the dose at any point in an isolated medium-size Japanese type house could be approximated by a simple parameter, i.e., the distance along a line through the burst point and the point of interest, equal in length to the distance from the surface where the line enters the house to the point of interest. From the experiments it was also concluded that, with additional measurements, the dose at any point in more complex houses or arrays of houses could be related to a few simple parameters.

1.2 OBJECTIVES

The chief objective of Program 39 was to determine the neutron- and gamma-ray-dose distributions in near replicas of Japanese type residences as a function of three parameters: (a) house size, (b) house orientation, and (c) relative position with respect to other houses. A secondary objective was the refinement of angular-distribution measurements made during Operation Plumbbob and the measurement of attenuation by slabs of house material as a function of angle with the burst-to-point-of-measurement axis.

REFERENCES

1. P. S. Harris, G. S. Hurst, H. H. Rossi, S. C. Sigoloff, and W. H. Langham, Operation Teapot Report, ITR-1167, April 1955. (Classified).
2. G. S. Hurst and R. H. Ritchie, Operation Plumbbob Report, WT-1504, Sept. 19, 1958. (Classified).

Chapter 2

INSTRUMENTATION

2.1 NEUTRON INSTRUMENTATION

The threshold detector system developed at Oak Ridge National Laboratory[1,2] was used for neutron measurements. Use of these detectors in the field has been described in detail.[3] The detector system included a set of fission foils surrounded by B^{10} (2 g/cm^2) and detectors of sulfur, gold, and gold with cadmium covers.

Neutron effective thresholds and cross sections for the various detectors currently used were as follows:

Detector	Threshold	Cross section
Pu^{239}	~4 kev	2.0×10^{-24} cm^2
Np^{237}	0.7 Mev	1.6×10^{-24} cm^2
U^{238}	1.5 Mev	0.55×10^{-24} cm^2
S	2.5 Mev	0.224×10^{-24} cm^2
Au and Au + Cd	Thermal	Direct calibration

After exposure the detectors were placed in a scintillation counter, and the net count was used to determine the neutron flux in the energy region above the threshold. The counting facilities were mounted in a van type trailer equipped with a-c voltage regulators and air conditioning.

2.2 GAMMA-RAY INSTRUMENTATION

The anhydrous tetrachloroethylene chemical dosimeter system[4,5] was used to measure gamma radiation. Ampoules containing the chemical were packed in Styrofoam, which was placed in a can designed to establish secondary-electron equilibrium and to attenuate thermal neutrons. This can, containing lithium between double walls of aluminum, was usually placed in an aluminum blast-proof container. The container system has been described previously.[5] After exposure the chemicals were analyzed in special spectrophotometers.*

In addition, a limited number of silver-activated metaphosphate glass rods[5-7] were placed in the lithium cans with the chemicals on the goal-post line of event X. The 1-mm-diameter by 6-mm-long rods were read on a commercially available† fluorometer.

---

*The gamma dosimeters were furnished by the Nucleonics Group of Edgerton, Germeshausen & Grier, Inc.; evaluations of the doses were also made by this group.

†Bausch and Lomb Optical Co. microdosimeter reader.

REFERENCES

1. G. S. Hurst, J. A. Harter, P. N. Hensley, W. A. Mills, M. Slater, and P. W. Reinhardt, Techniques of Measuring Neutron Spectra with Threshold Detectors: Tissue Dose Determination, Rev. Sci. Instr., 27: 153-156 (1956).
2. P. W. Reinhardt and F. J. Davis, Improvements in the Threshold Detector Method of Fast Neutron Dosimetry, Health Physics, 1: 169-175 (1958).
3. G. S. Hurst and R. H. Ritchie, Operation Plumbbob Report, WT-1504, Sept. 19, 1958. (Classified).
4. S. C. Sigoloff, Fast Neutron Insensitive Chemical Gamma-Ray Dosimeter, Nucleonics, 14(10): 54 (1956).
5. G. S. Hurst and R. H. Ritchie (Eds.), Radiation Accidents: Dosimetric Aspects of Neutron and Gamma-Ray Exposures, USAEC Report ORNL-2748, pp.70-71, Oak Ridge National Laboratory, Nov. 2, 1959.
6. J. H. Schulman and H. W. Etzel, Small Volume Dosimeter for X Rays and Gamma Rays, Science, 118: 184 (1953).
7. W. T. Thornton and J. A. Auxier, Some X-Ray and Fast Neutron Response Characteristics of Silver Metaphosphate Glass Dosimeters, USAEC Report ORNL-2912, Oak Ridge National Laboratory, Aug. 11, 1960.

Chapter 3

DESCRIPTION OF FACILITIES AND PROCEDURES

3.1 HOUSES

3.1.1 Construction of Houses

Owing to the uniformity of materials and construction techniques used in typical Japanese dwellings, it is possible to measure radiation-attenuation characteristics of a few sample houses and to apply the resulting information to a large number of houses.[1,2] However, to construct several exact replicas of Japanese houses at NTS would have been prohibitively expensive and time consuming. The use of a suitable domestic material, especially one that could be utilized easily in sheet form, would materially reduce both cost and time. The typical Japanese residence has exterior and interior walls of mud, fiber, and oyster-shell composition and a roof of wood, mud, and tile.[2]

Neutron- and gamma-ray-attenuation measurements had been made previously for wall and roof sections of Japanese residences. These sections were fabricated at ORNL from materials imported from Japan. In addition, slabs of many domestic construction materials were procured for testing. Neutron- and gamma-attenuation measurements were made for all these materials.[3] A polonium-boron neutron source was used with an ethylene-polyethylene absolute dosimeter.[4] Sources of Co^{50}, Cs^{137}, and Ra^{224} and a C-CO_2 ionization chamber were used to make the gamma-attenuation measurements. Cement-asbestos board, under several trade names, was found to approximate closely the neutron-attenuation to gamma-attenuation ratio of both Japanese walls and roofs. The radiation-attenuation of the Japanese exterior walls and roofs was equal to that of 1.75 in. of the cement-asbestos board; 2.00 in. of the cement-asbestos board was needed to simulate the interior walls of a Japanese house.*

Basic Japanese design was followed throughout the construction of the houses, but details were simplified. The typical framing used 4-in. by 4-in. vertical wood on approximately 3-ft centers. Horizontal 4-in. by 4-in. beams were placed in typical positions, and roof framing was of typical Japanese structure. Nailed joints were used instead of the more complicated Japanese joints. Figure 3.1 shows the framing of one of the houses. The wood frame was filled with cement-asbestos board of the appropriate thickness, the board being held in place by 1-in. by 1-in. strips of wood, as shown in Fig. 3.2. The diagonal bracing shown in Fig. 3.2 was used to strengthen the house during transportation and was removed when the house was in place. Recovery of the detectors postshot was facilitated by kerfing, or scoring, the wall panels on both sides (Fig. 3.3) to weaken them and decrease the coarseness of the debris. The parts of a

*These dimensions are applicable to Johns-Manville Transite. The density of cement-asbestos board by other trade names is slightly different.

Japanese house which would contribute negligibly to the attenuation of radiation were omitted (Fig. 3.4). These included thin wood and/or paper doors, paper or glass windows, and the thin wooden ceilings. The floors were constructed of plywood. No mats, plumbing, or other furnishings were included in the structures.

Three types of houses were selected for this study. The first type, type A (Fig. 3.4), was a facsimile of the single-story houses of medium size used in Operation Plumbbob. Type B houses were larger two-story residences, and type C houses were small one-story structures (Fig. 3.5). Seven houses were constructed for the experiments; two type A houses, two type B houses, and three type C houses. The houses were constructed at a central location and were transported by truck to their exposure positions.

3.1.2 Installation of Instrumentation

A ½-in. steel cable was strung through each to form a three-dimensional grid to distribute the detectors throughout the volume of each house and to facilitate recovery of the detectors following the detonation. A minimum of 100 ft of cable extended from each house to ensure that it would be accessible for recovery. The detectors were clamped to the cables with U bolts, as shown in Fig. 3.6. The detectors were always mounted on the side of the cable toward Ground Zero (GZ). The detectors were recovered after the explosion by pulling the cables out of the houses with six-wheel-drive military trucks to areas where the radiation intensity was sufficiently low to permit removal without excessive personnel exposure. The detectors were then detached and sent to the counting facility.

3.2 COLLIMATORS

The collimators used in Operation Plumbbob[1] were reconditioned and used during Operation Hardtack, Phase II. The collimators were placed at 20-ft intervals along arcs at 750, 1000, and 1020 yards from GZ and were oriented at various elevation and azimuthal angles. Figure 3.7 shows a typical installation of collimators. One pair of gamma collimators was placed face-to-face to shield the detectors completely and to allow a determination of the shielding efficiency of the collimators. The openings of some of the collimators were covered with slabs of cement-asbestos board or boxes of sand; collimators with identical orientations were covered with 0, 1, 2, 3, or 4 uniform slabs of cement-asbestos board or 0, 3, 6, or 9 in. of sand. The unit thickness of the cement-asbestos board slabs was 1.75 in., the thickness of the roofs and external walls of the houses. These slabs of cement-asbestos board on the collimator openings were used to determine the radiation-attenuation characteristics of this material as a function of the angle of incident radiation. The sand attenuators were used to relate Operation Hardtack, Phase II, measurements to the measurements made in Operation Plumbbob.

3.3 GOAL POSTS

Detectors for determining the air doses (gamma exposure dose and neutron first-collision tissue dose) were placed on appropriately positioned goal posts[2] (Fig. 3.8). Recovery of the detectors from the goal posts was achieved by removing the entire crossbar.

3.4 PLACEMENT OF HOUSES, COLLIMATORS, AND GOAL POSTS

3.4.1 Event X

This device was detonated on a balloon 1500 ft above Yucca Flat. Seven houses, ten goal posts, and fifty collimators on the 1000-yard arc (gamma ray only) were used.

(a) *Goal-post Placements.* The air dose at the houses and collimators was measured using goal-post assemblies located as shown in the vicinity map, Fig. 3.9. The placement permitted dose and flux measurements as functions of distance and angle of arc.

(b) *House Placements.* Figure 3.10, the plot plan of the house area for this event, shows the location and orientation of the houses. Houses 5, 6, and 7 (types C, A, and B, respectively) were oriented with side 1 toward GZ. Side 1 is the open or windowed side of the house. In Japan such a side characteristically faces south. These houses were used to study the effects of size of house on dose distribution. Houses 1 and 3 (types A and B, respectively) were oriented with side 1 rotated 90° clockwise from GZ. These houses could be compared with houses 6 and 7, respectively, for determining the effect of orientation on the dose distribution. Houses 2 and 4 (type C houses) also with side 1 rotated 90° clockwise from GZ, were located directly behind houses 1 and 3, respectively. The separation distances were 4 ft. This arrangement was used to study the effect of mutual shielding. The centers of houses 1, 3, 5, 6, and 7 were located at 150-ft intervals on an arc of radius 1000 yards from GZ. A view of the houses is shown in Fig. 3.11; the camera faced the houses on the GZ side at an angle of approximately 45°.

(c) *Collimator Placement.* Because all the available neutron detectors were used in the houses in this event, only gamma measurements were made in the collimators. The 50 collimators were located on two arcs with radii of 1000 and 1020 yards from GZ. Figure 3.9, a vicinity map, shows the location of the collimator lines.

3.4.2 Event Y

All seven houses were repaired and used on event Y. In addition, 62 gamma collimators, 10 neutron collimators, and 10 goal posts were instrumented.

(a) *Goal Post Placement.* Figure 3.12, a vicinity map, shows the placement of the 10 goal posts instrumented for this event.

(b) *House Placement.* As shown in Fig. 3.13, a plot plan, house 1 was rotated clockwise in place through 45°. House 2 was moved to a position 4 ft from house 4, the original orientation having been retained. This arrangement permitted the determination of effects of lateral shielding by comparison of the results with those from the direct shielding investigation in event X. Houses 3 and 4 remained in place. House 5 was retained with its previous orientation and location to determine the reproducibility of measurements. House 6 was moved to a position beside, and 4 ft from, house 7. This configuration permitted the effect of lateral mutual shielding between a two-story and a one-story house to be studied. An aerial view of the houses and collimators in position for this event is shown in Fig. 3.14; GZ is to the left.

(c) *Collimator Placement.* The gamma collimators were arranged along the same lines as in the previous event (Fig. 3.12).

3.4.3 Event Z

Only six houses were available for use in event Z. They included two type A houses, one type B, and three type C. One A house was modified by closing all the openings with cement-asbestos board, thus producing a closed shell. Because only six houses were used, more neutron detectors were available to be used in collimators. The vicinity map is shown in Fig. 3.15.

(a) *House Placements.* House 1 was rotated 135° counterclockwise so that side 1 faced GZ, as shown on the plot plan, Fig. 3.16. It was compared with the other A house, house 6, on which the exterior openings had been closed, Fig. 3.17. House 6 was moved back to the position it had occupied in event X, with side 1 toward GZ. The original orientation and position of house 7 was not changed. House 5 was rotated 180° in place. Houses 2 and 4, the other C houses, were placed along a radius passing through house 5 at distances of 1500 and 1250 yards, respectively, and were rotated 90° clockwise. This group was used to study the effects of a change in angle of elevation of the burst point with respect to the house. The ratio of the percentage of the radiation incident on the walls and the roof would vary among houses 2, 4, and 5.

(b) *Collimator Placement.* Neutron and gamma collimators were used along the arc of radius 1000 yards as in events X and Y, as shown in Fig. 3.15. In addition, 20 neutron collimators and 21 gamma collimators were placed on an arc of radius 750 yards from GZ.

REFERENCES

1. G. S. Hurst and R. H. Ritchie, Operation Plumbbob Report, WT-1504, Sept. 19, 1958. (Classified).
2. R. H. Ritchie and G. S. Hurst, Penetration of Weapons Radiation: Application to the Hiroshima-Nagasaki Studies, Health Physics, 1: 390 (1959).
3. Health Physics Division Annual Progress Report, USAEC Report ORNL-2806, pp.121-124, Oak Ridge National Laboratory, Oct. 23, 1959.
4. E. B. Wagner and G. S. Hurst, Advances in the Standard Proportional Counter Method of Fast Neutron Dosimetry, Rev. Sci. Inst., 29: 153 (1958).

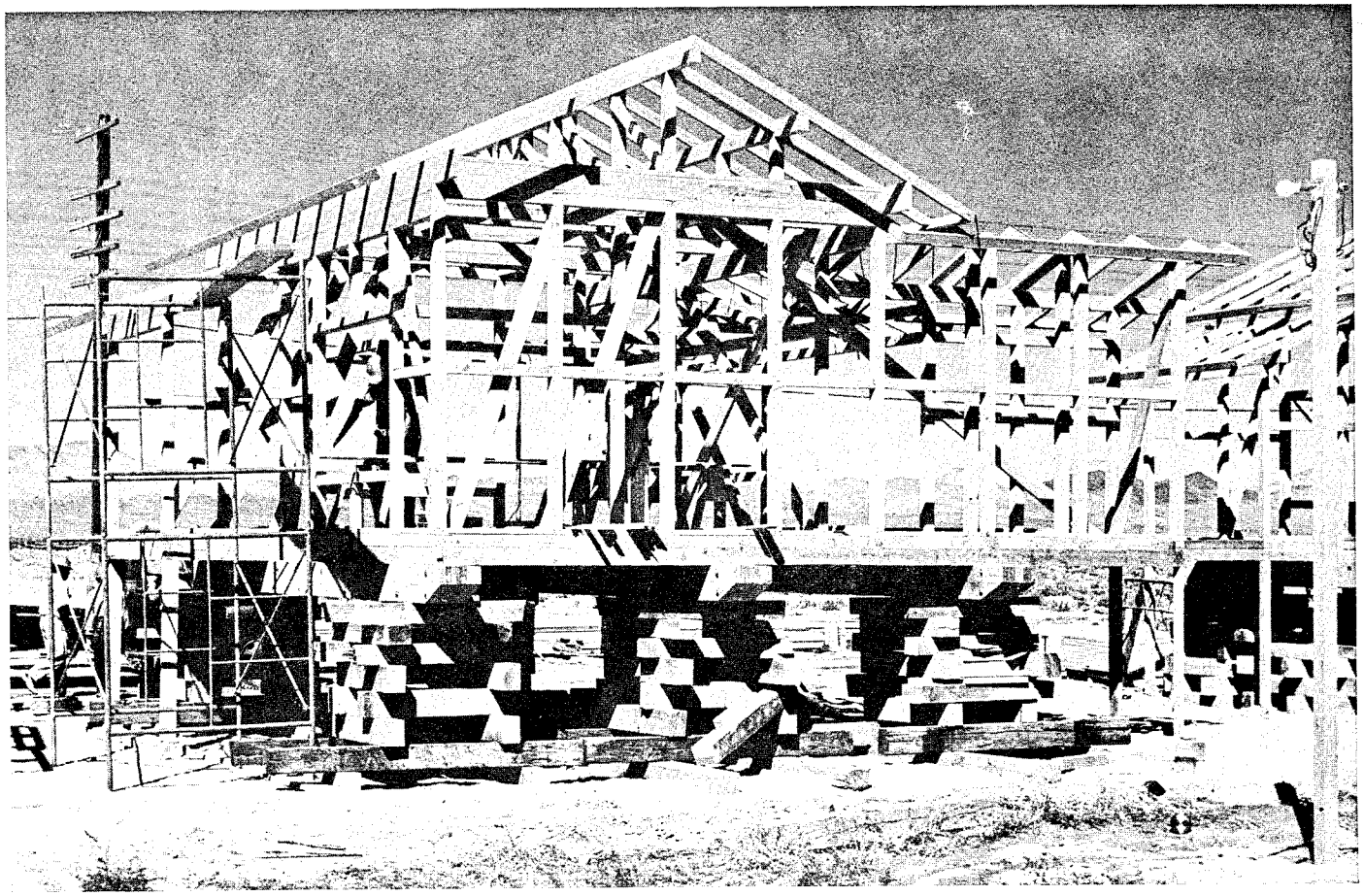

Fig. 3.1— Framing of typical house.

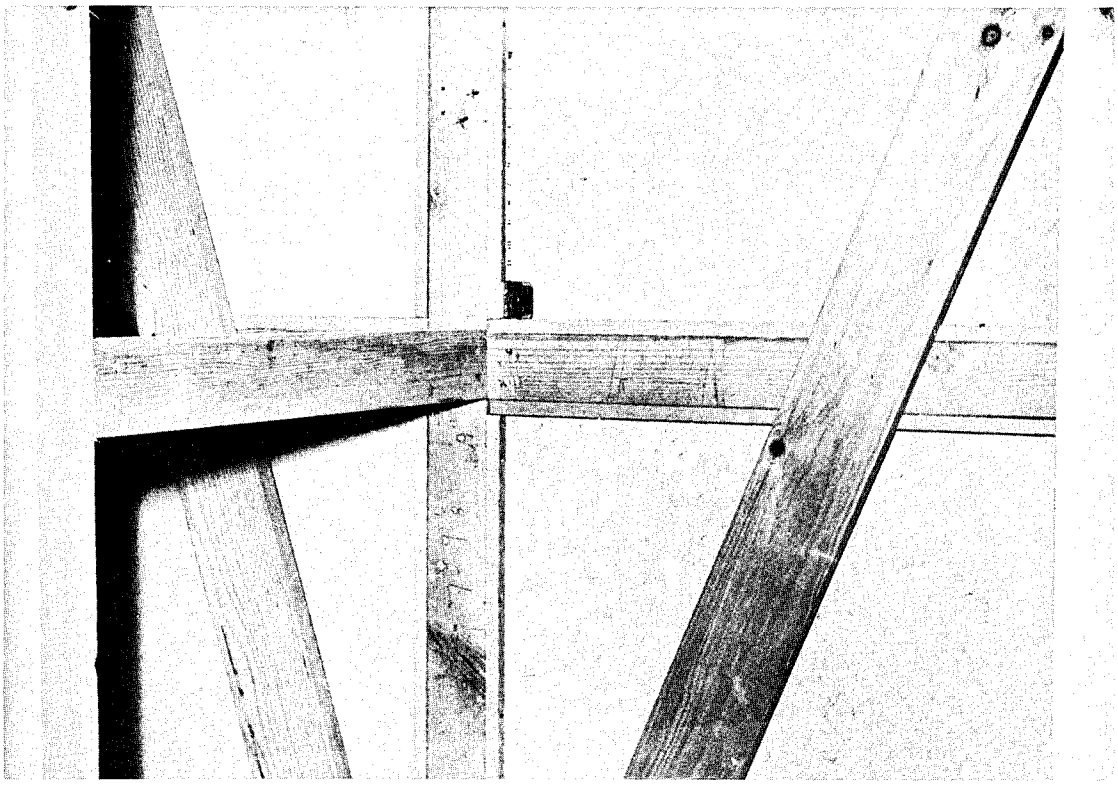

Fig. 3.2— Method of holding panels in place.

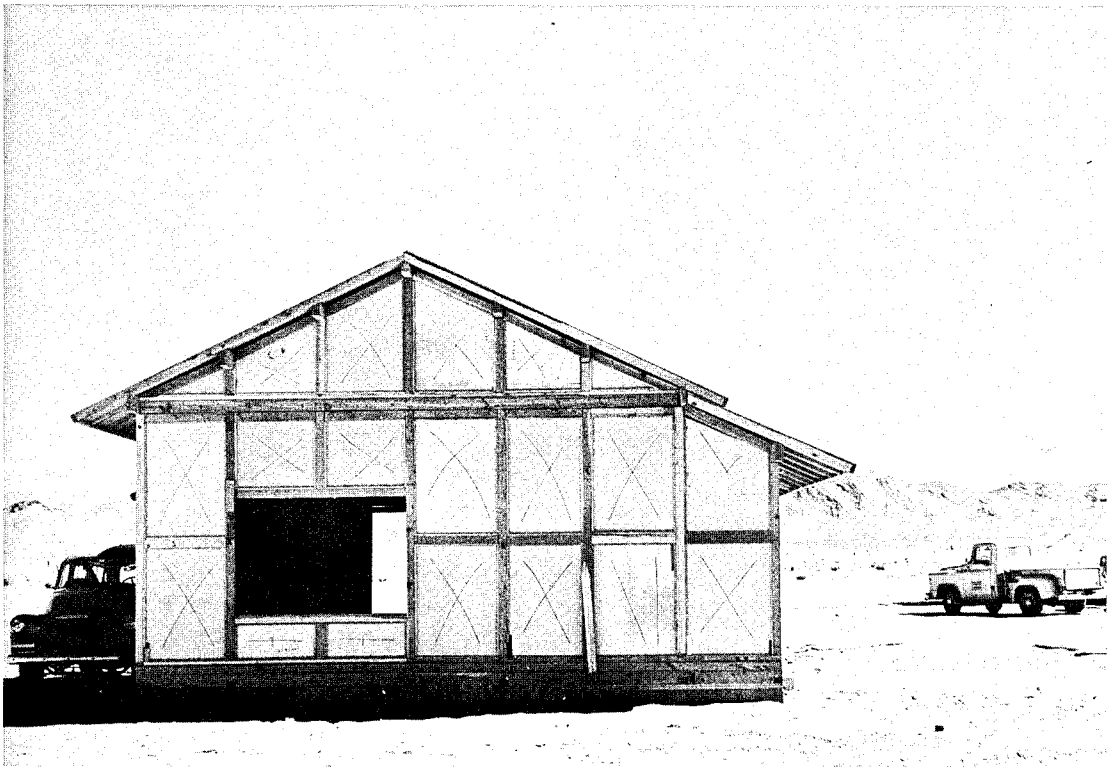

Fig. 3.3— Typical kerfing of house panels.

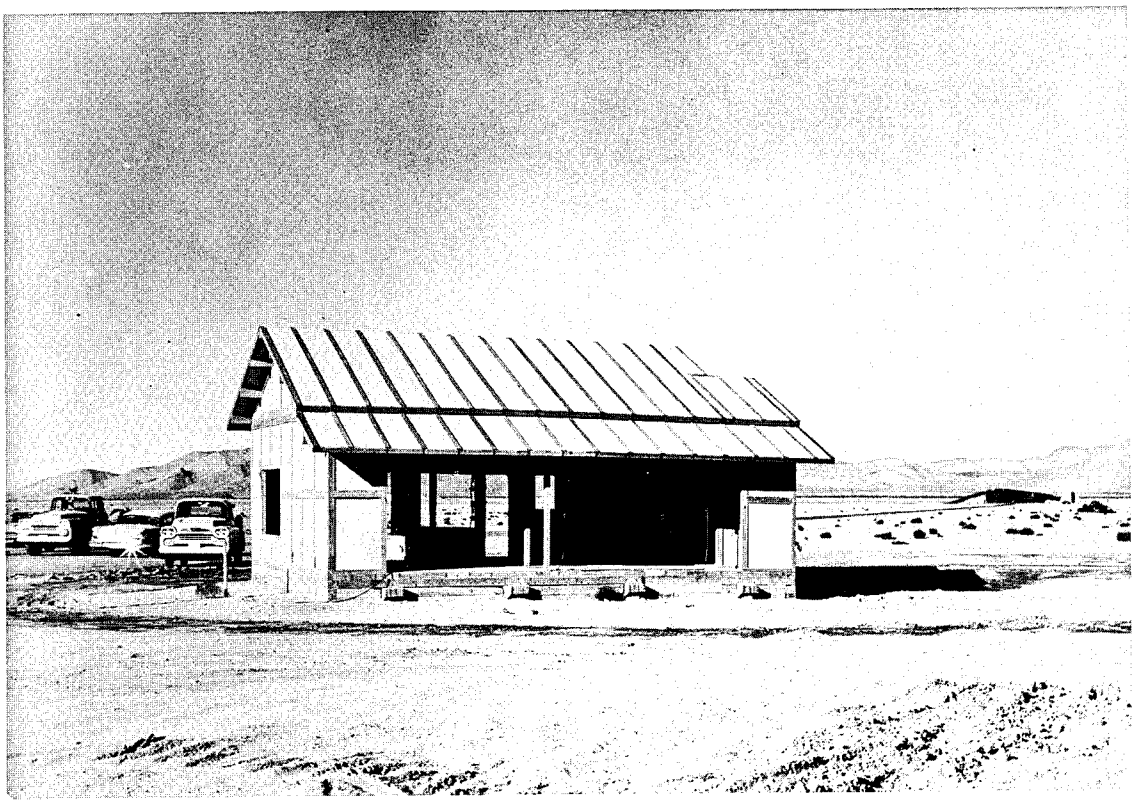

Fig. 3.4 — Type A house.

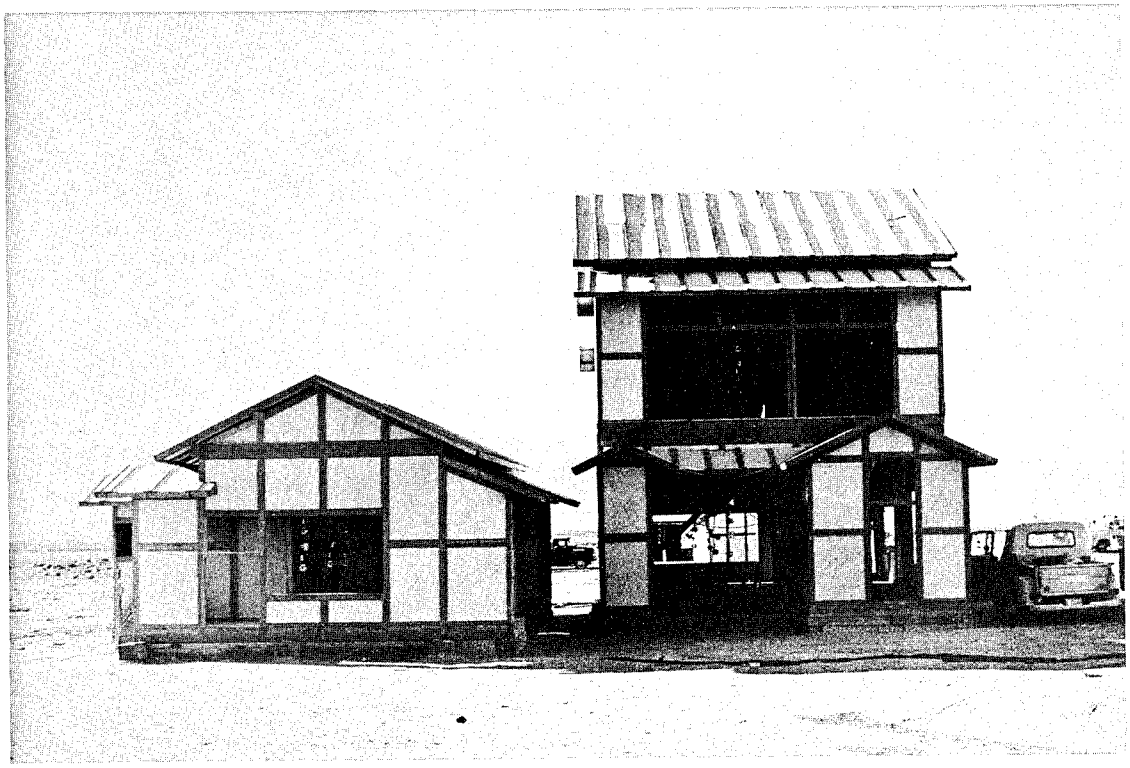

Fig. 3.5— Type B (left) and type C houses (right).

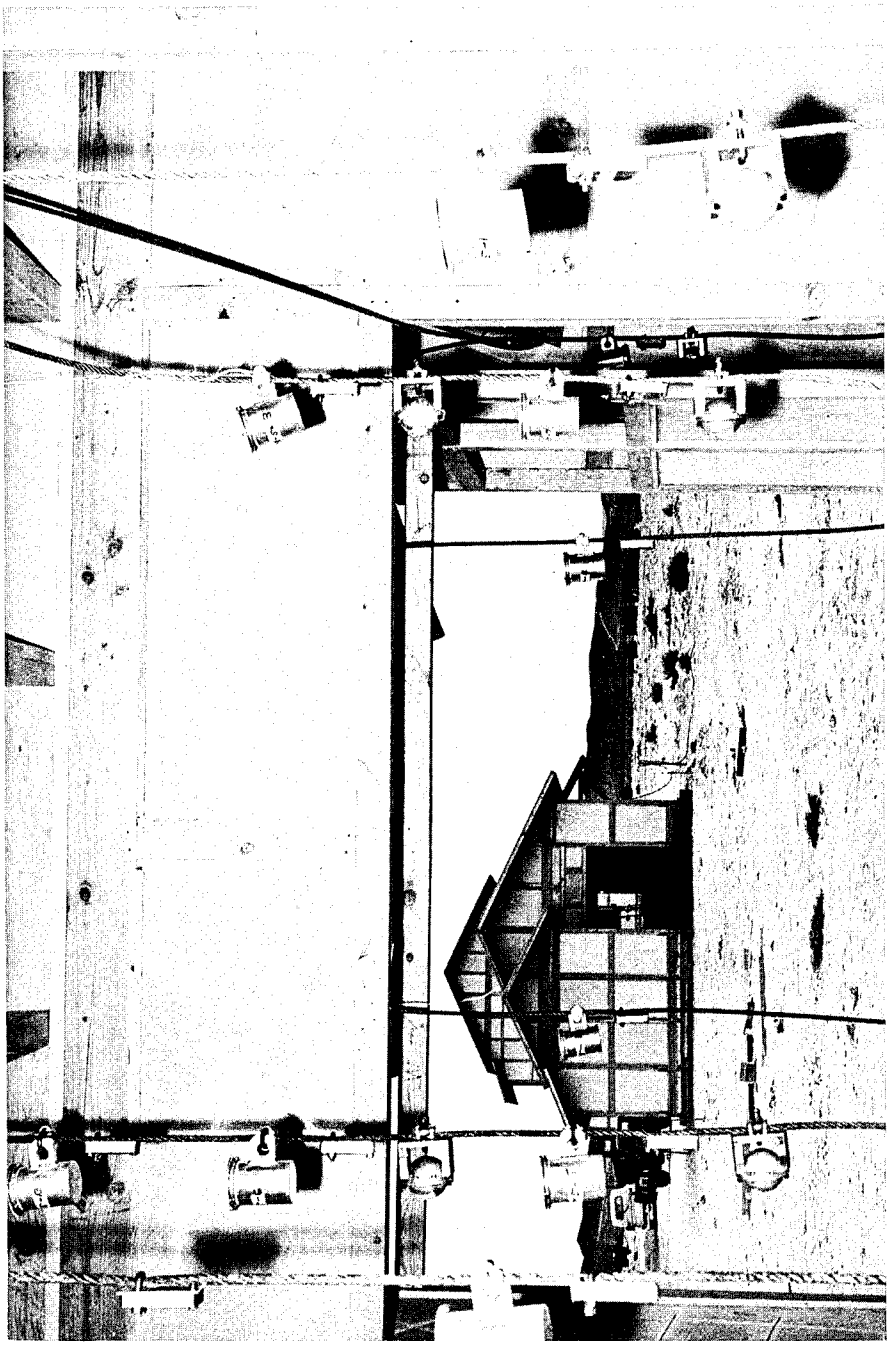

Fig. 3.6— Detectors in place on cable.

Fig. 3.7—Collimators in place.

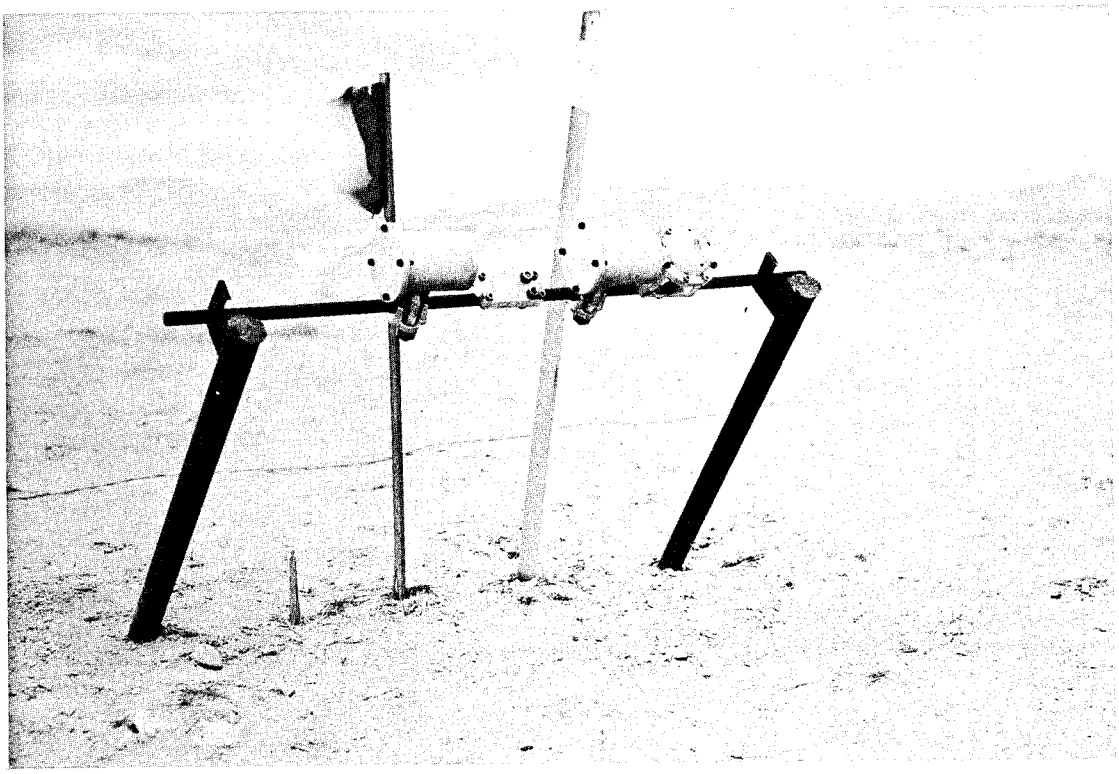

Fig. 3.8—Goal-post installation.

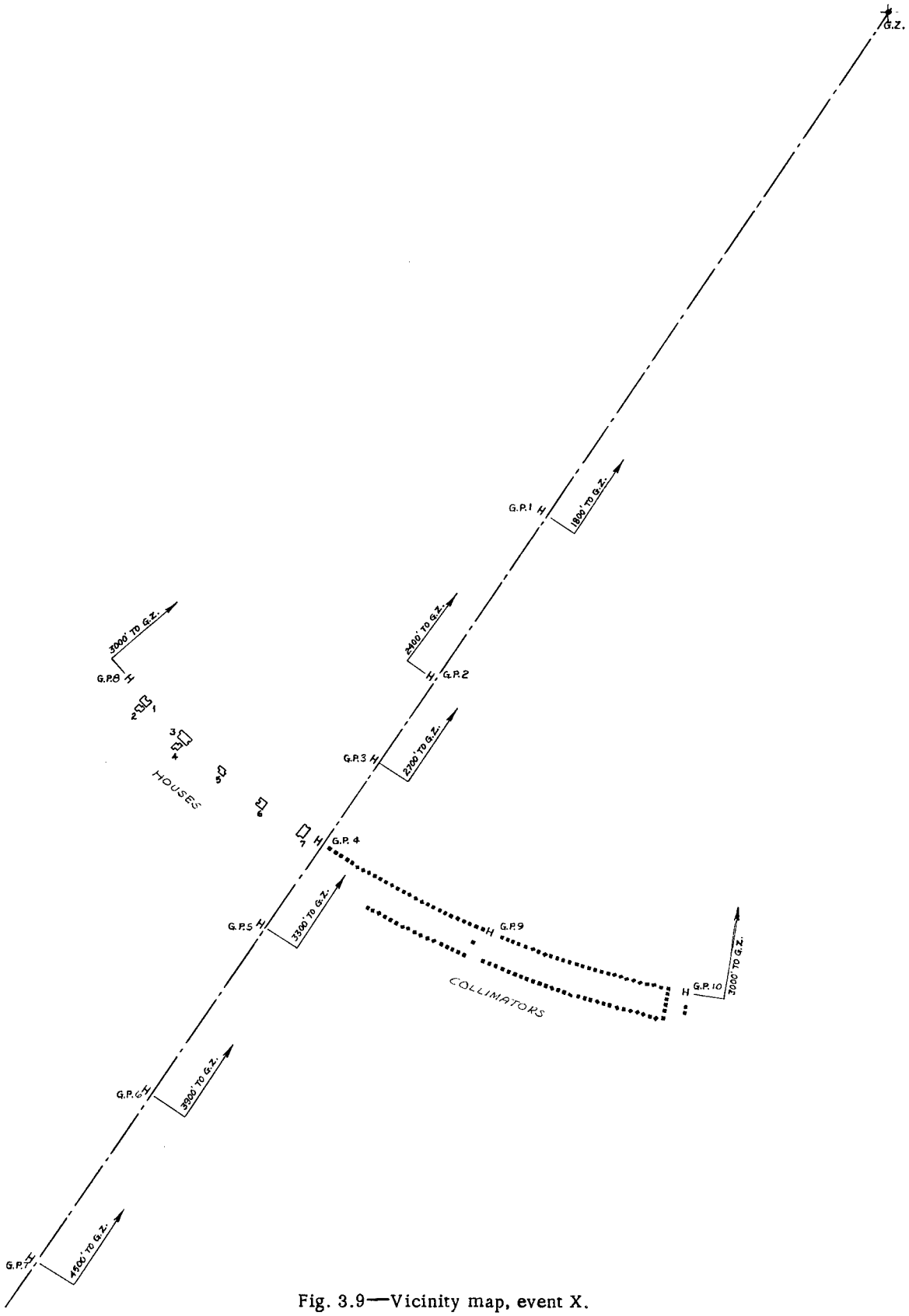

Fig. 3.9—Vicinity map, event X.

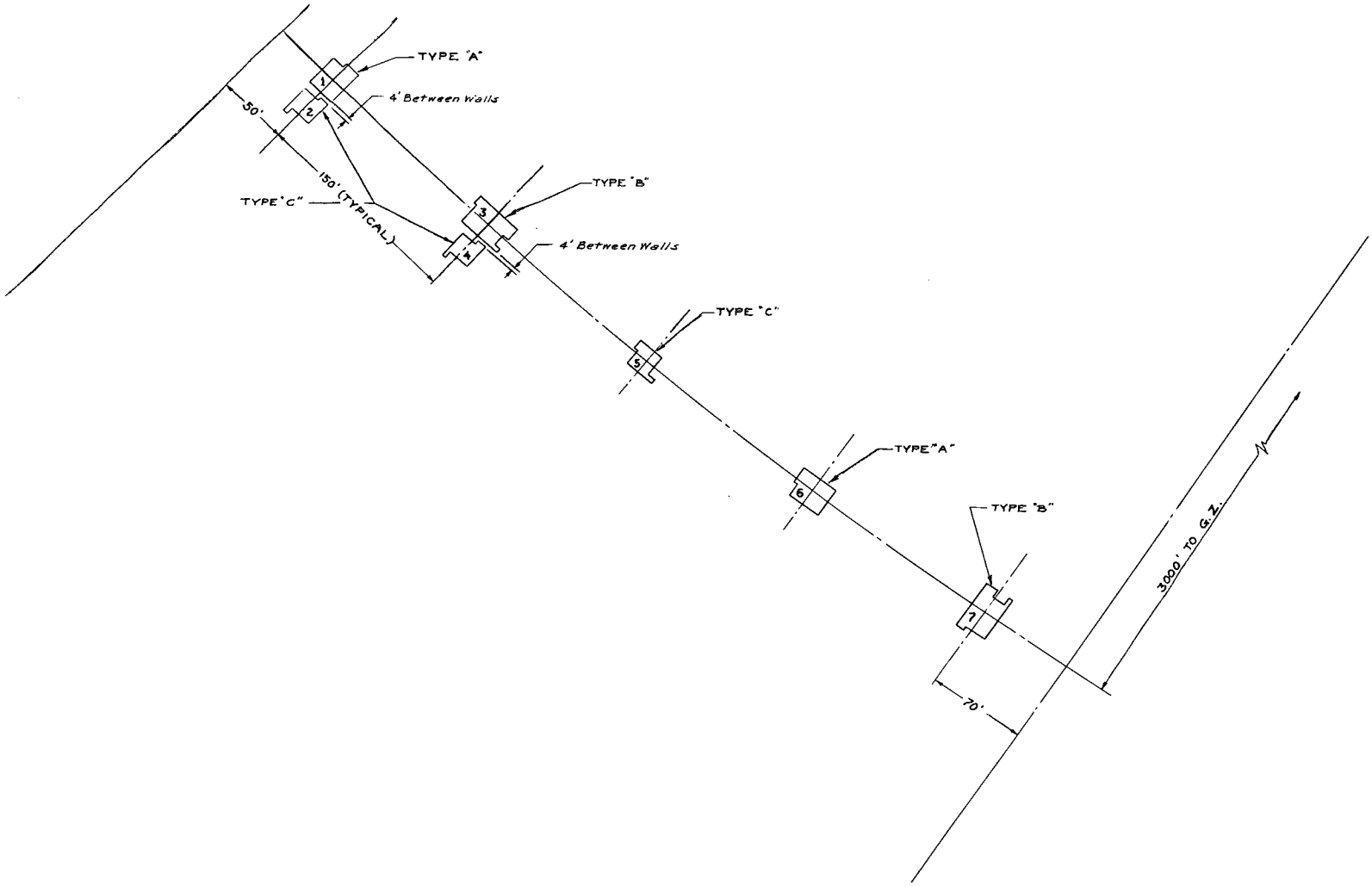

Fig. 3.10—House-array plot plan, event X.

Fig. 3.11—View of array, event X.

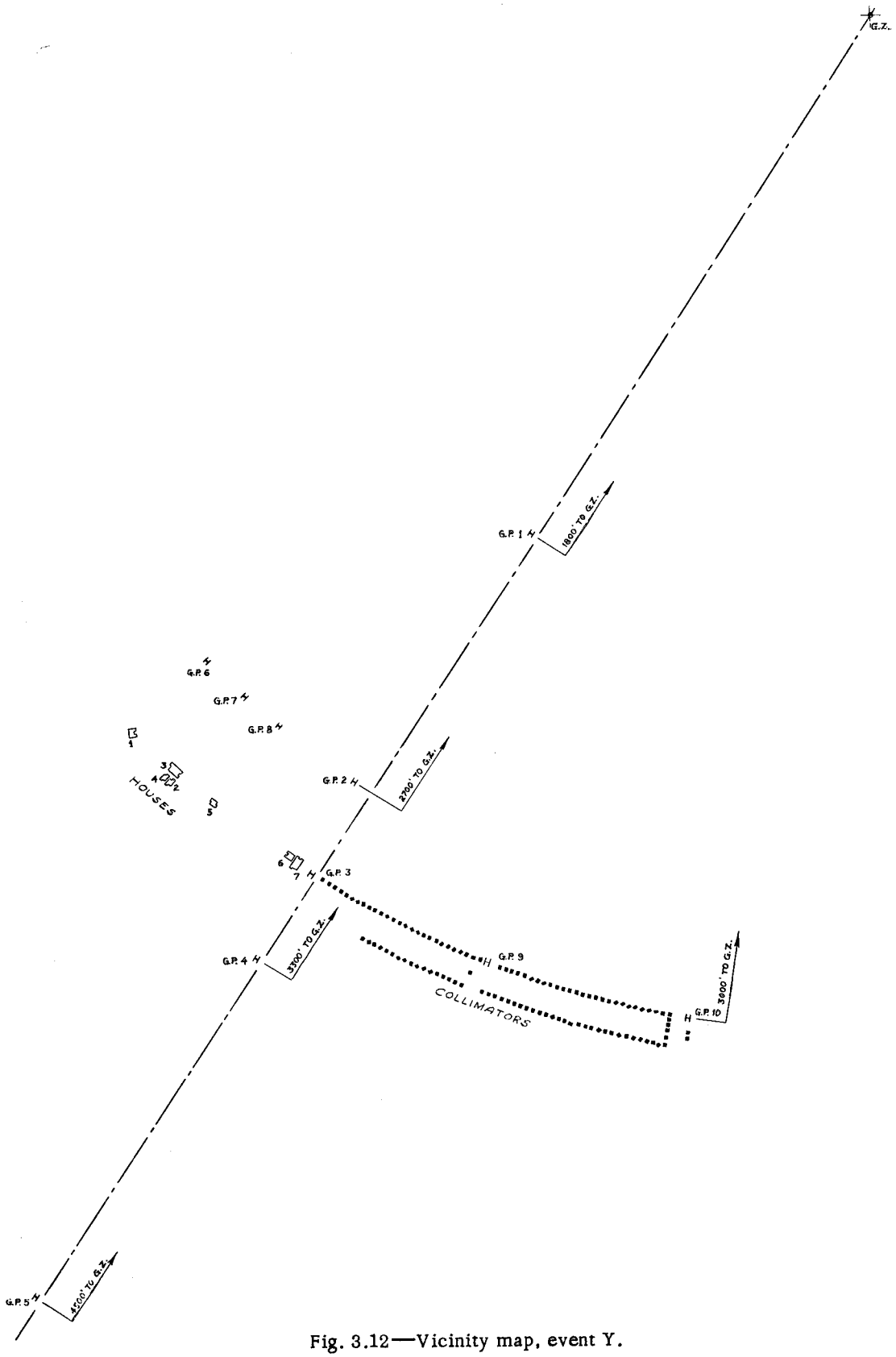

Fig. 3.12—Vicinity map, event Y.

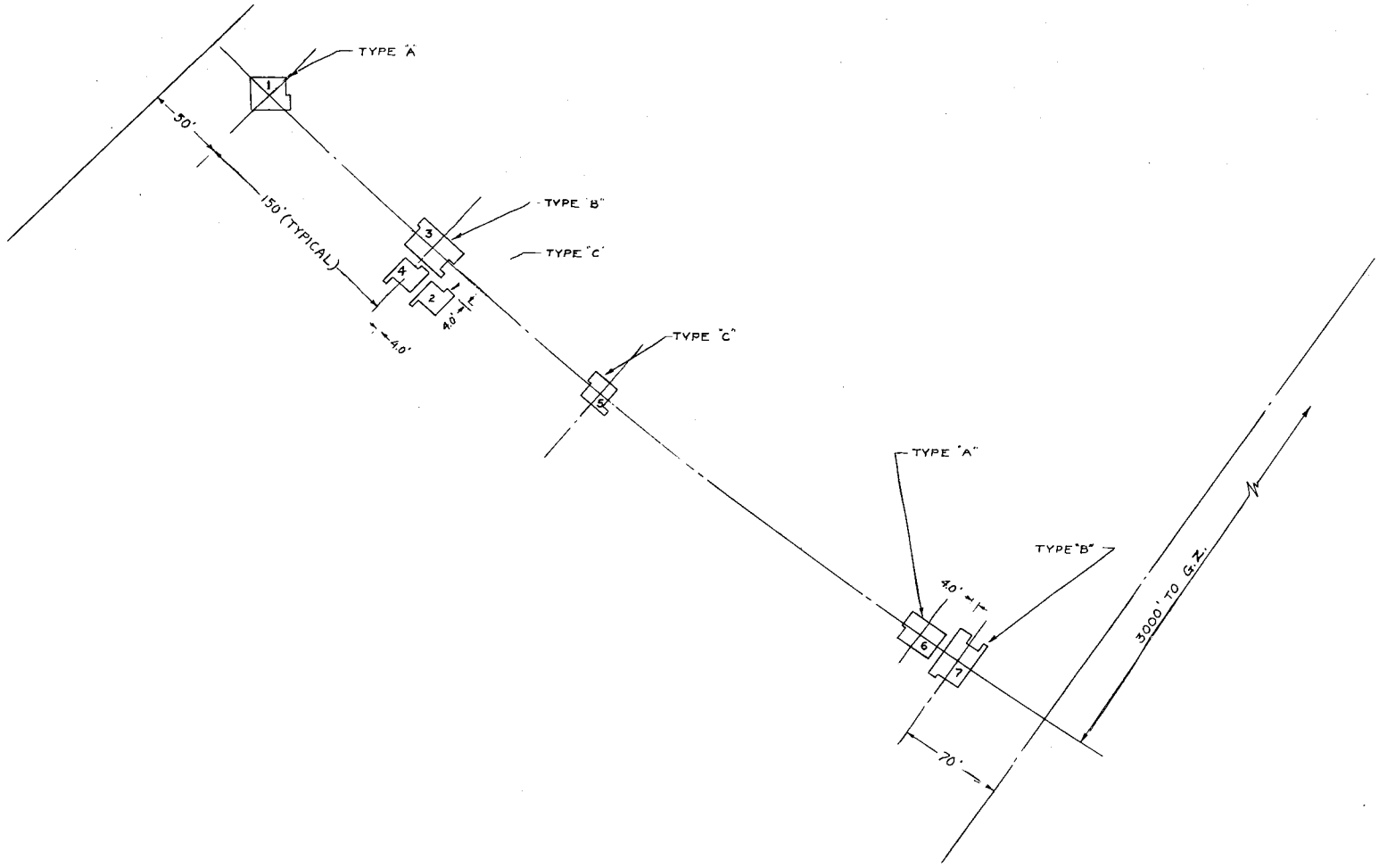

Fig. 3.13—House-array plot plan, event Y.

Fig. 3.14— View of array, event Y.

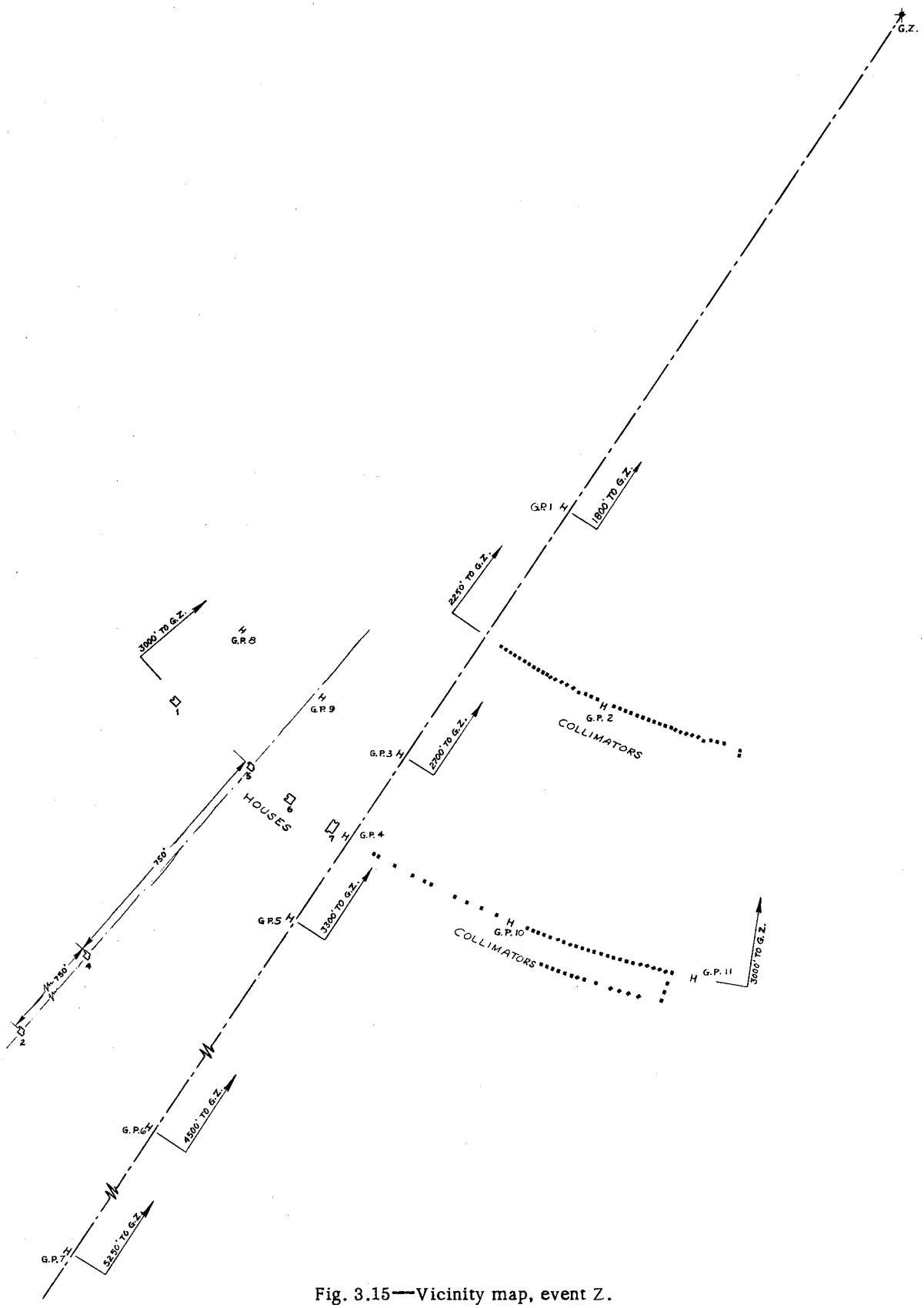

Fig. 3.15—Vicinity map, event Z.

[redacted]

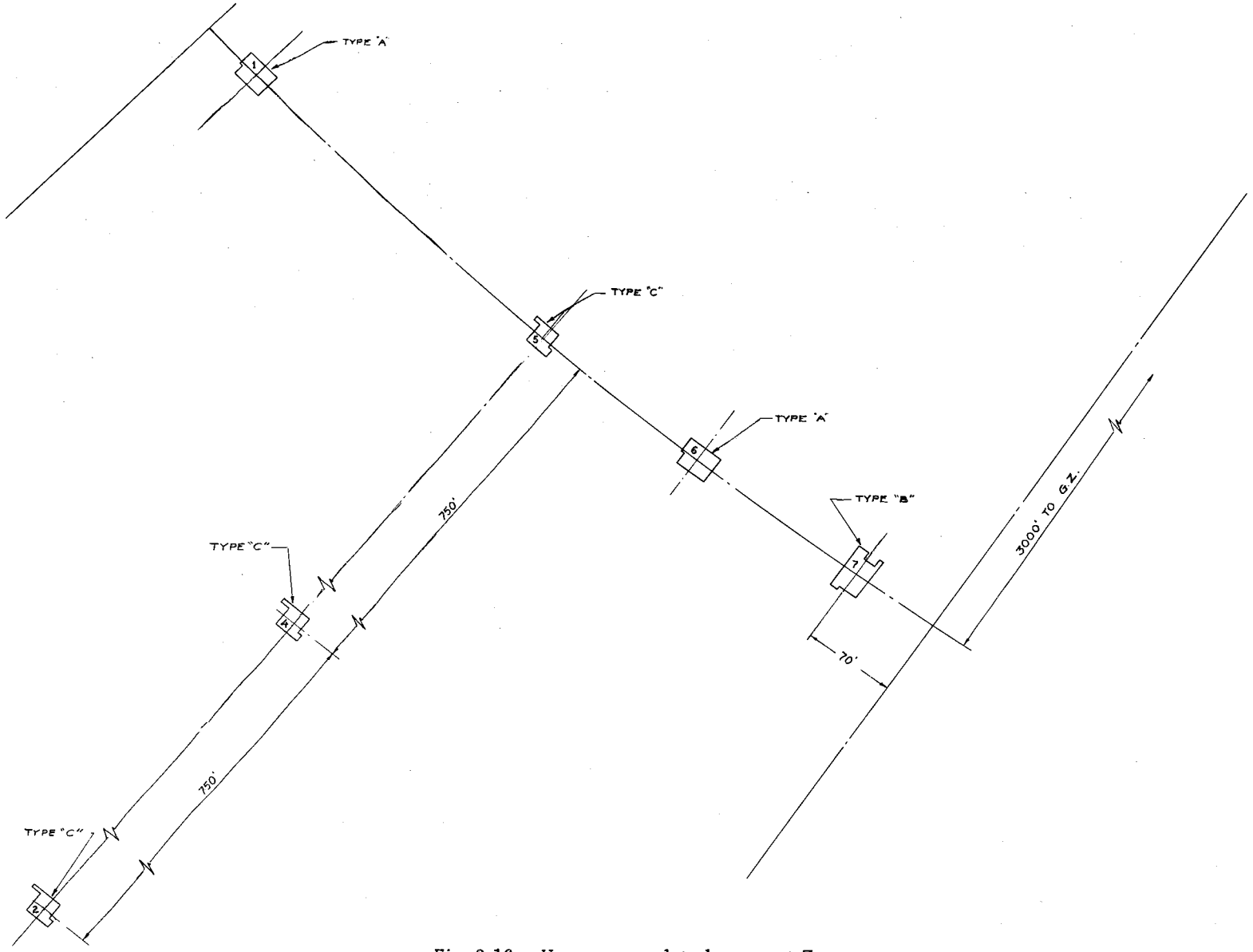

Fig. 3.16—House-array plot plan, event Z.

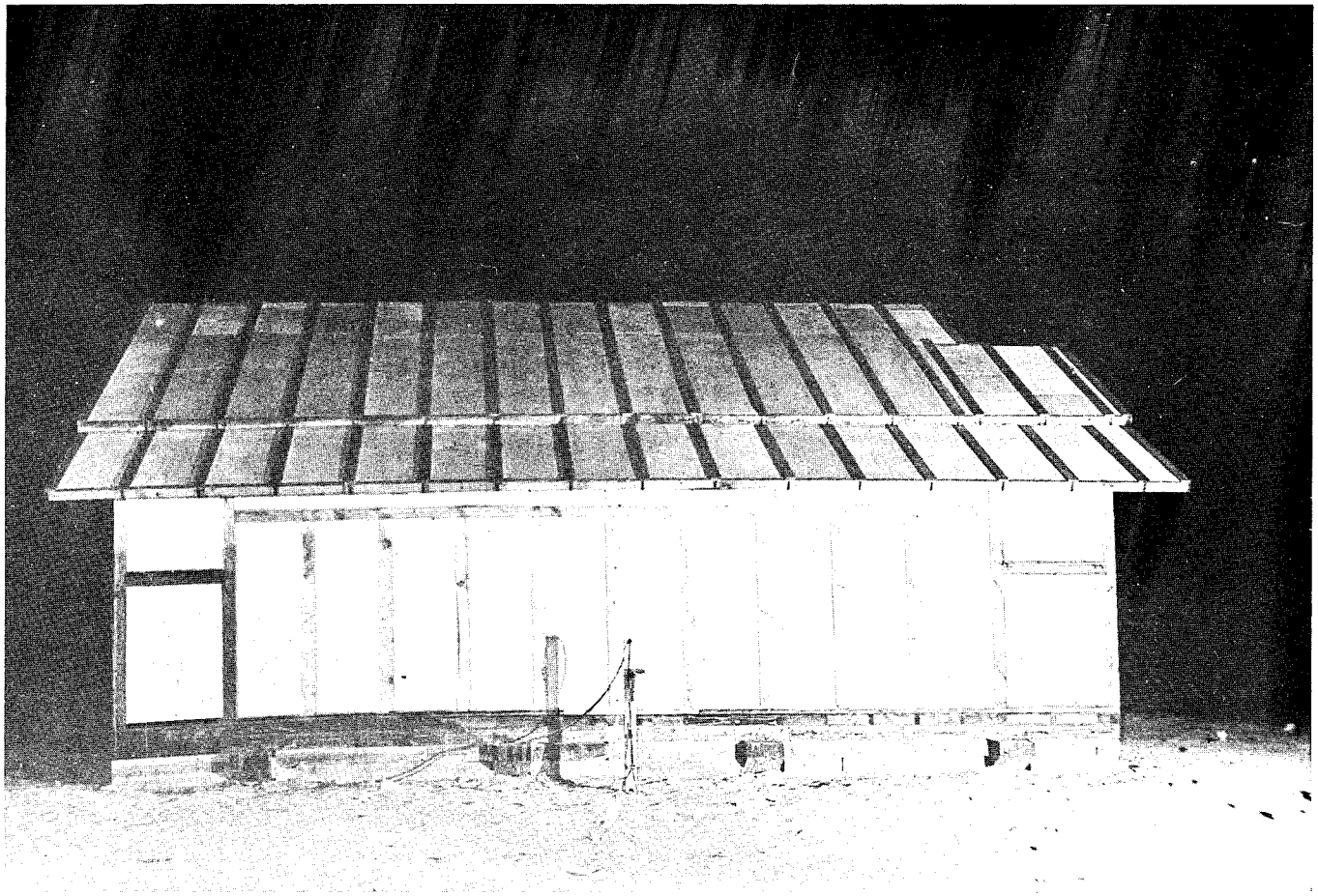

Fig. 3.17 — Shell house, type A.

Chapter 4

PRESENTATION OF DATA

4.1 NEUTRON AND GAMMA-RAY MEASUREMENTS IN AIR

Goal posts were positioned along a radial line passing through GZ and between the arc segment occupied by the houses and that occupied by the collimators (Figs. 3.9, 3.12, and 3.15). Installations were made at points from 600 to 1750 yards from GZ and also along arcs at 900 and 1000 yards. $R^2\phi$ and R^2D, where ϕ is neutron flux, D is neutron dose, and R is the slant range (distance from burst to detector) as functions of distance from burst, all normalized to a dose of 1000 rads at the 1000-yard arc, are given in Figs. 4.1, 4.2, and 4.3 for events X, Y, and Z, respectively. The gamma-ray air-dose data are given in the same manner but are normalized to 1000, 2000, and 4000 r at the 1000-yard arc for events X, Y, and Z, respectively, in Fig. 4.4. Glass dosimeter readings for event X normalized to 500 r at 1000 yards also appear in Fig. 4.4.

4.2 NEUTRON AND GAMMA-RAY MEASUREMENTS IN COLLIMATORS

Neutron dose and spectrum as functions of polar angle were measured at 1000 yards from GZ on event Y and at 750 and 1000 yards on event Z. Angular distribution, as measured at 1000 yards, on event Z without inserts in the collimators is shown in Fig. 4.5. The neutron-energy distributions as functions of polar angle, distance from GZ, and thickness of slabs of Transite and sand are shown in Figs. 4.6, 4.7, 4.8, and 4.9.

Gamma-dose distribution was also measured as a function of polar angle. Figure 4.10 shows angular distribution at 750 yards for event Z. Some slab penetration measurements are given in Figs. 4.11 and 4.12.

4.3 NEUTRON AND GAMMA-RAY MEASUREMENTS IN HOUSES

4.3.1 Event X

The house array is shown in Fig. 3.11. Neutron- and gamma-dose distributions for all houses in this event are shown relative to air dose at 1000 yards from GZ as indicated by the key (Fig. 4.13) in Figs. 4.14 through 4.22. Typical neutron-flux and dose histograms are presented for points in air (goal posts) 4 ft in front of the house, in the center of the house, and 4 ft behind the house in Figs. 4.23 through 4.26, respectively. "Front" and "rear" of house as used here refer to the side of the house nearest and the side of the house farthest from GZ, respectively. In addition, a composite of neutron-flux and -dose measurements made in type B houses on the several events is plotted against slant penetration (distance from detector to point where radiation enters house along line to burst point) in Fig. 4.27.

4.3.2 Event Y

The house array is shown in Fig. 3.14. Neutron- and gamma-dose distributions for each of the houses in this event are given in Figs. 4.28 through 4.36.

4.3.3 Event Z

Neutron- and gamma-dose distributions for the houses in this array, Fig. 3.16, are given in Figs. 4.37 through 4.43.

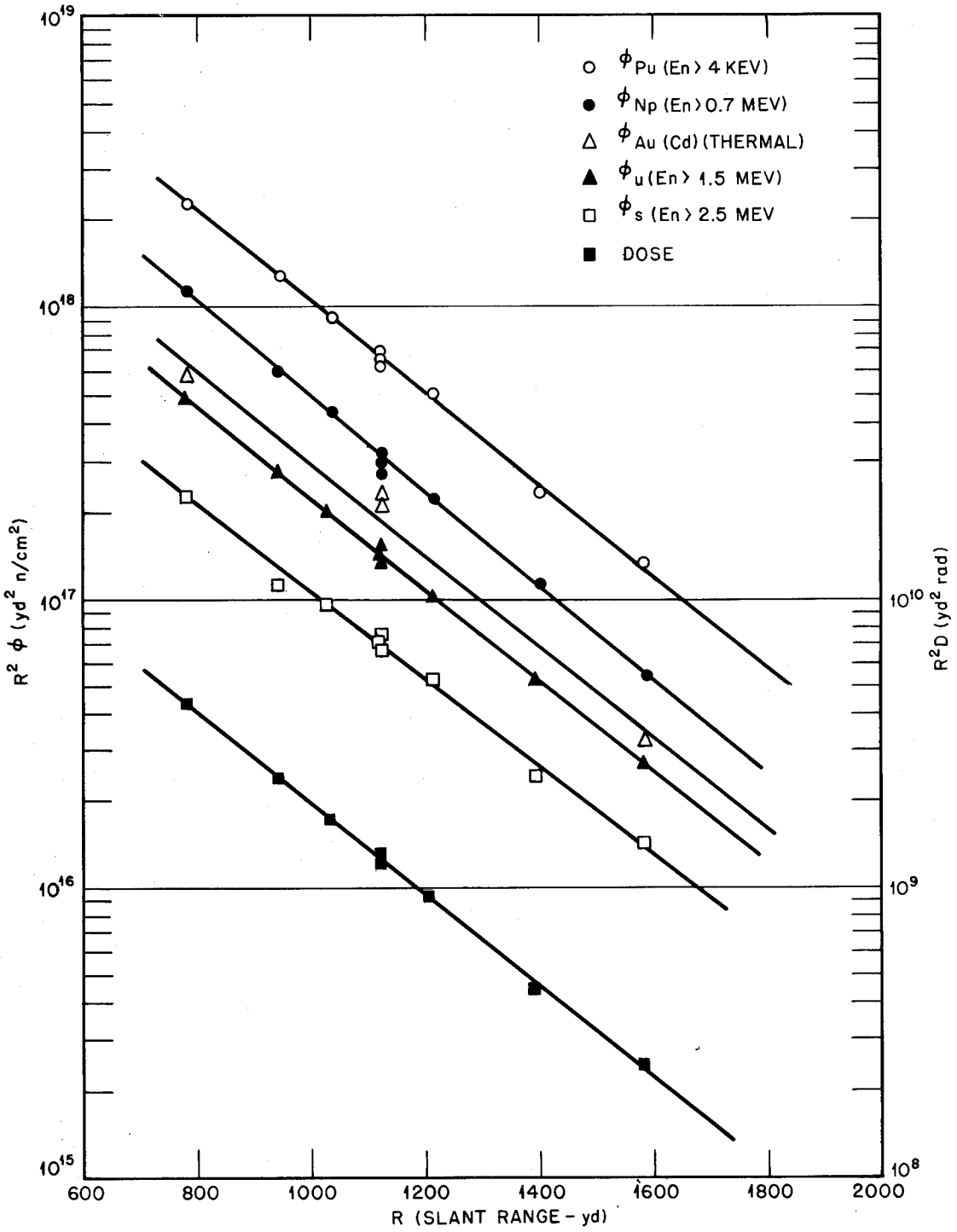

Fig. 4.1—$R^2\phi$ and R^2D vs. slant range for neutrons, event X.

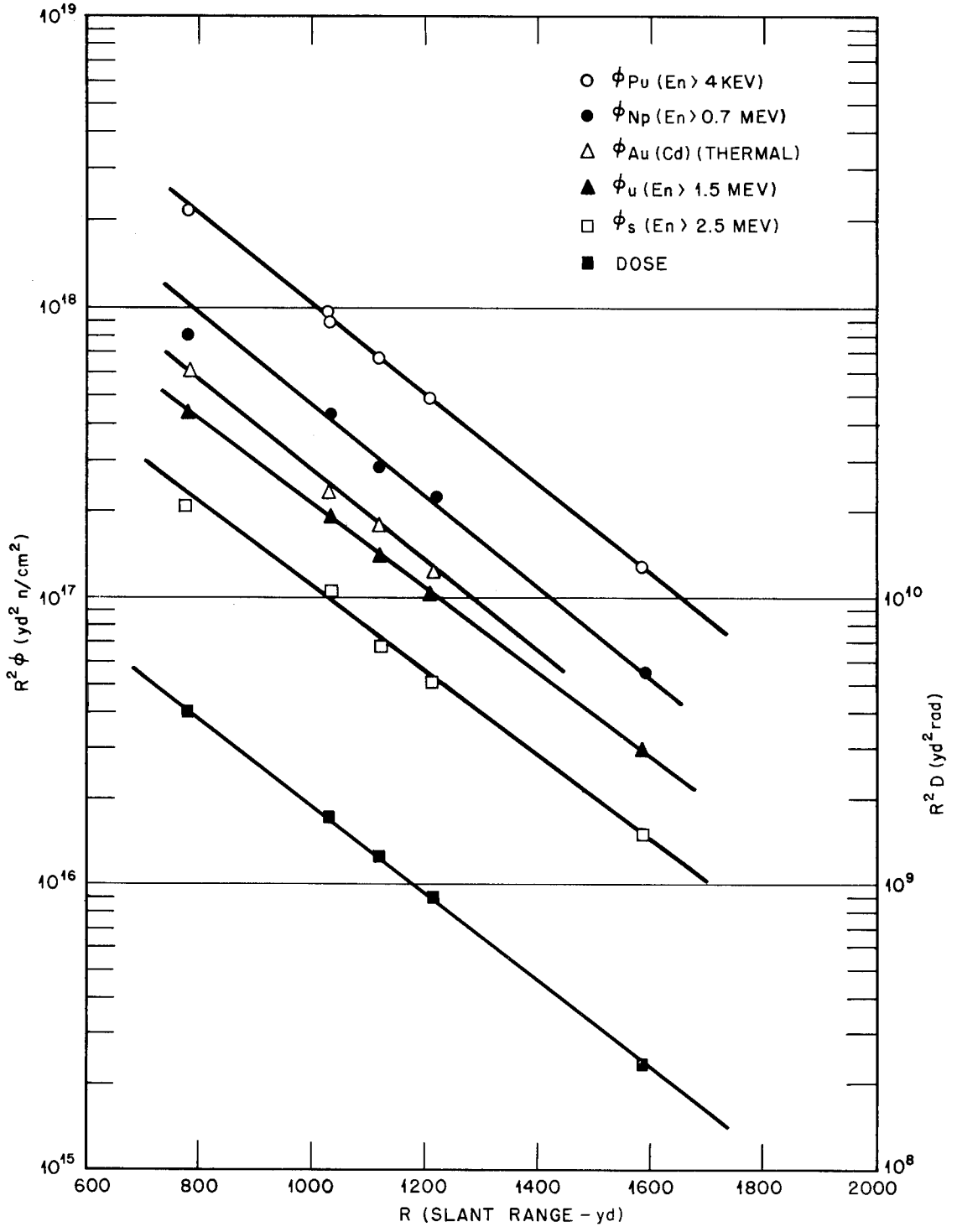

Fig. 4.2—$R^2\phi$ and R^2D vs. slant range for neutrons, event Y.

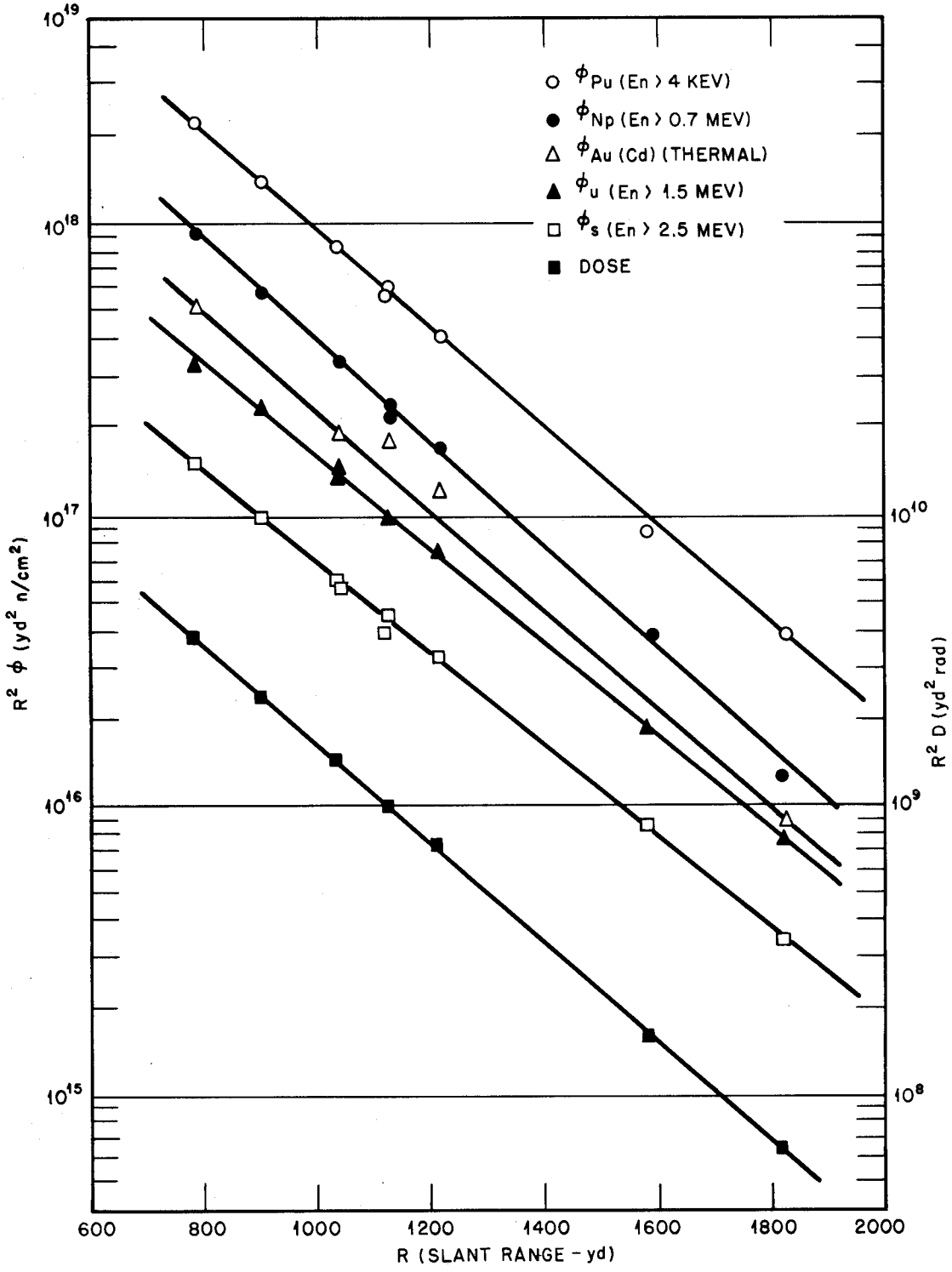

Fig. 4.3—$R^2\phi$ and R^2D vs. slant range for neutrons, event Z.

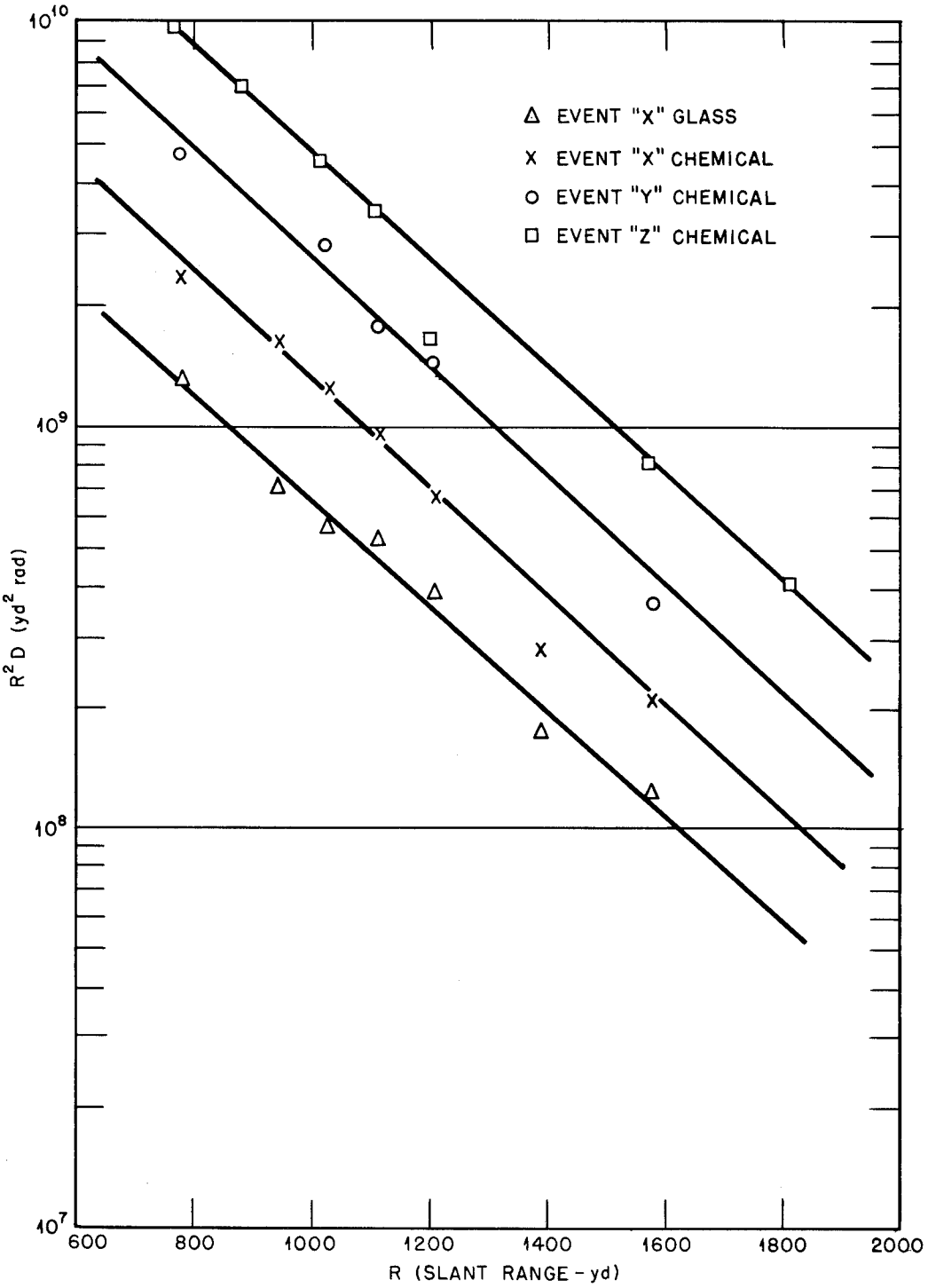

Fig. 4.4—R^2D vs. slant range for gamma rays, events X, Y, and Z.

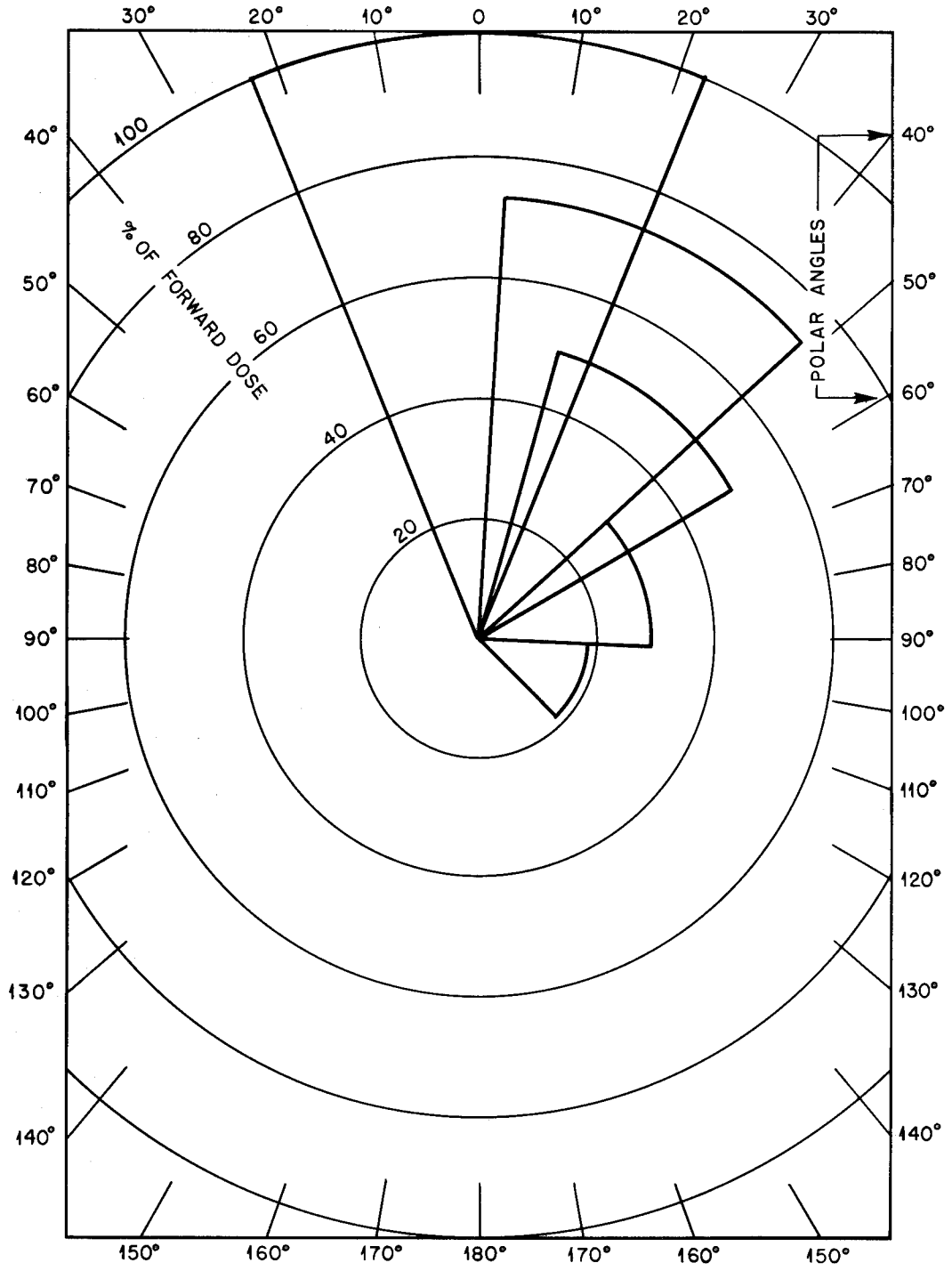

Fig. 4.5—Angular distribution of neutron dose at 1000 yards.

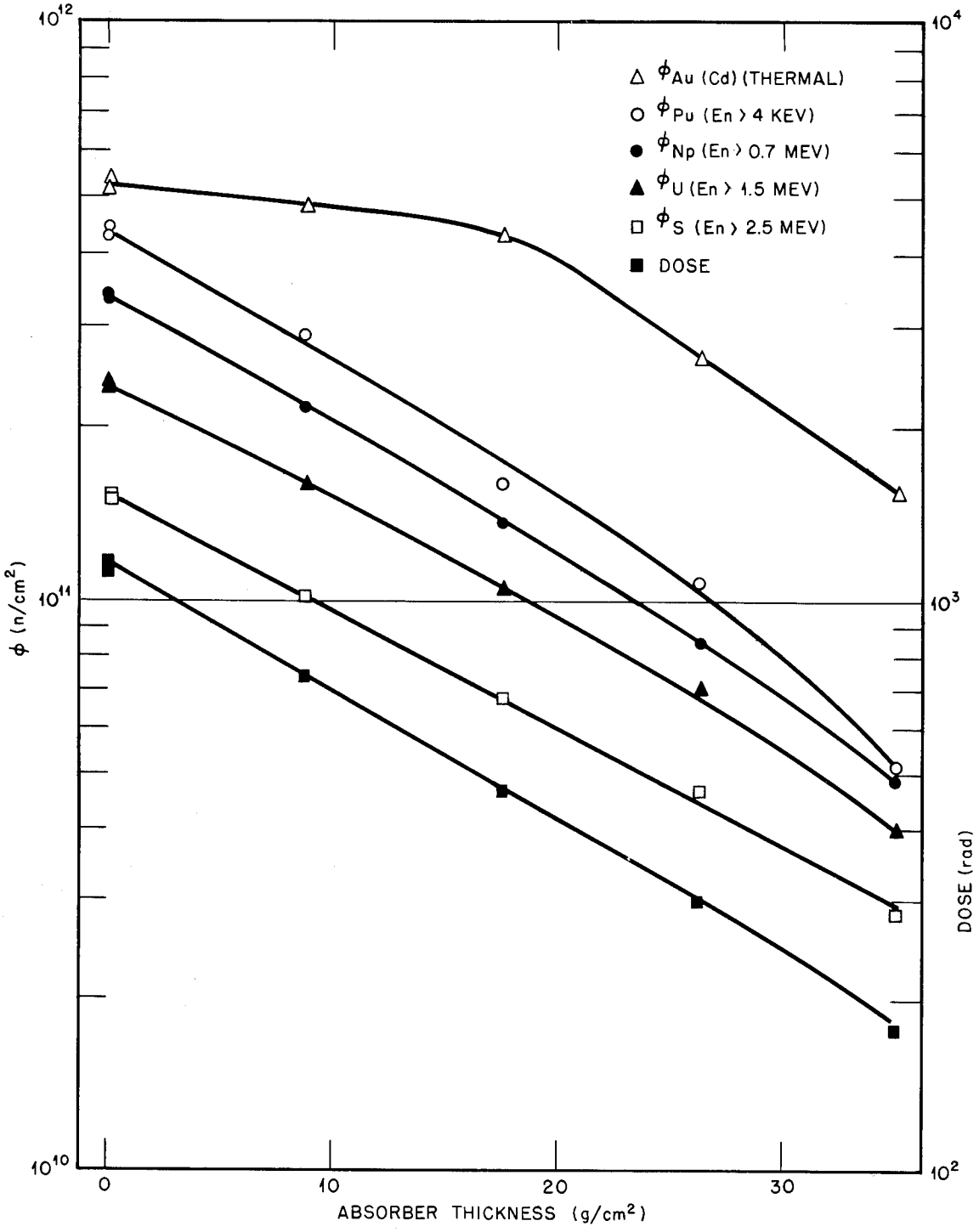

Fig. 4.6—Neutron attenuation by Transite at 750 yards, 0° polar angle.

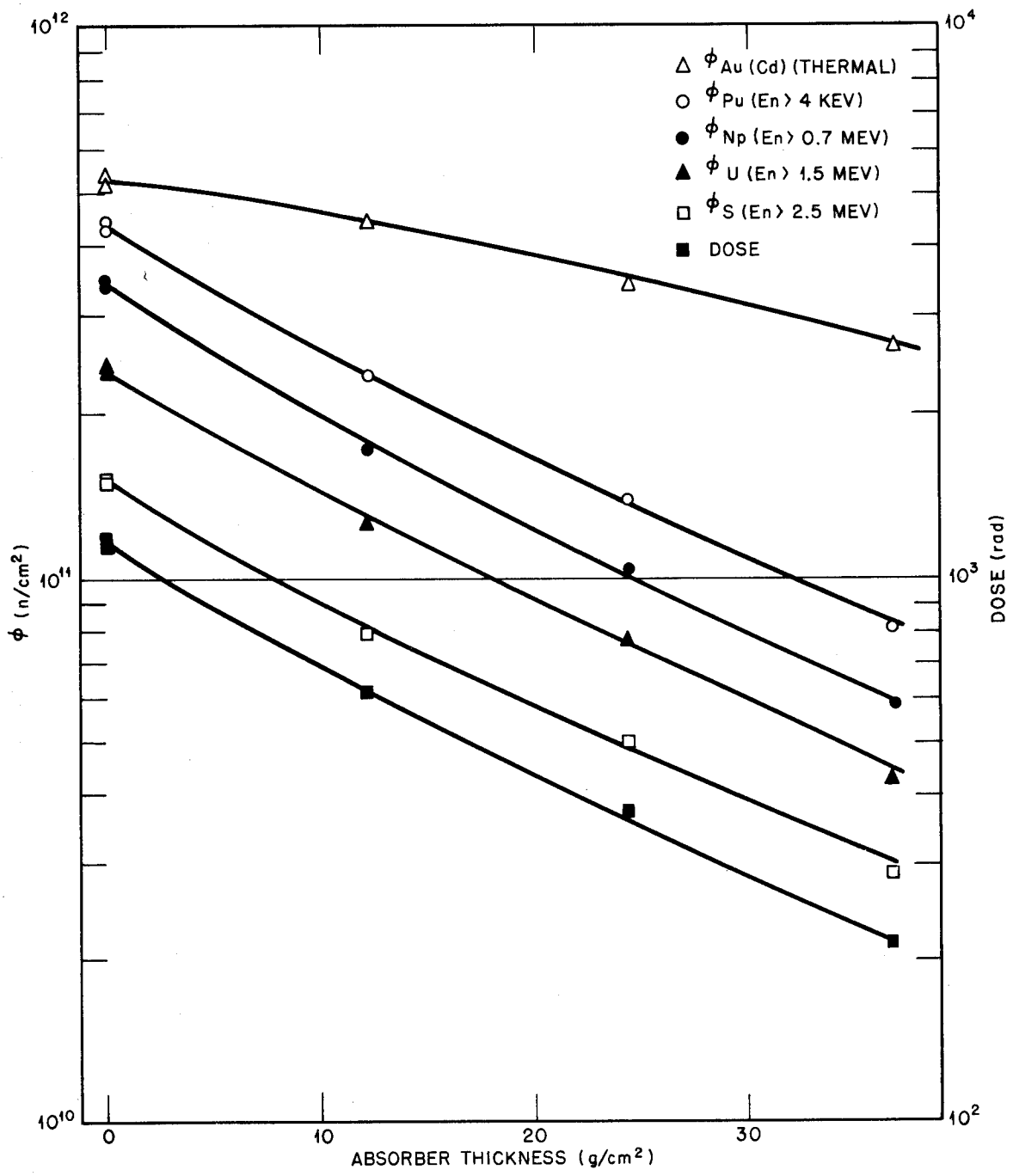

Fig. 4.7—Neutron attenuation by sand at 750 yards, 0° polar angle.

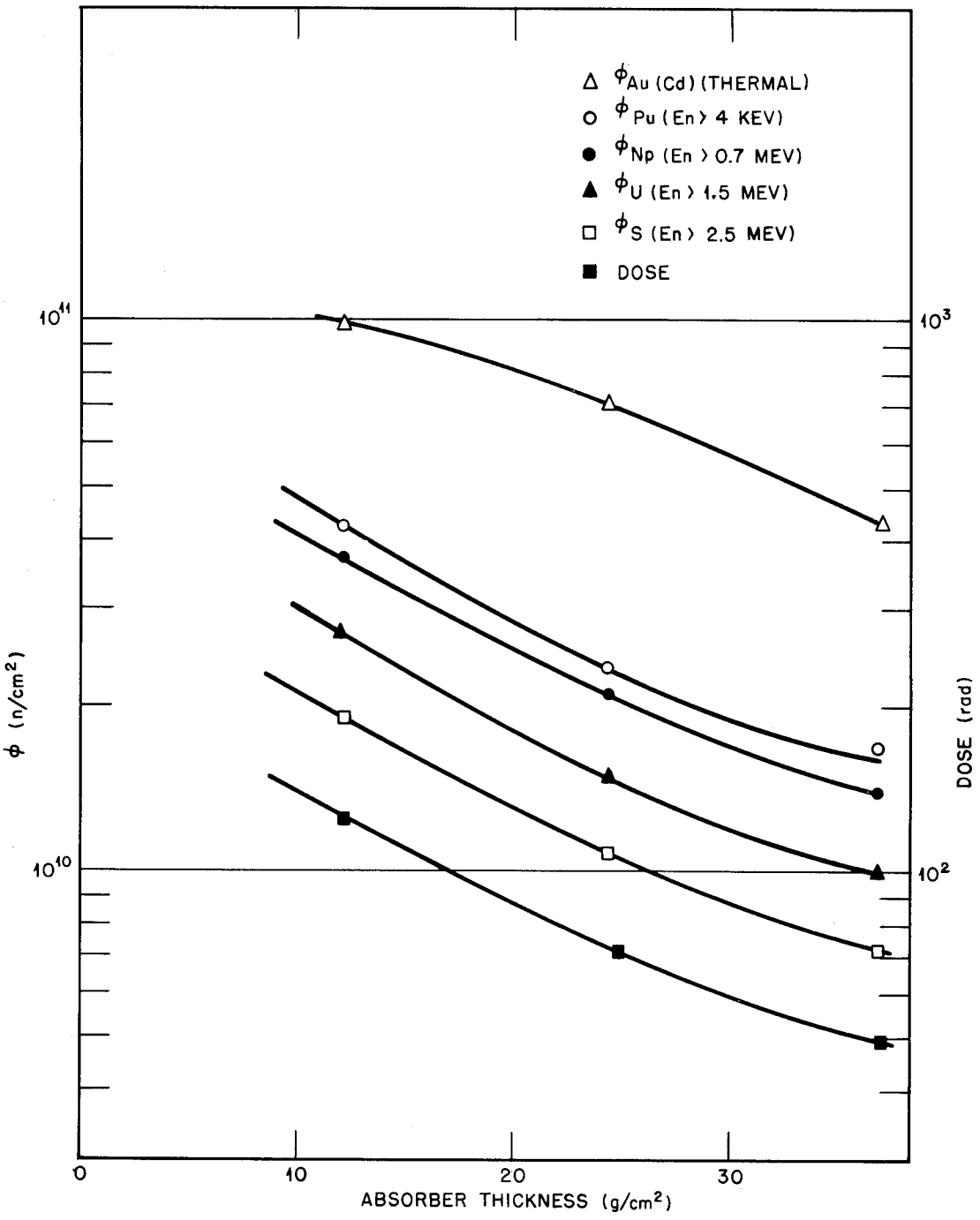

Fig. 4.8—Neutron attenuation by sand at 1000 yards, 0° polar angle.

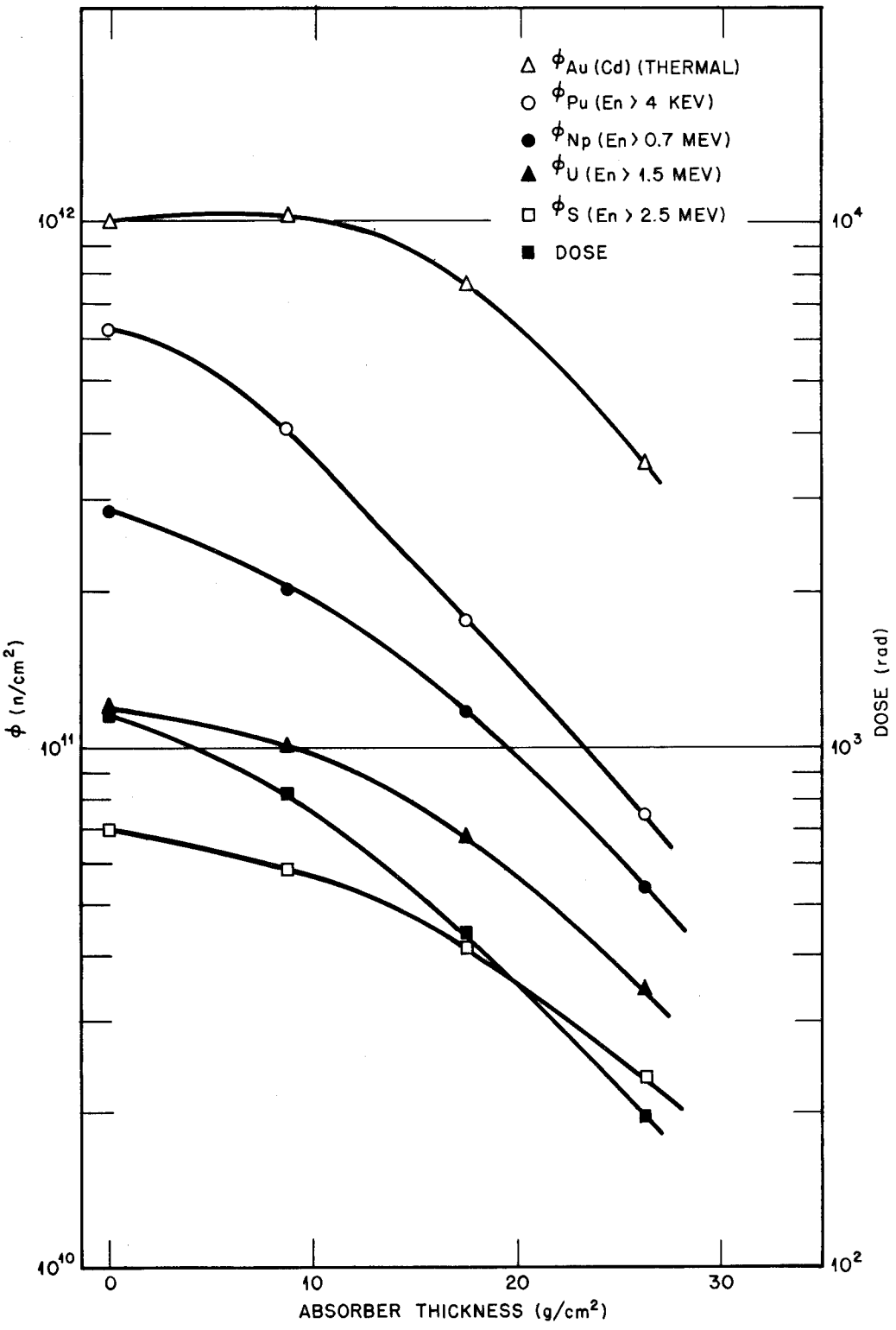

Fig. 4.9—Neutron attenuation by Transite at 750 yards, 36° polar angle.

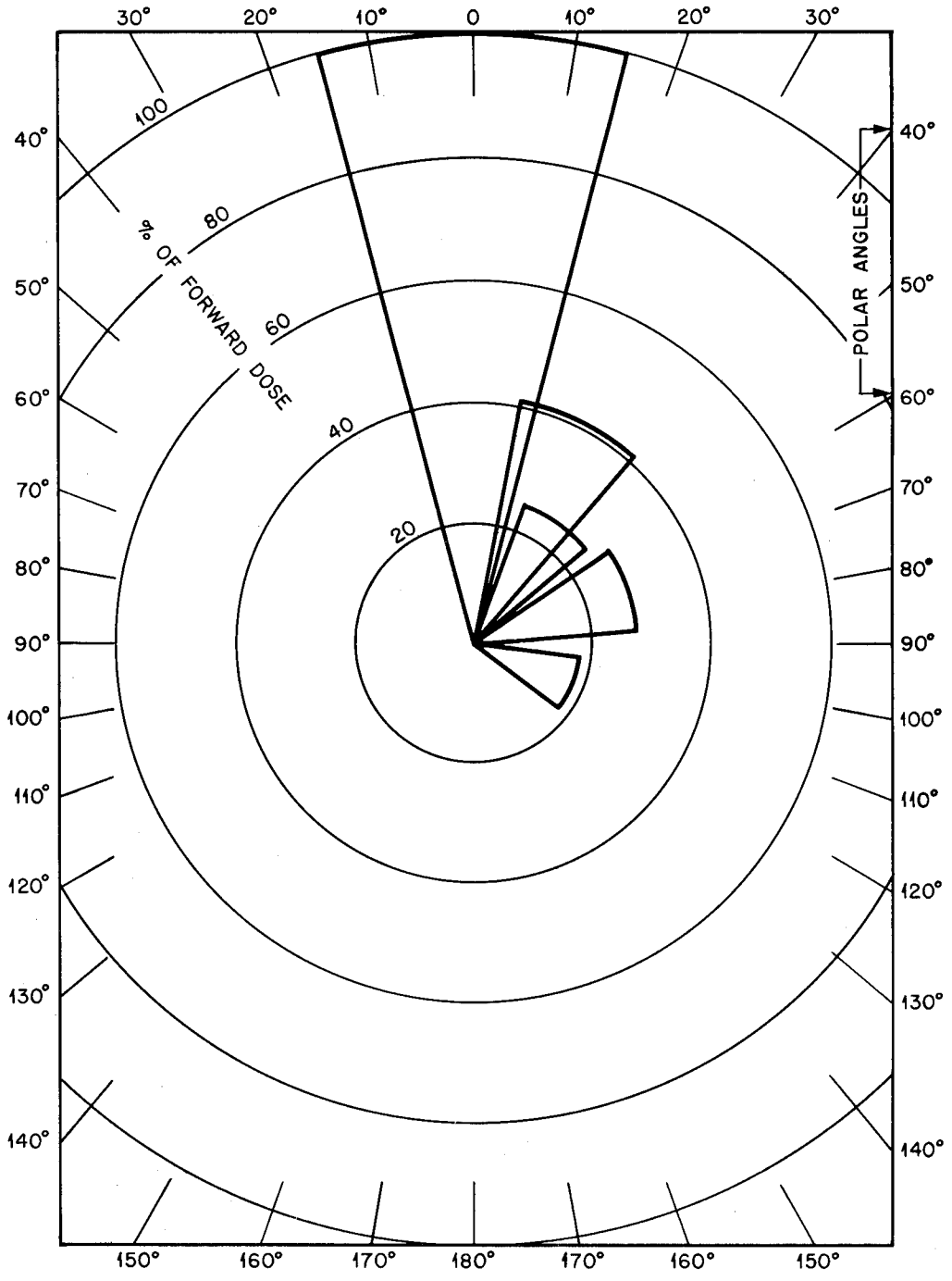

Fig. 4.10—Angular distribution of gamma-ray dose at 750 yards, event Z.

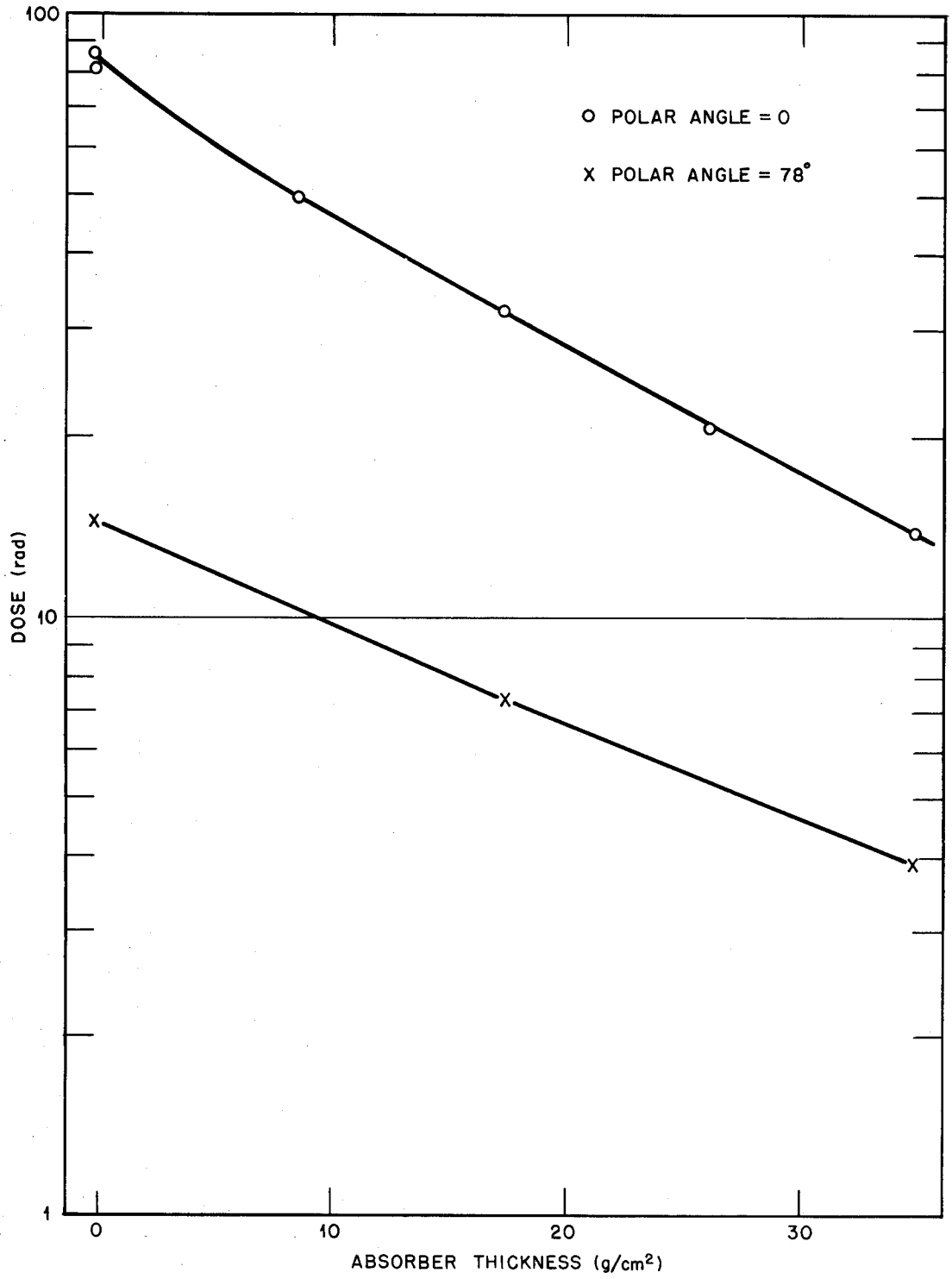

Fig. 4.11—Gamma-ray attenuation by Transite at 1000 yards.

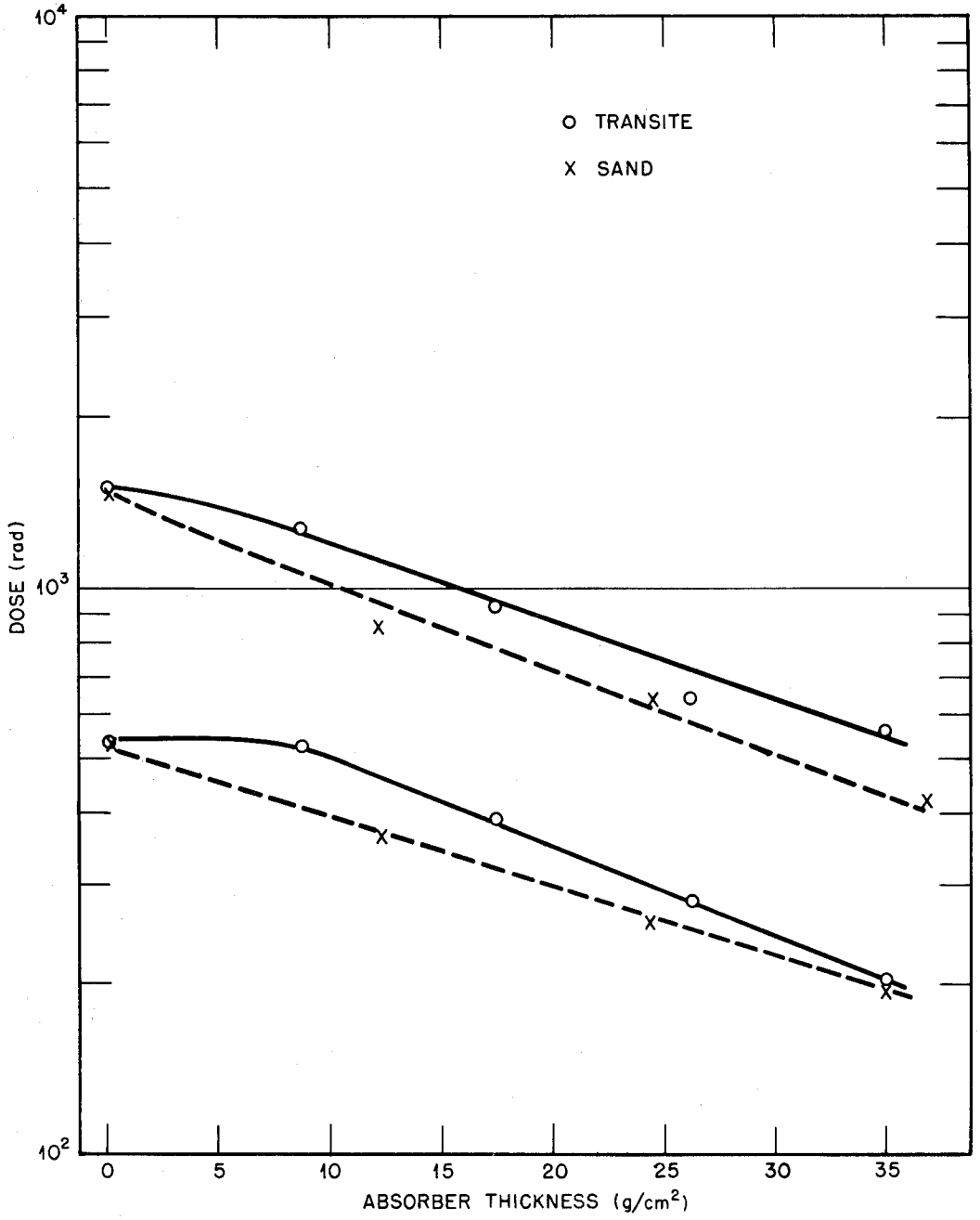

Fig. 4.12—Gamma-ray attenuation by Transite and sand at 750 and 1000 yards.

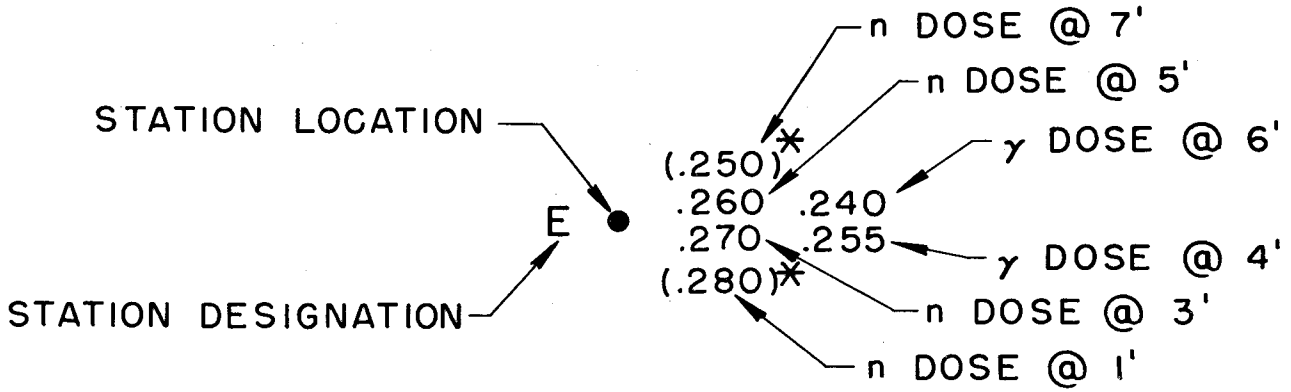

*PARENTHESES INDICATE DOSE WHEN ESTIMATED FROM S FLUX ONLY.

NOTE:
BLANK SPACE IN ANY POSITION INDICATES NO MEASUREMENT AT THAT LOCATION.

Fig. 4.13—Key to house dose-distribution diagrams.

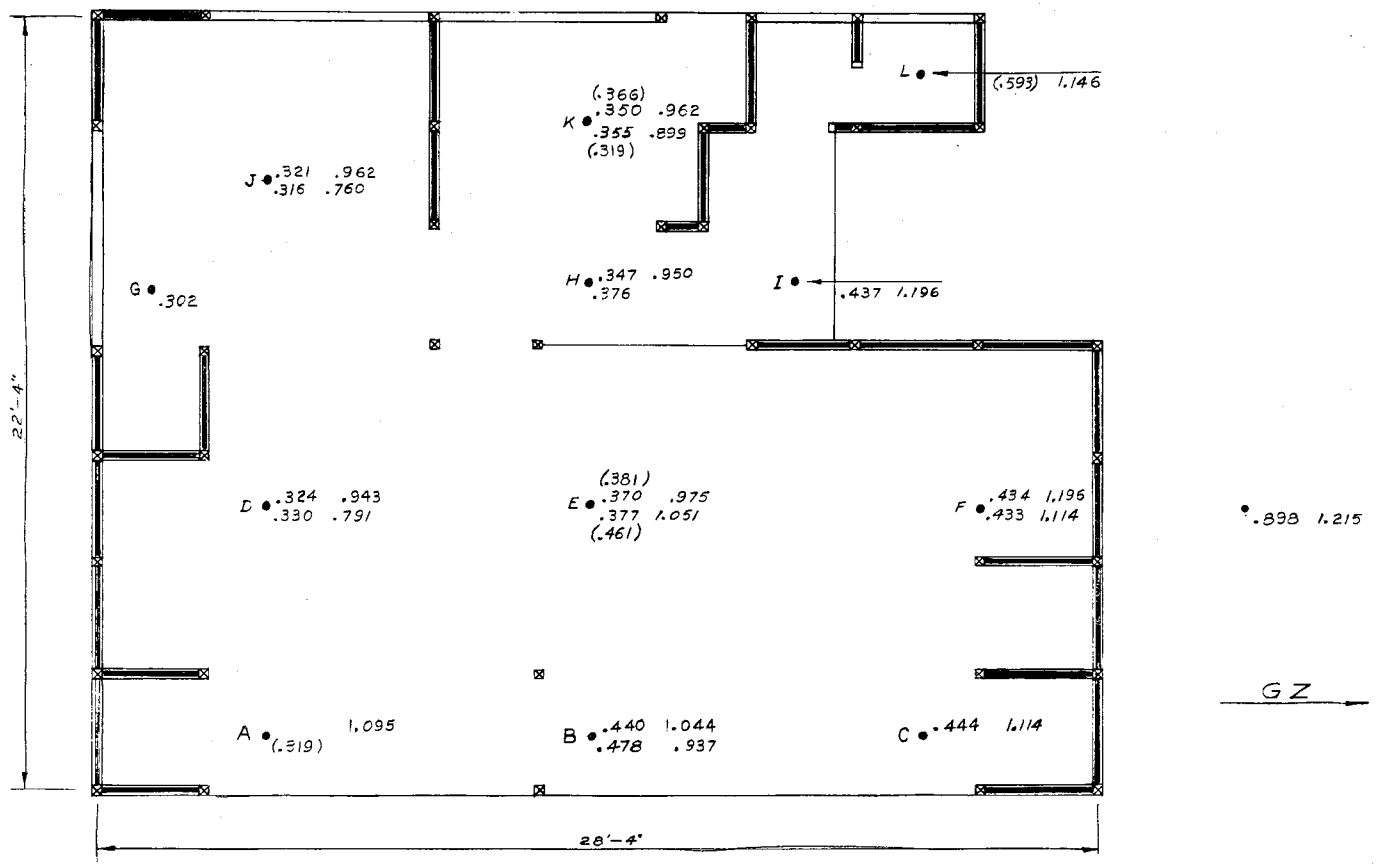

Fig. 4.14—Relative gamma- and neutron-dose distributions in house 1, event X.

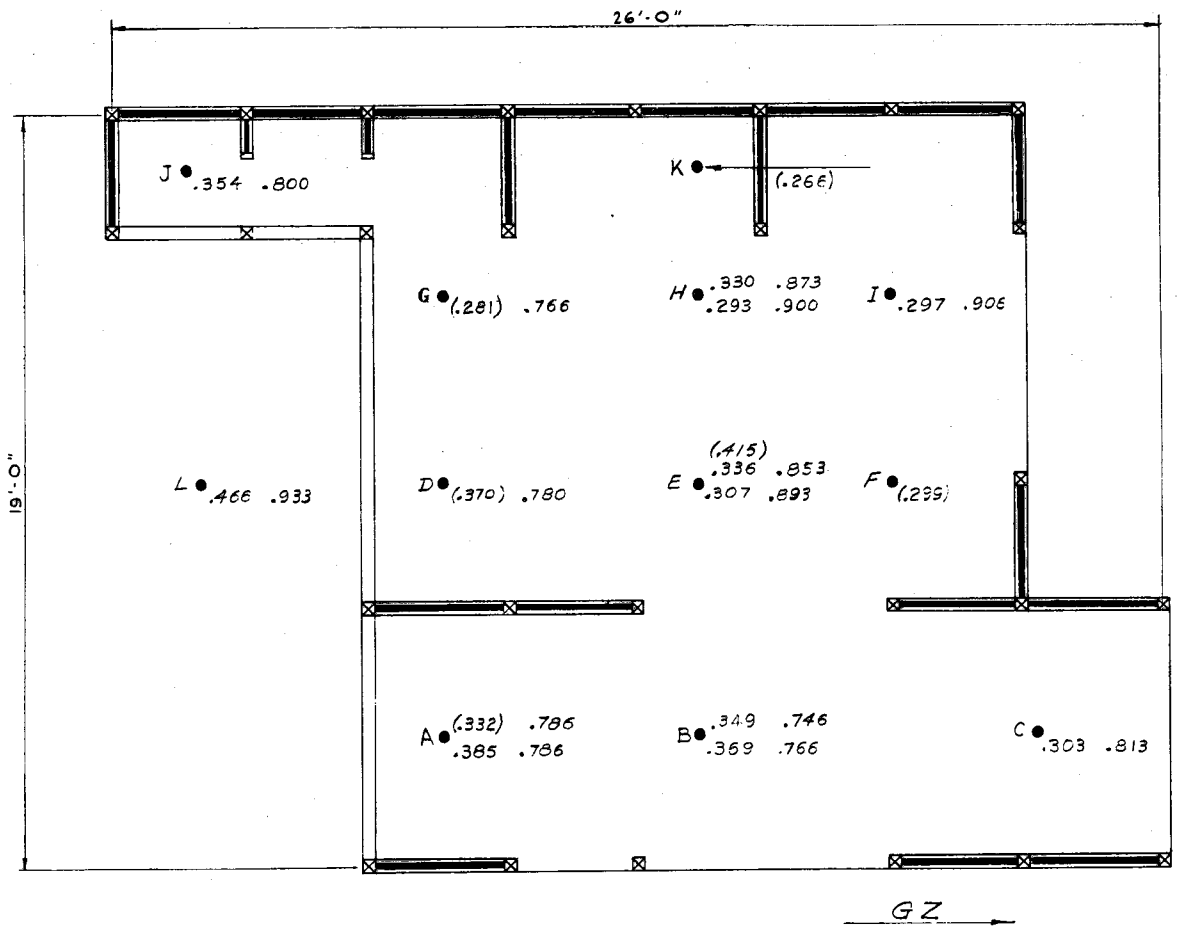

Fig. 4.15—Relative gamma- and neutron-dose distributions in house 2, event X.

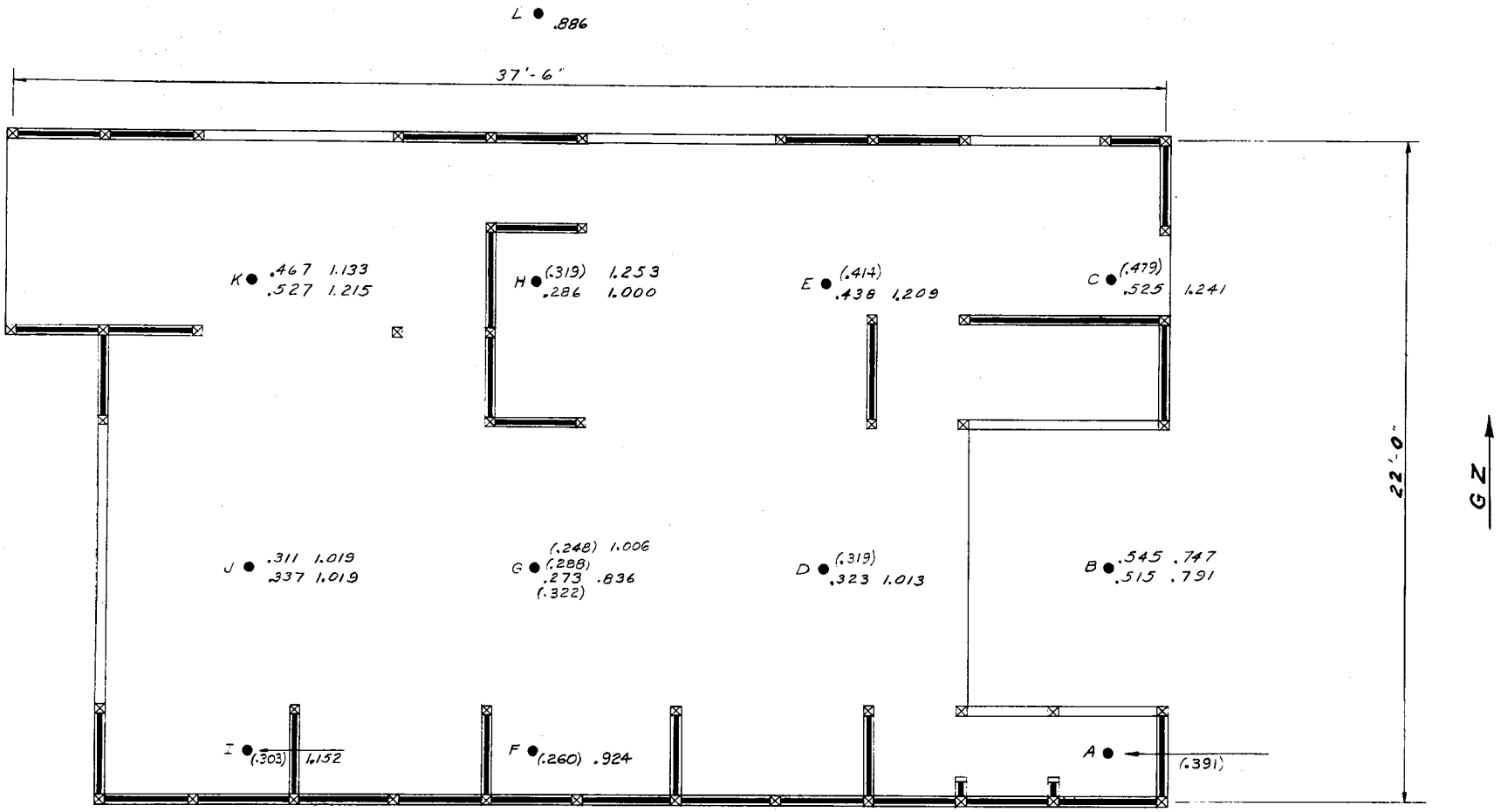

Fig. 4.16—Relative gamma- and neutron-dose distributions in house 3, first floor, event X.

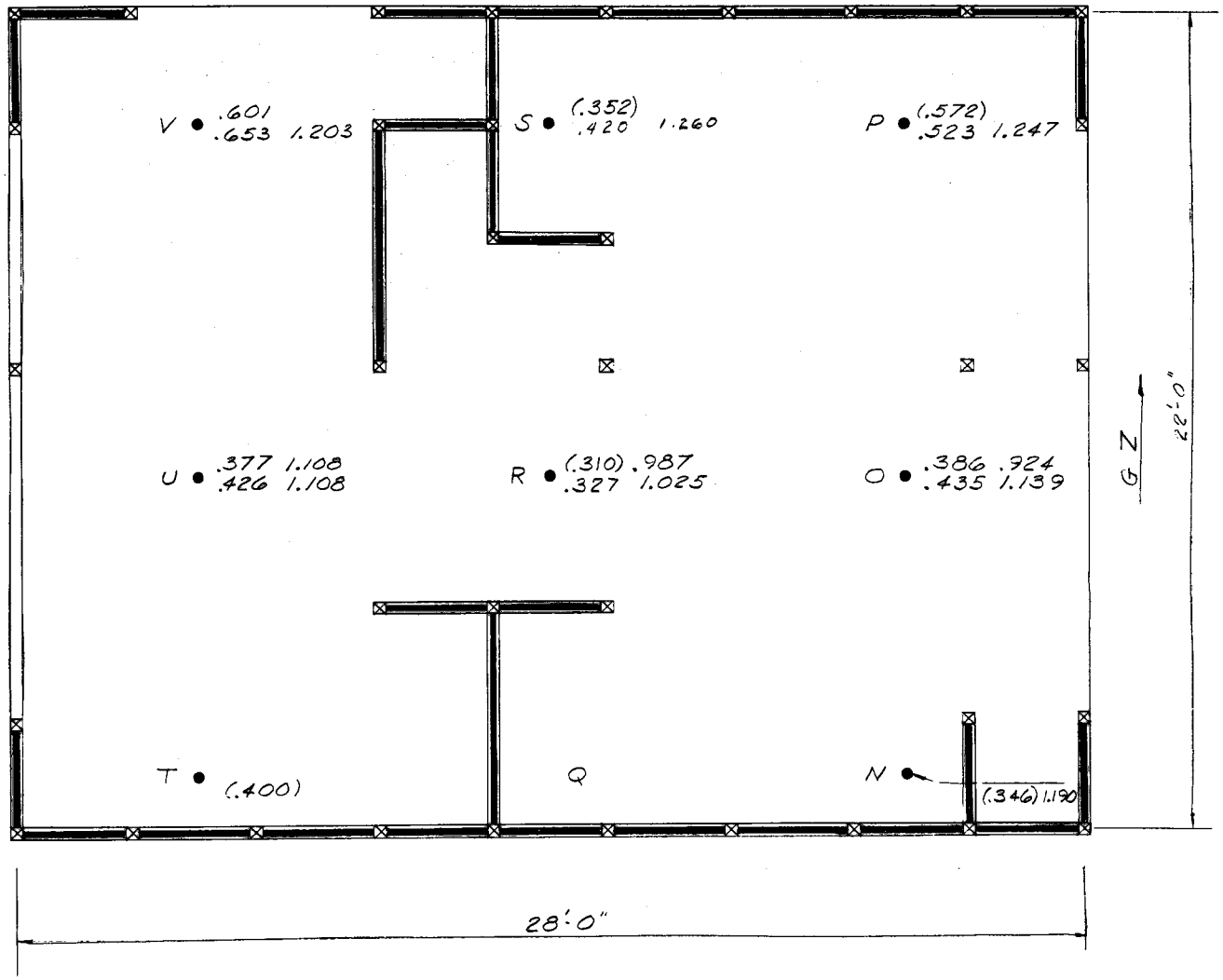

Fig. 4.17—Relative gamma- and neutron-dose distributions in house 3, second floor, event X.

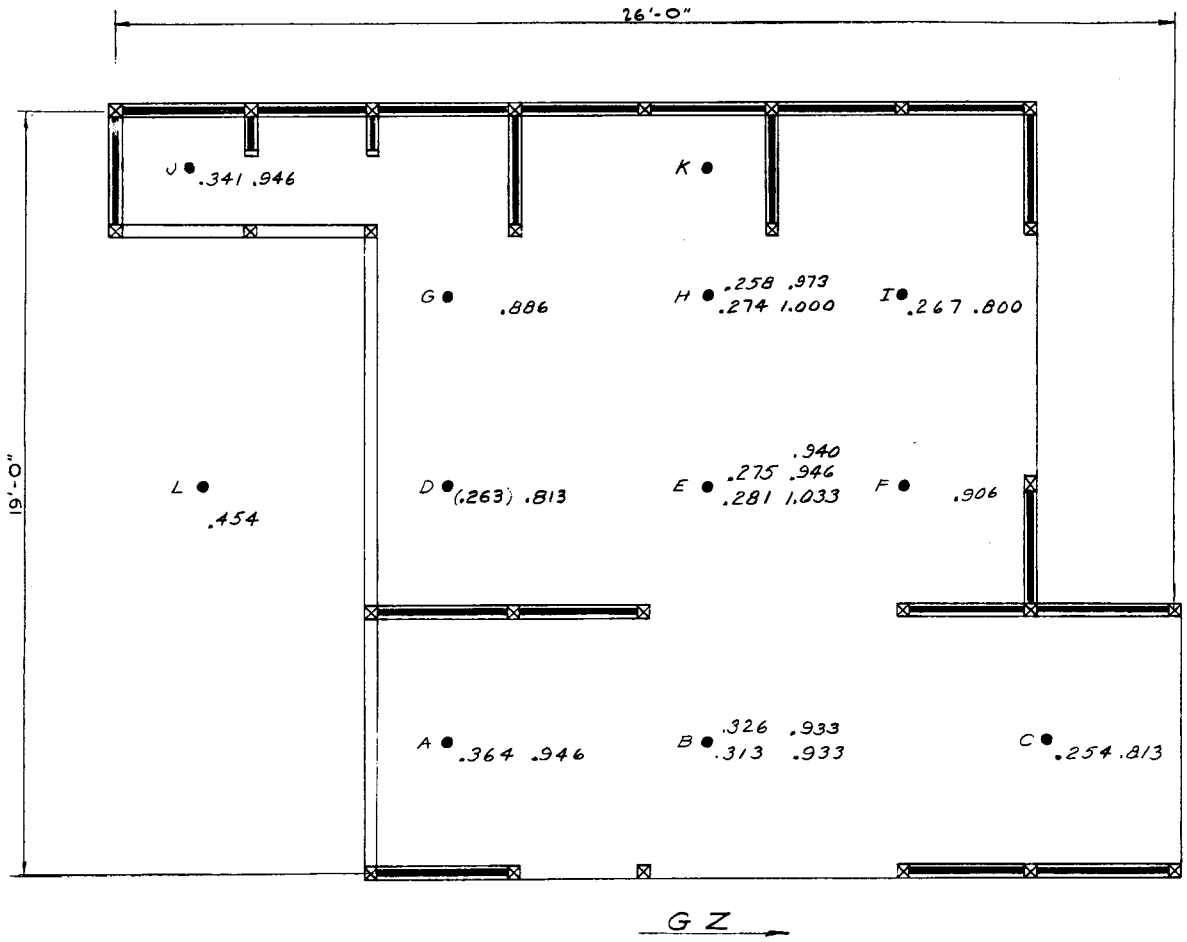

Fig. 4.18—Relative gamma- and neutron-dose distributions in house 4, event X.

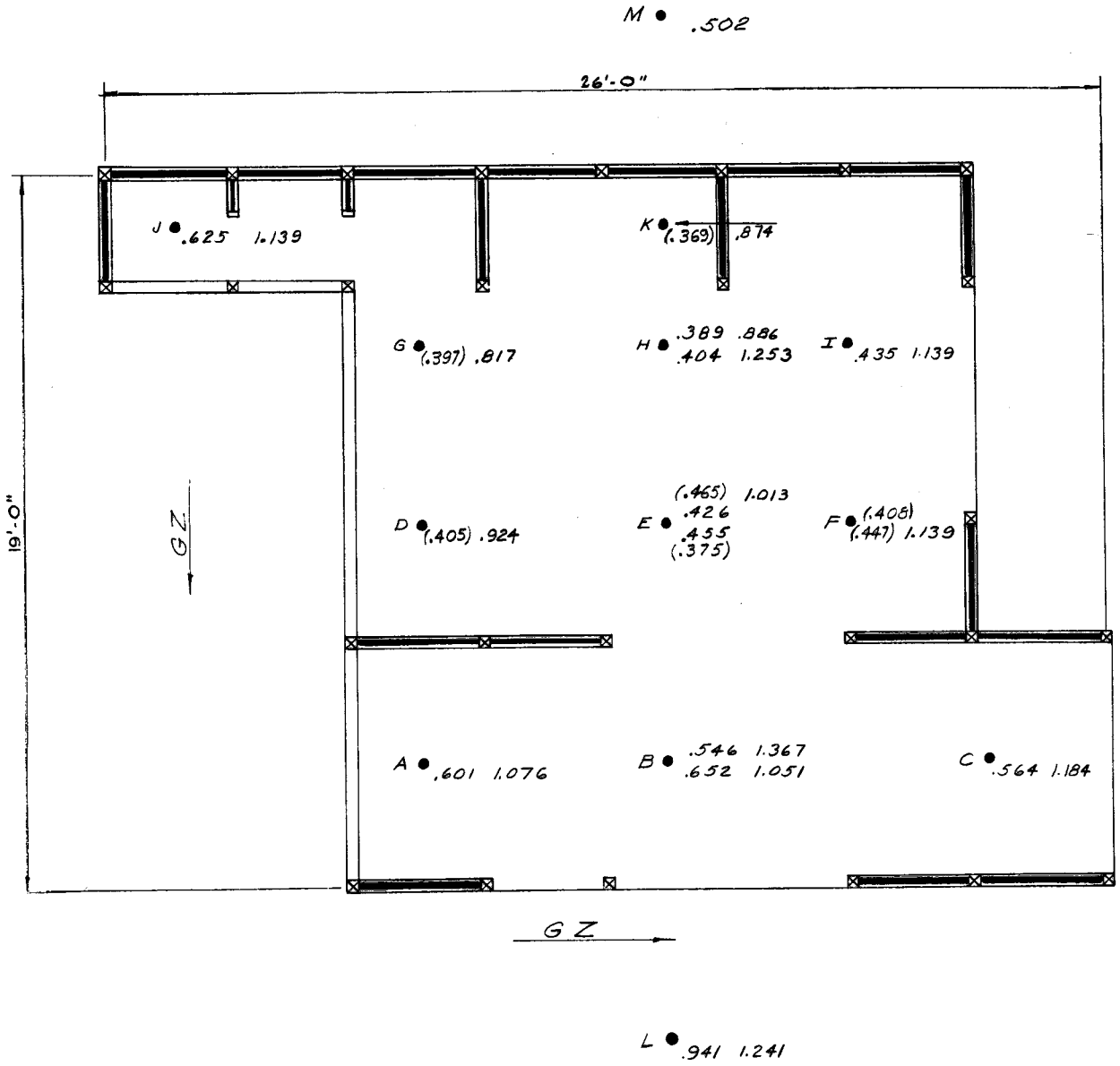

Fig. 4.19—Relative gamma- and neutron-dose distributions in house 5, event X.

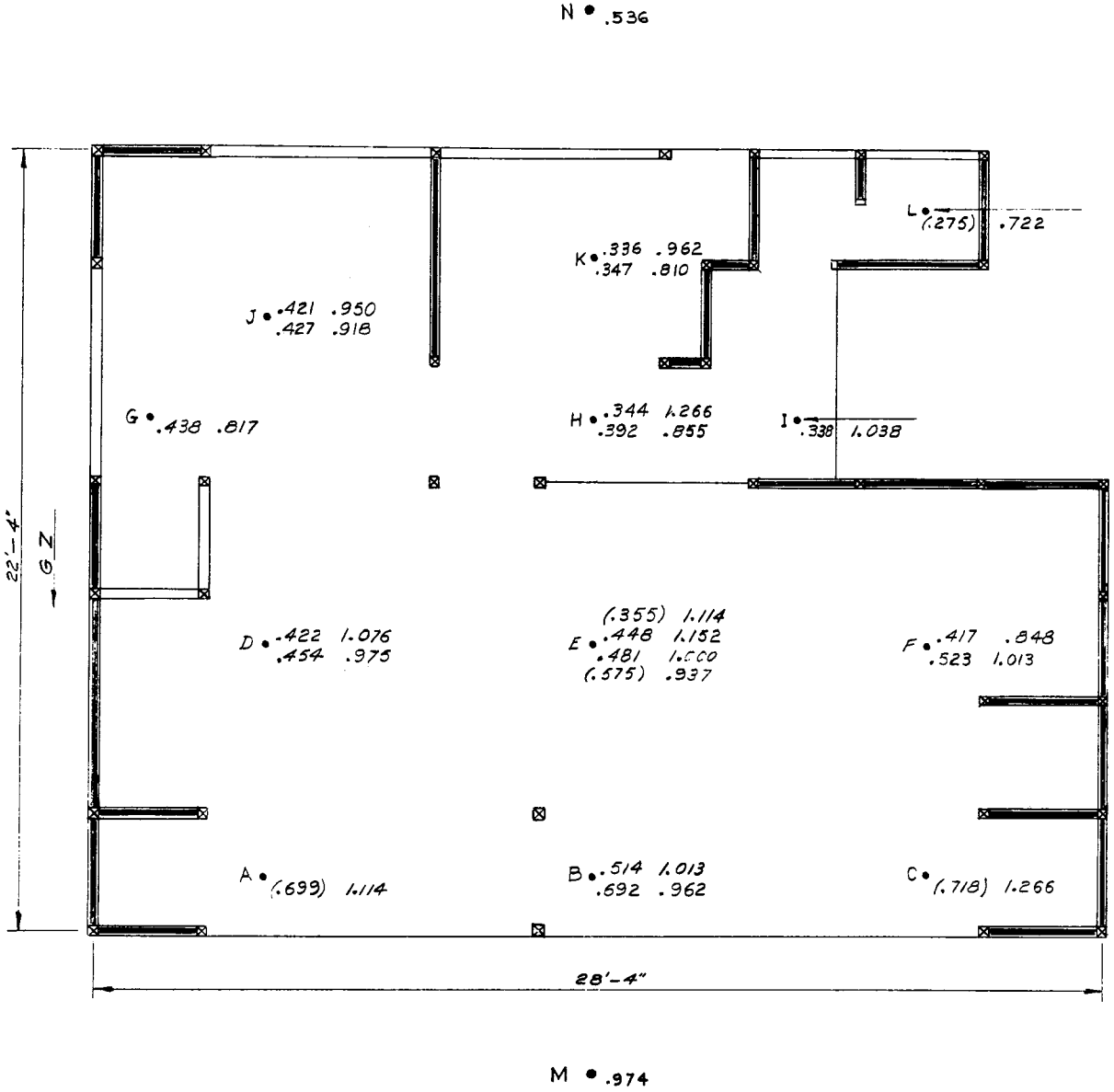

Fig. 4.20—Relative gamma- and neutron-dose distributions in house 6, event X.

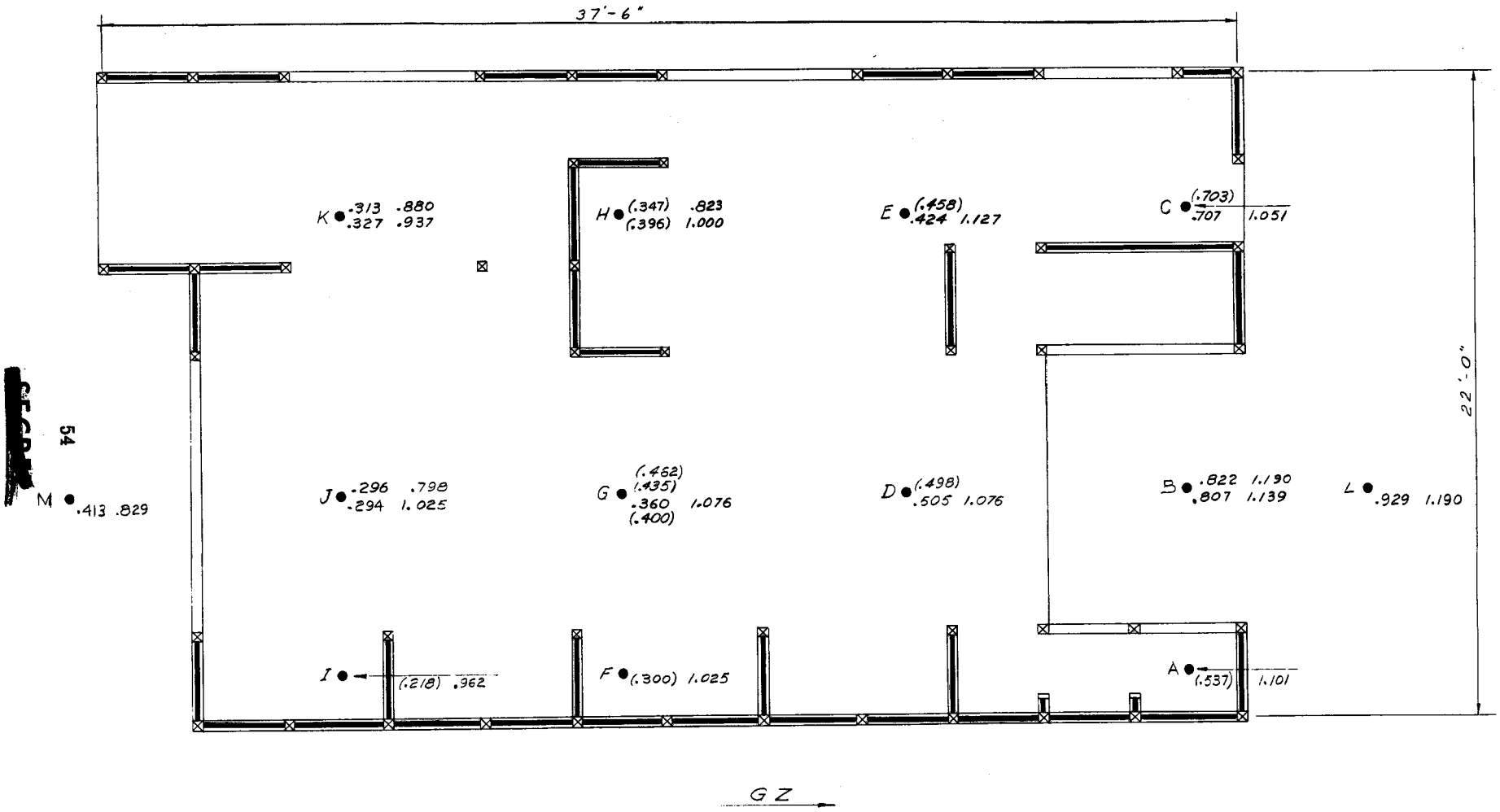

Fig. 4.21—Relative gamma- and neutron-dose distributions in house 7, first floor, event X.

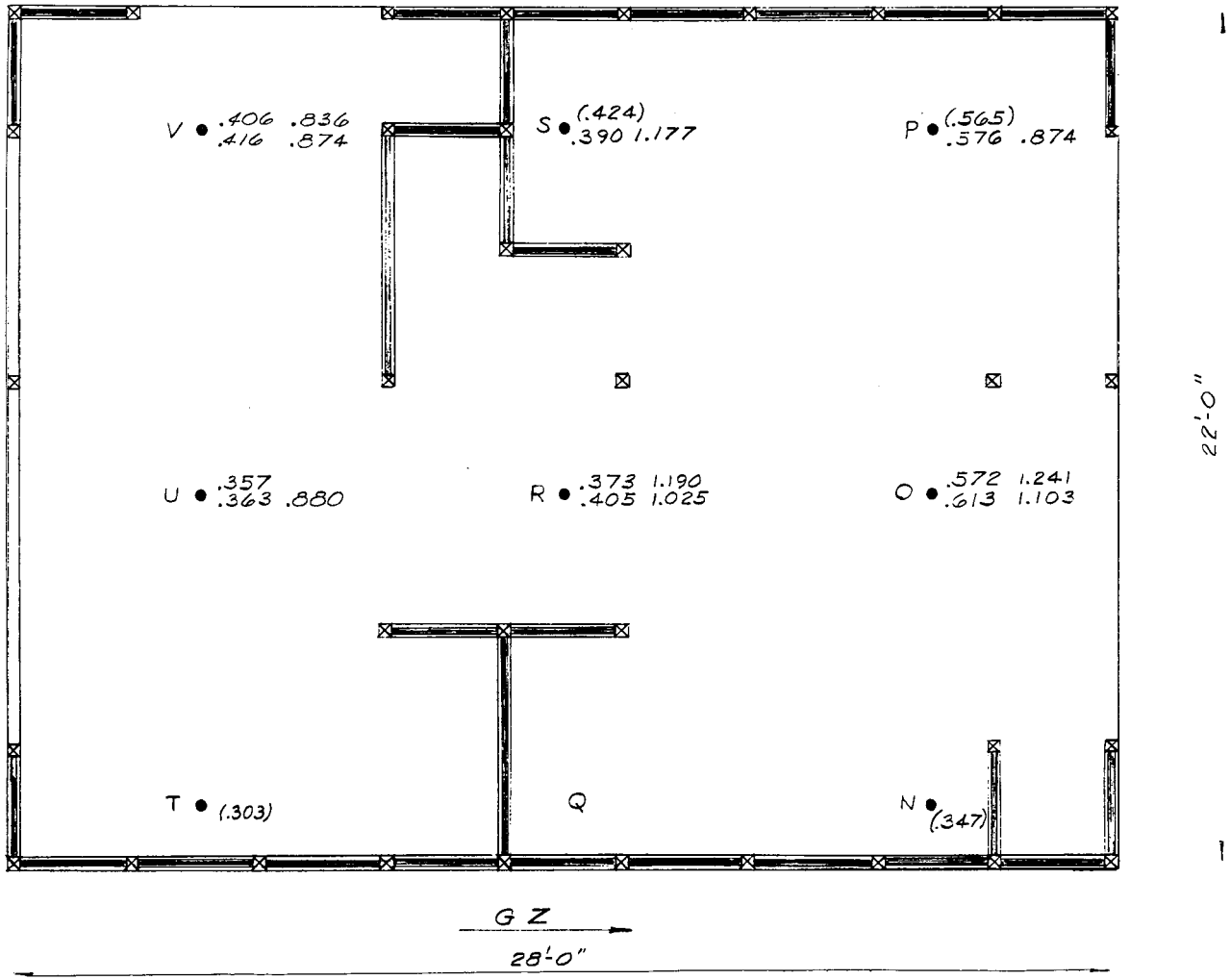

Fig. 4.22—Relative gamma- and neutron-dose distributions in house 7, second floor, event X.

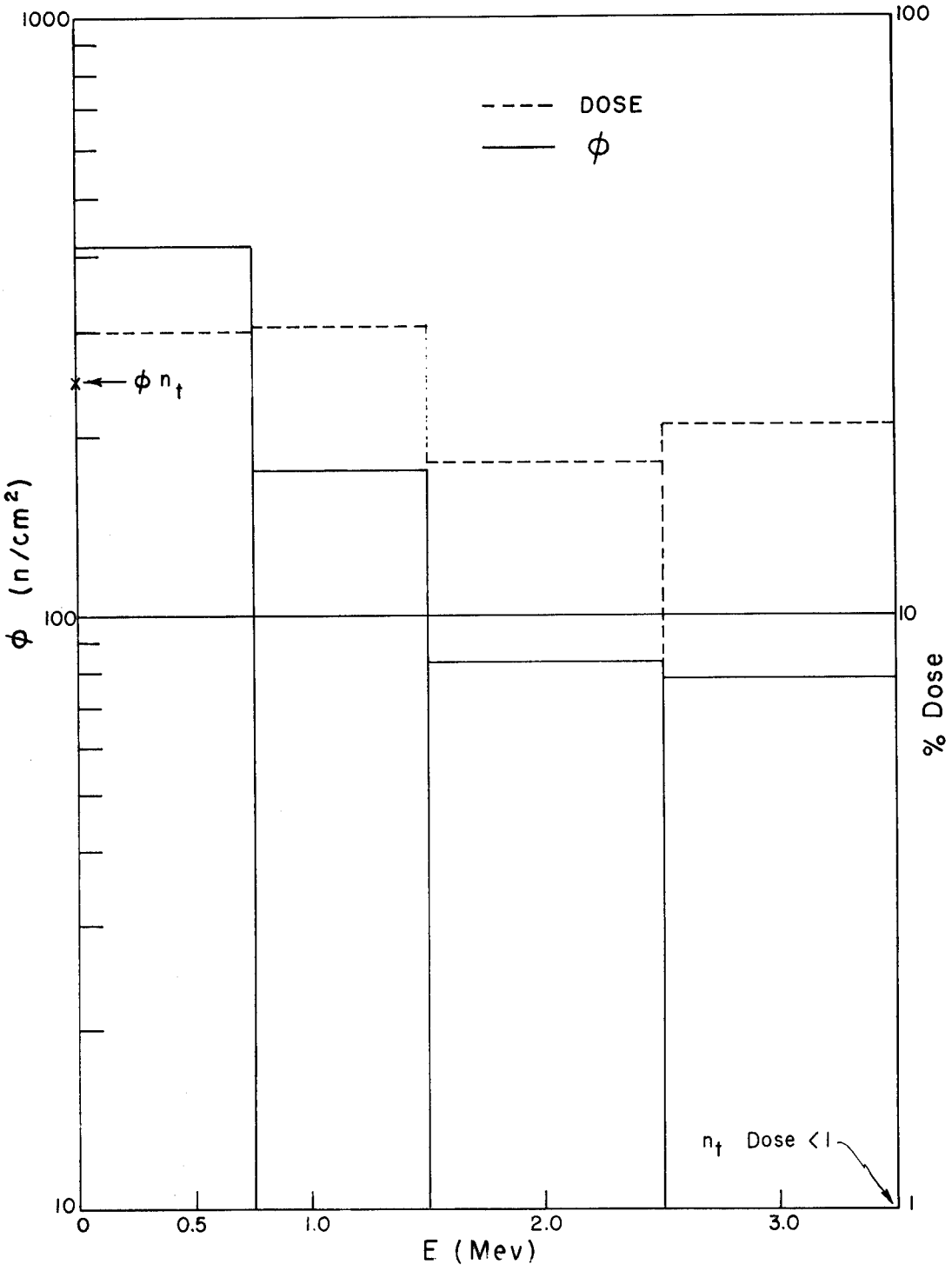

Fig. 4.23—Flux and dose histogram, air.

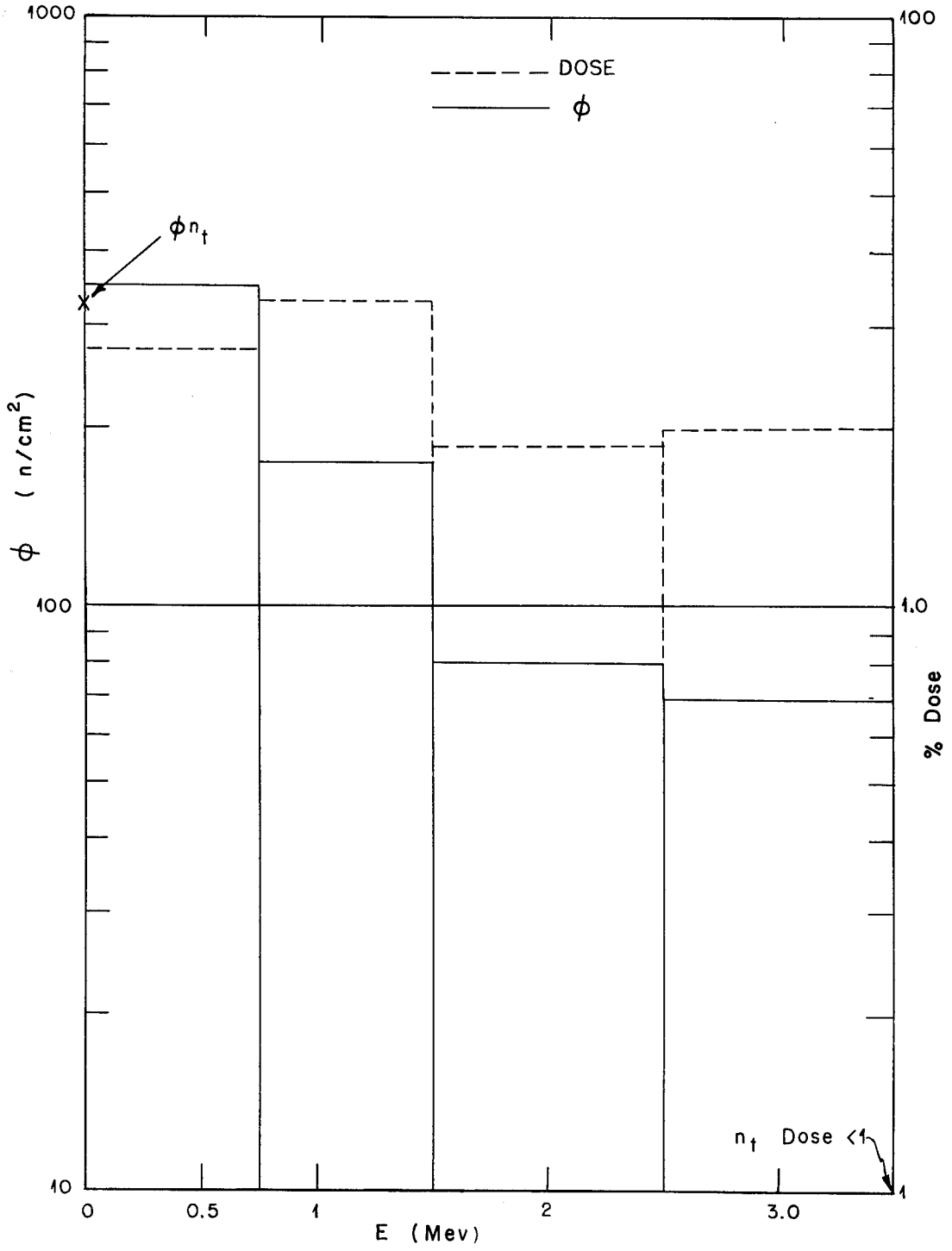

Fig. 4.24—Flux and dose histogram at 4 ft in front of house.

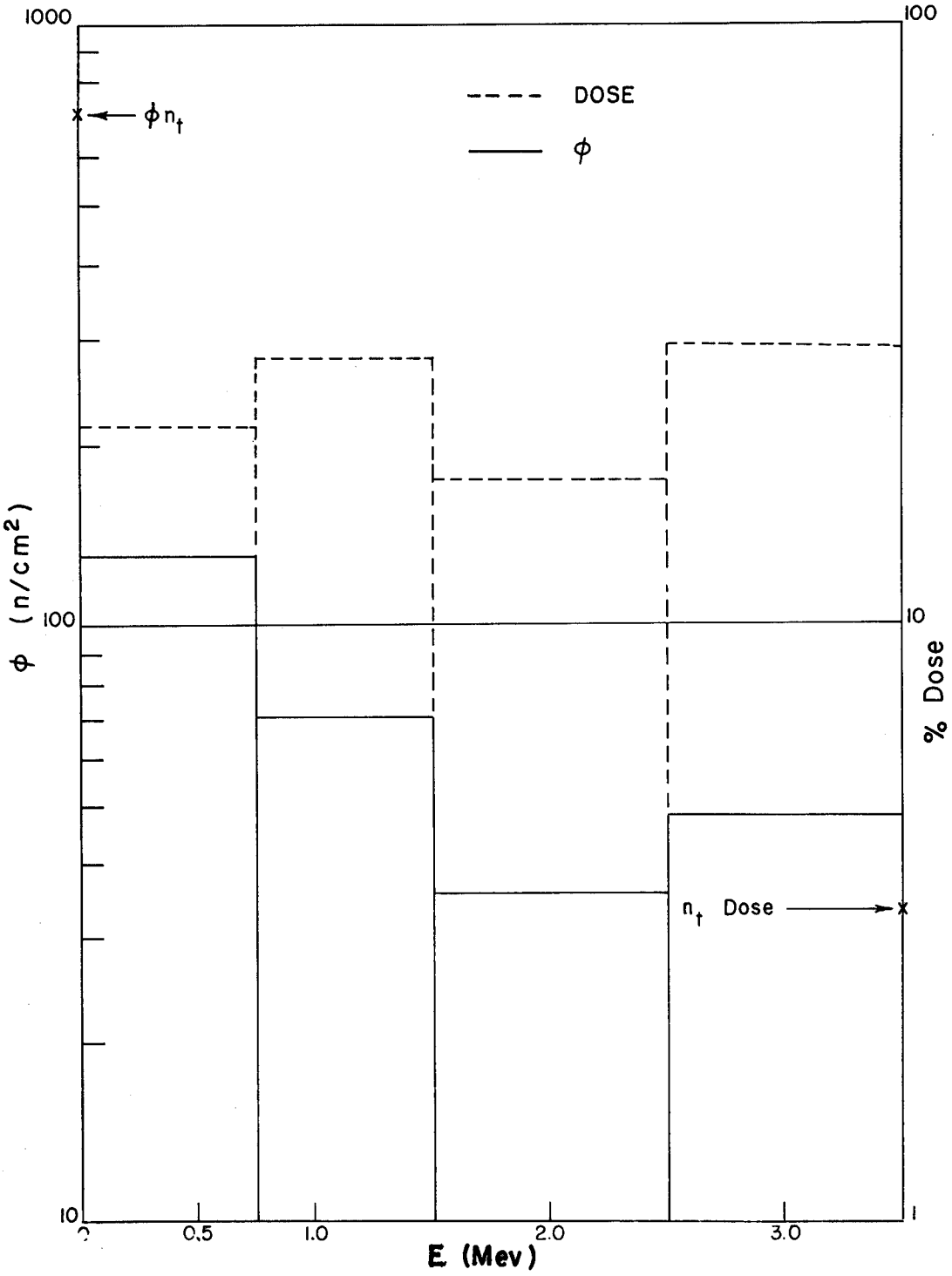

Fig. 4.25—Flux and dose histogram at center of house.

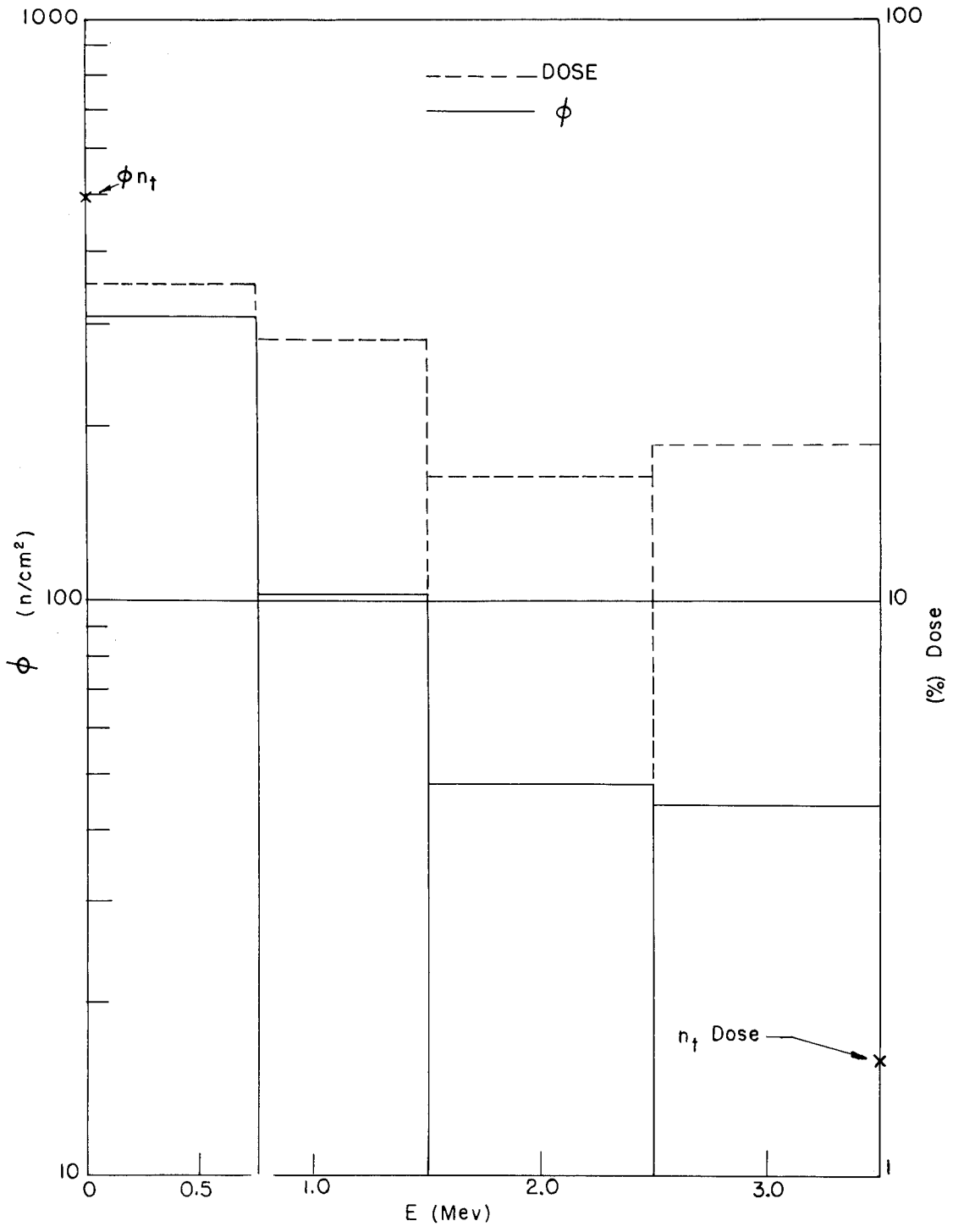

Fig. 4.26—Flux and dose histogram at 4 ft to rear of house.

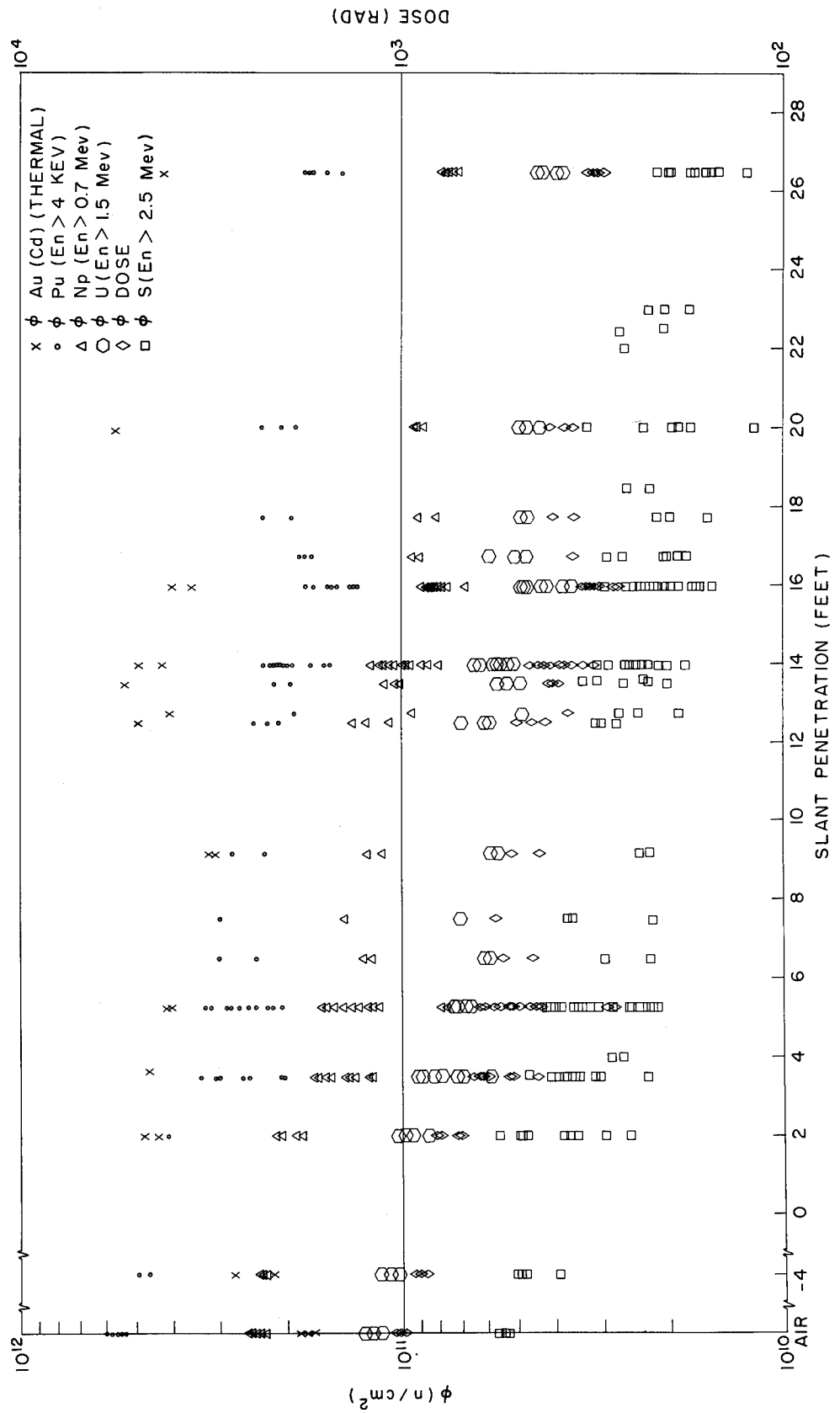

Fig. 4.27—Neutron flux and dose distribution vs. slant penetration, type B house.

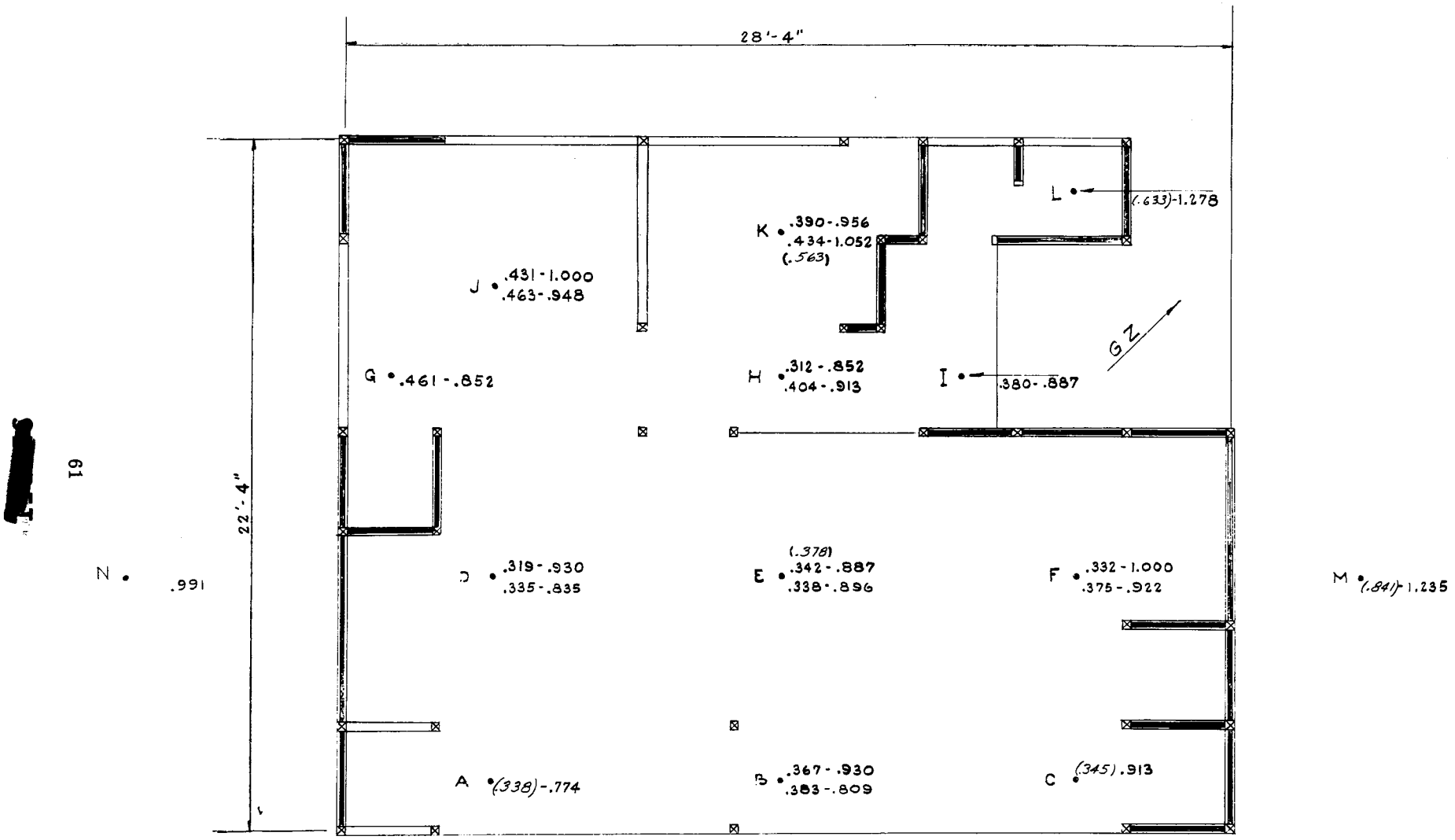

Fig. 4.28—Relative gamma- and neutron-dose distributions in house 1, event Y.

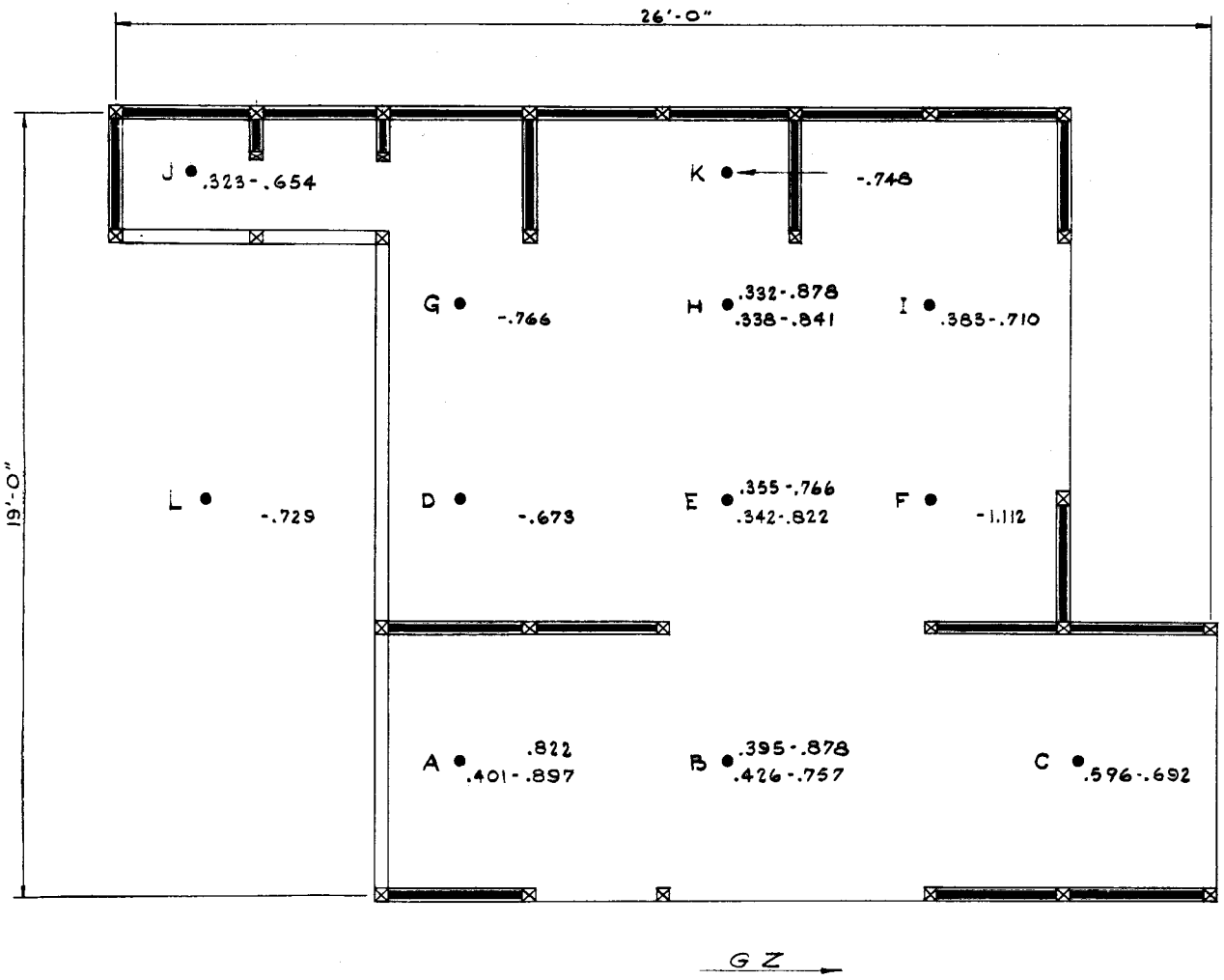

Fig. 4.29—Relative gamma- and neutron-dose distributions in house 2, event Y.

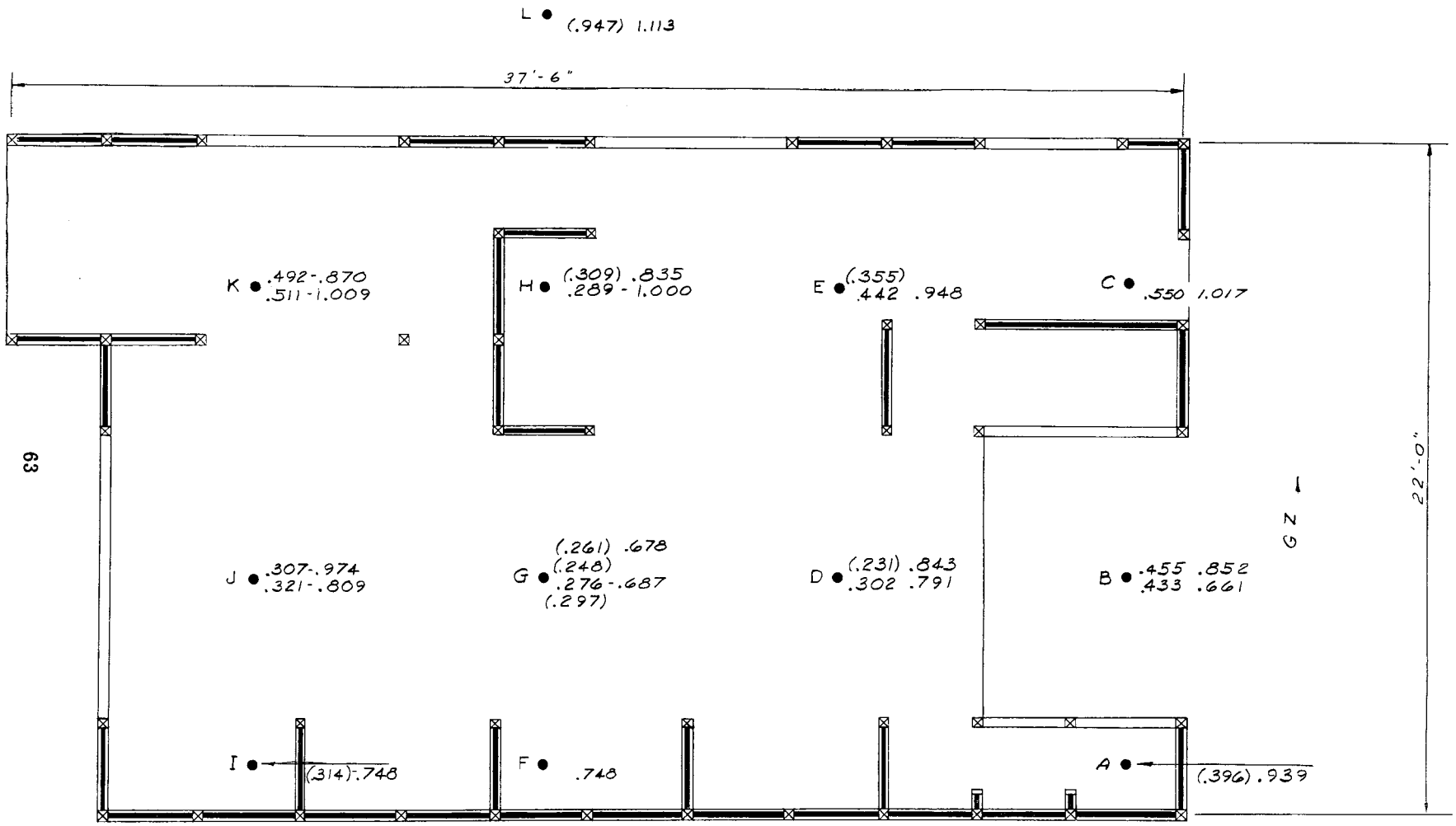

Fig. 4.30—Relative gamma- and neutron-dose distributions in house 3, first floor, event Y.

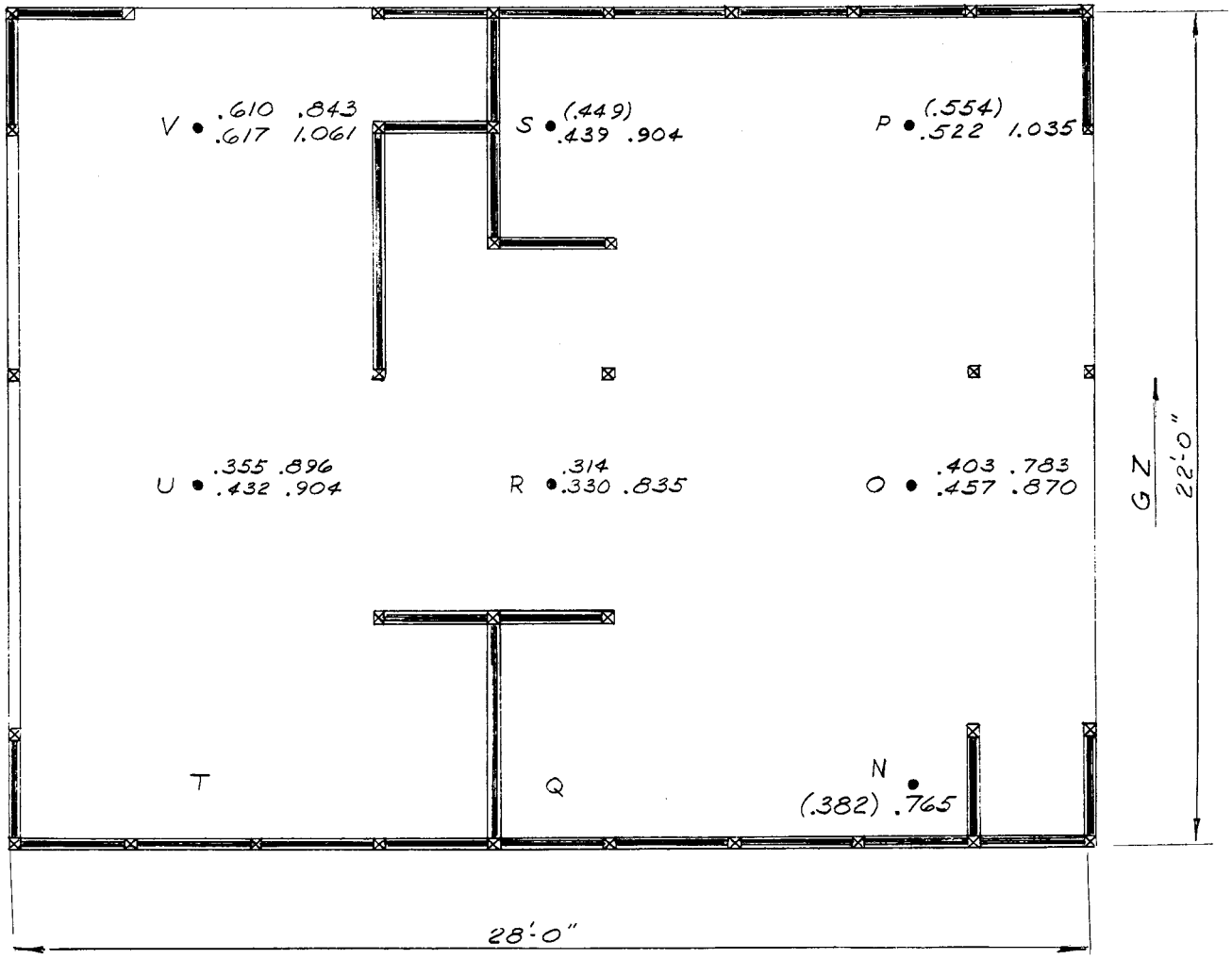

Fig. 4.31—Relative gamma- and neutron-dose distributions in house 3, second floor, event Y.

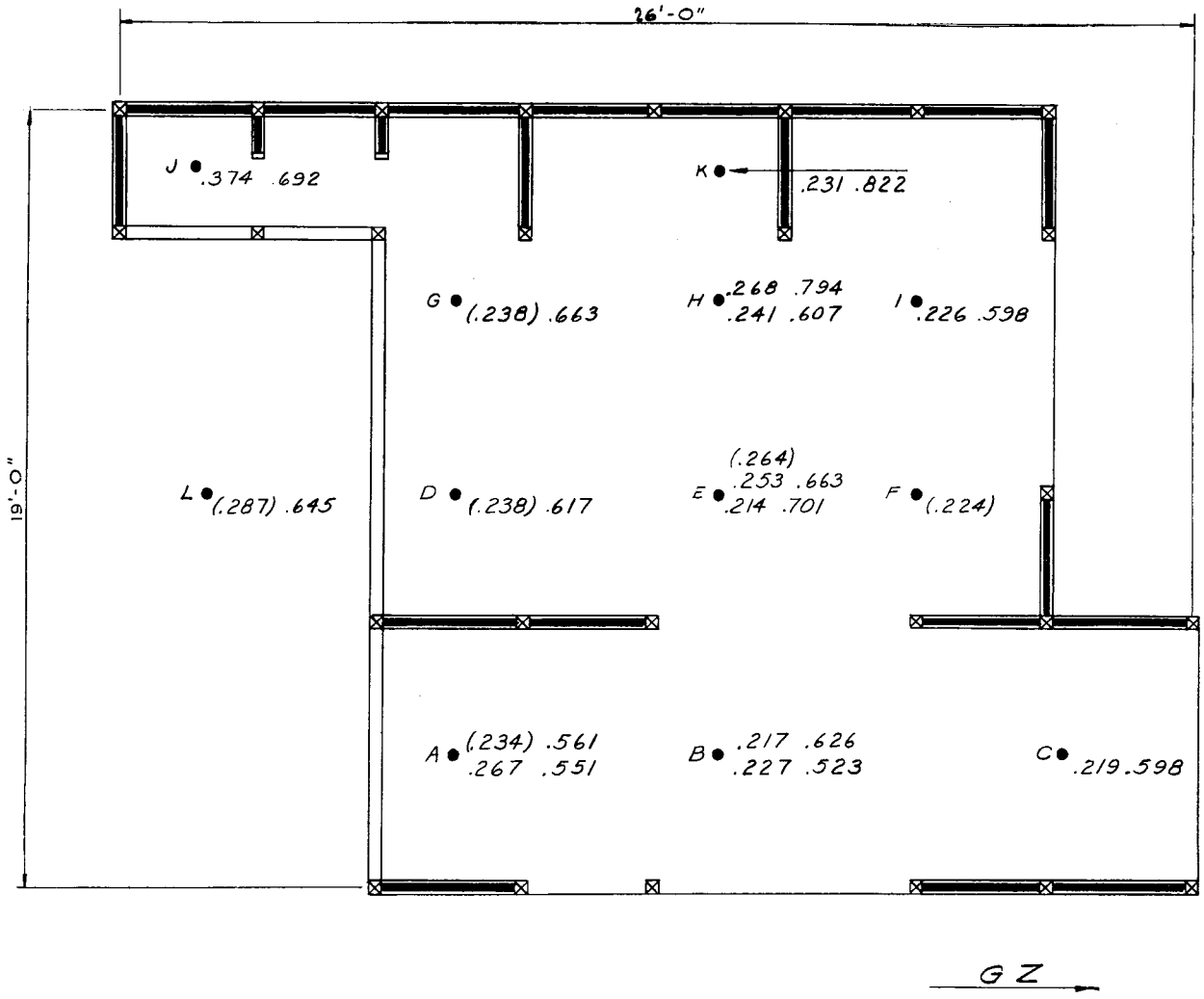

Fig. 4.32—Relative gamma- and neutron-dose distributions in house 4, event Y.

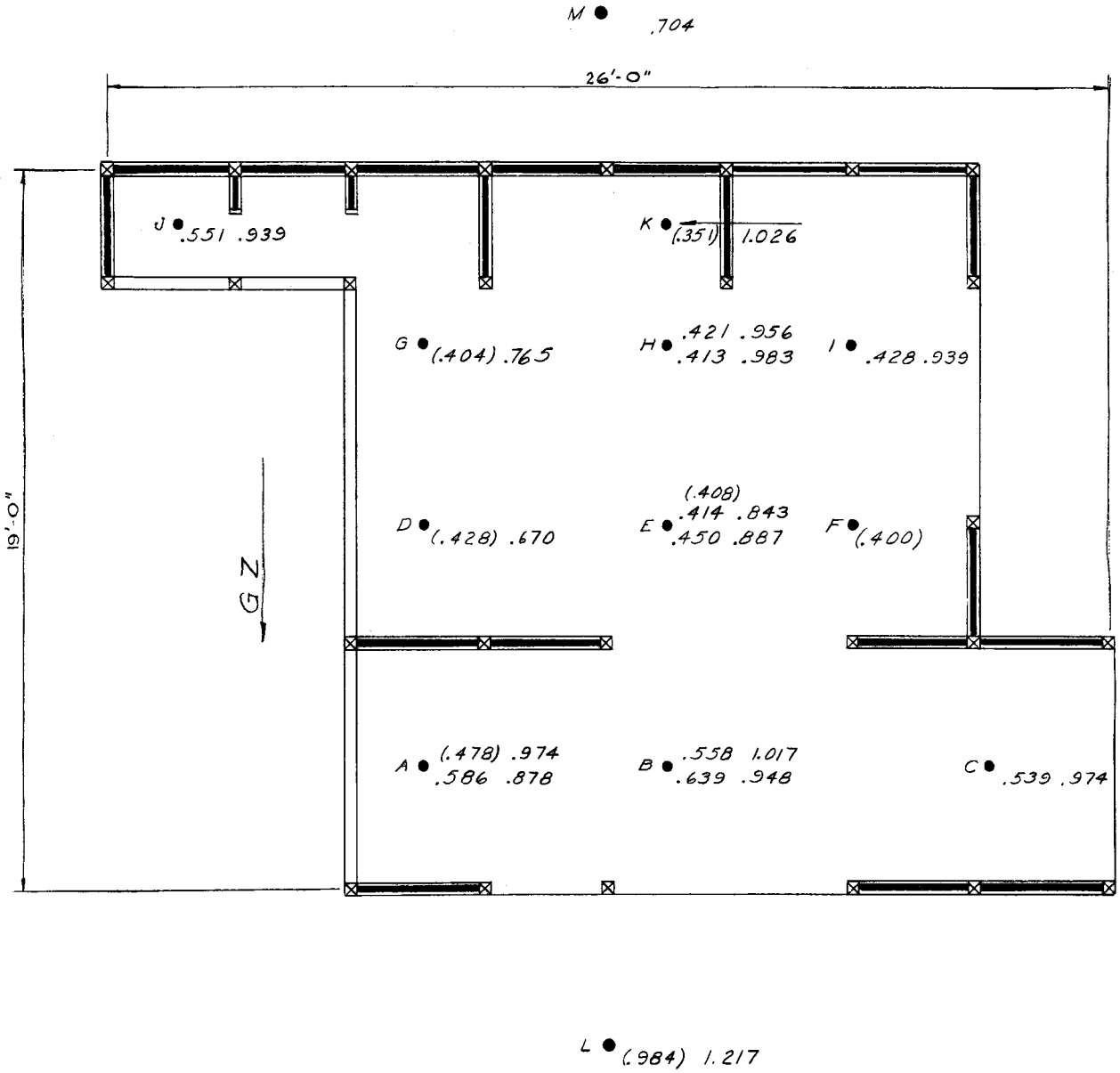

Fig. 4.33—Relative gamma- and neutron-dose distributions in house 5, event Y.

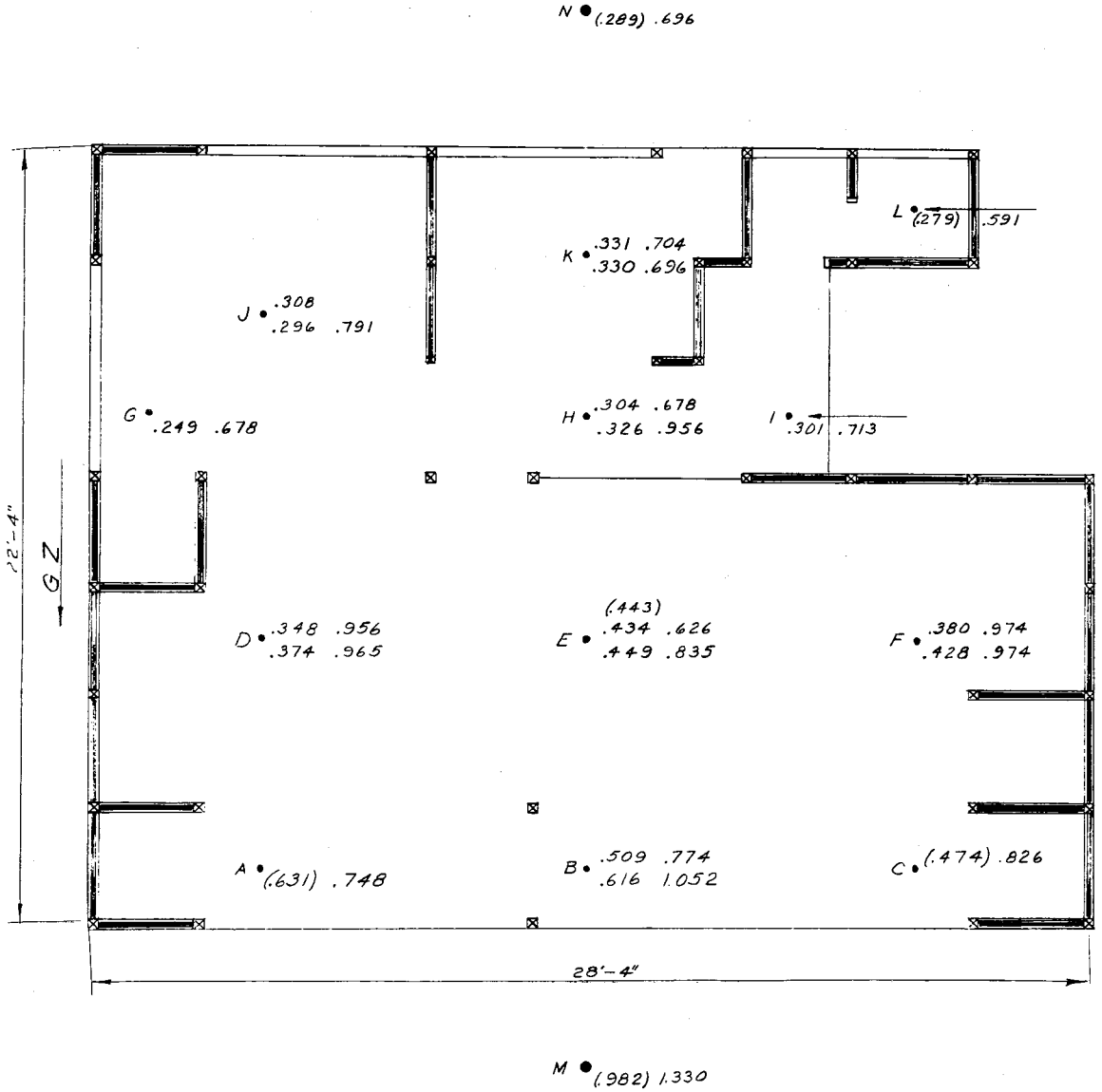

Fig. 4.34—Relative gamma- and neutron-dose distributions in house 6, event Y.

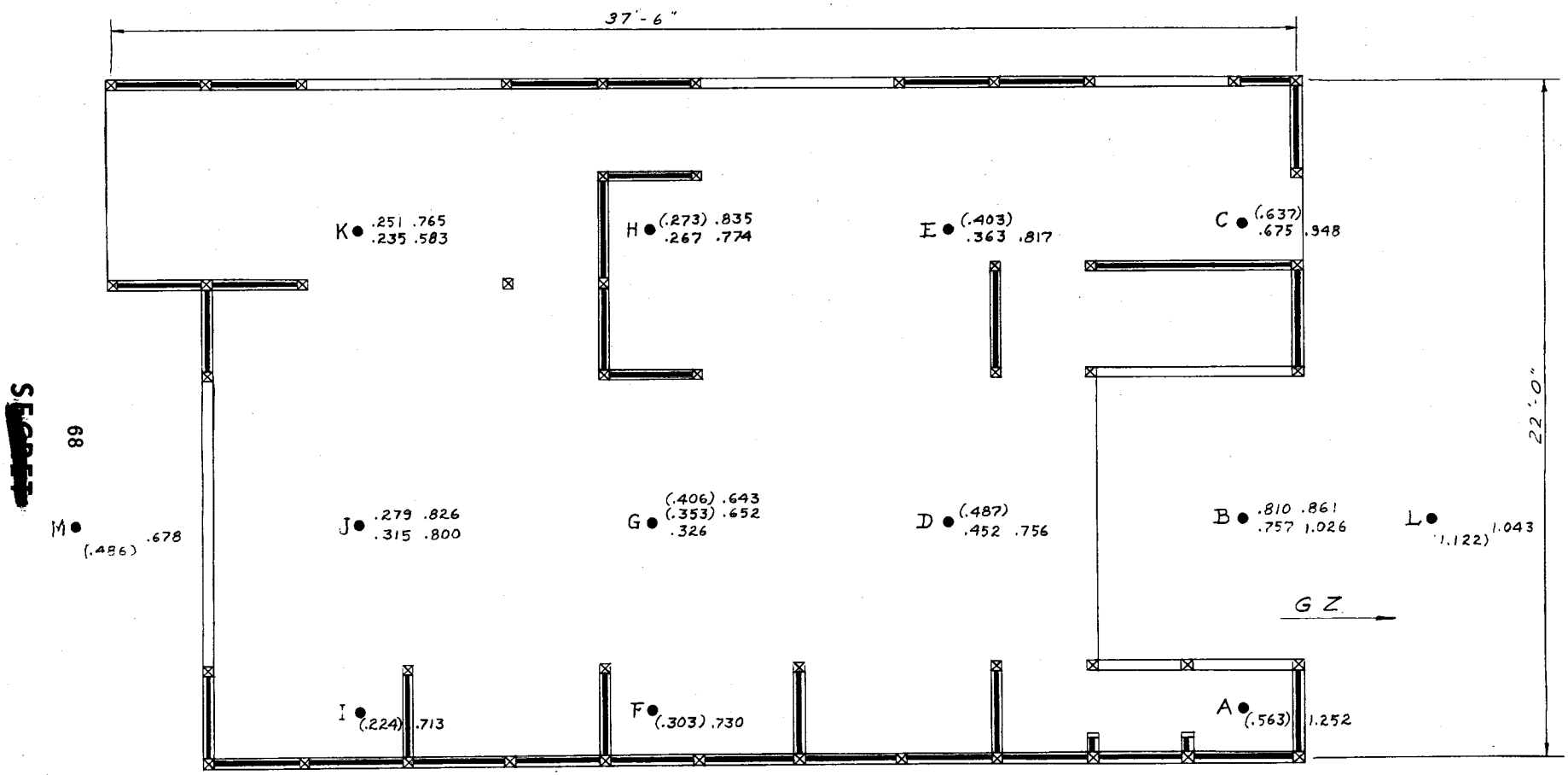

Fig. 4.35—Relative gamma- and neutron-dose distributions in house 7, first floor, event Y.

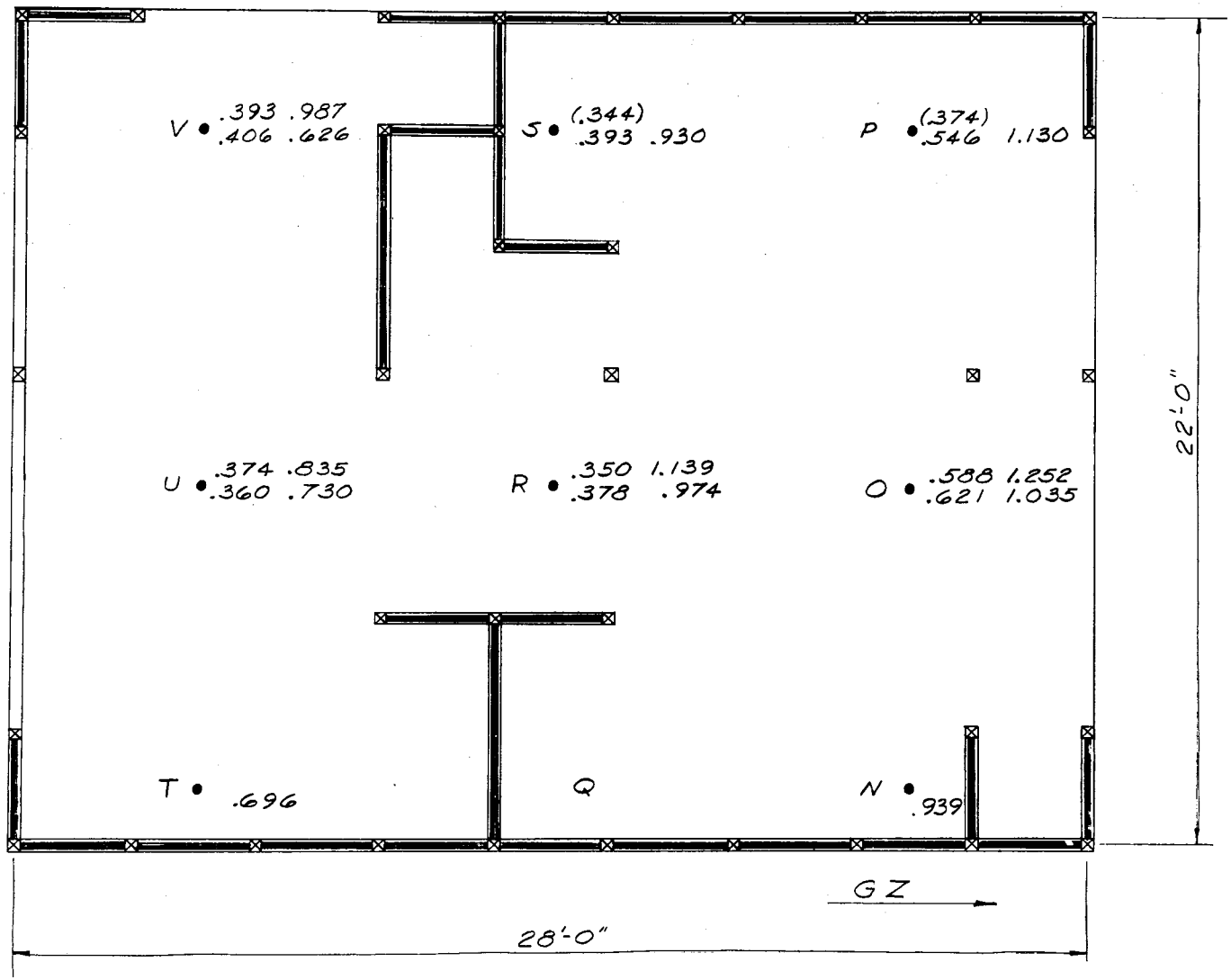

Fig. 4.36—Relative gamma- and neutron-dose distributions in house 7, second floor, event Y.

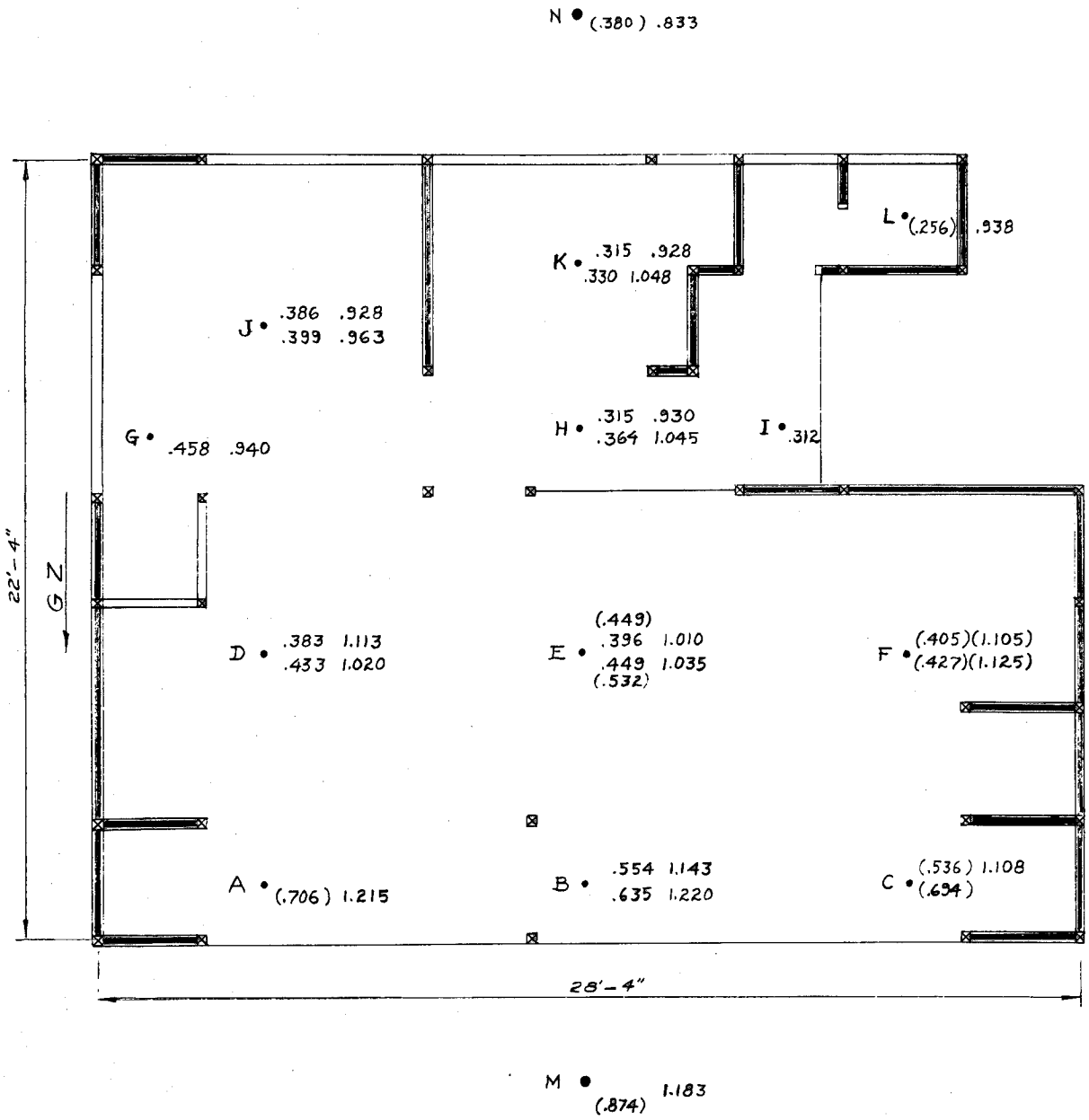

Fig. 4.37—Relative gamma- and neutron-dose distributions in house 1, event Z.

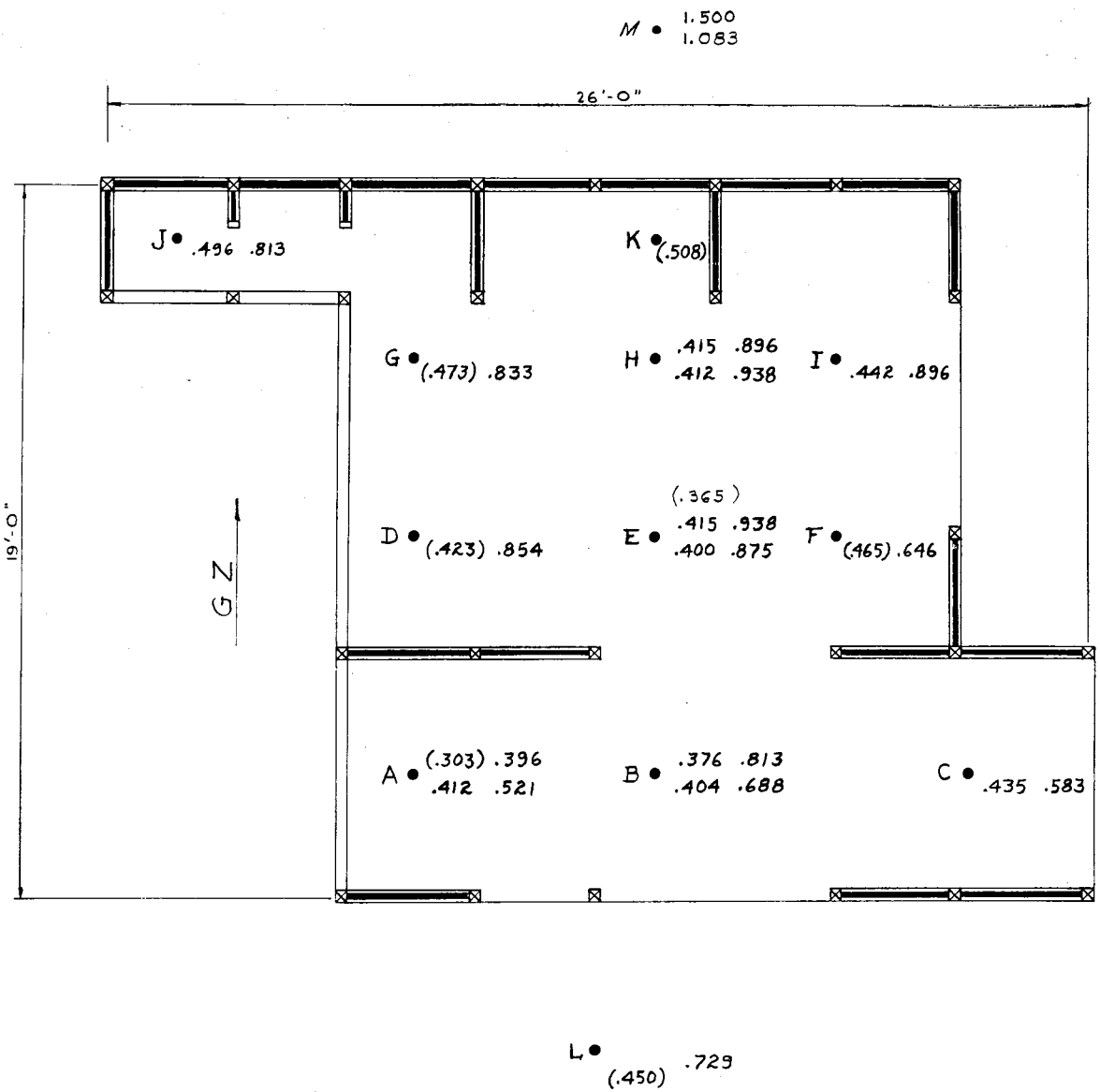

Fig. 4.38—Relative gamma- and neutron-dose distributions in house 2, event Z.

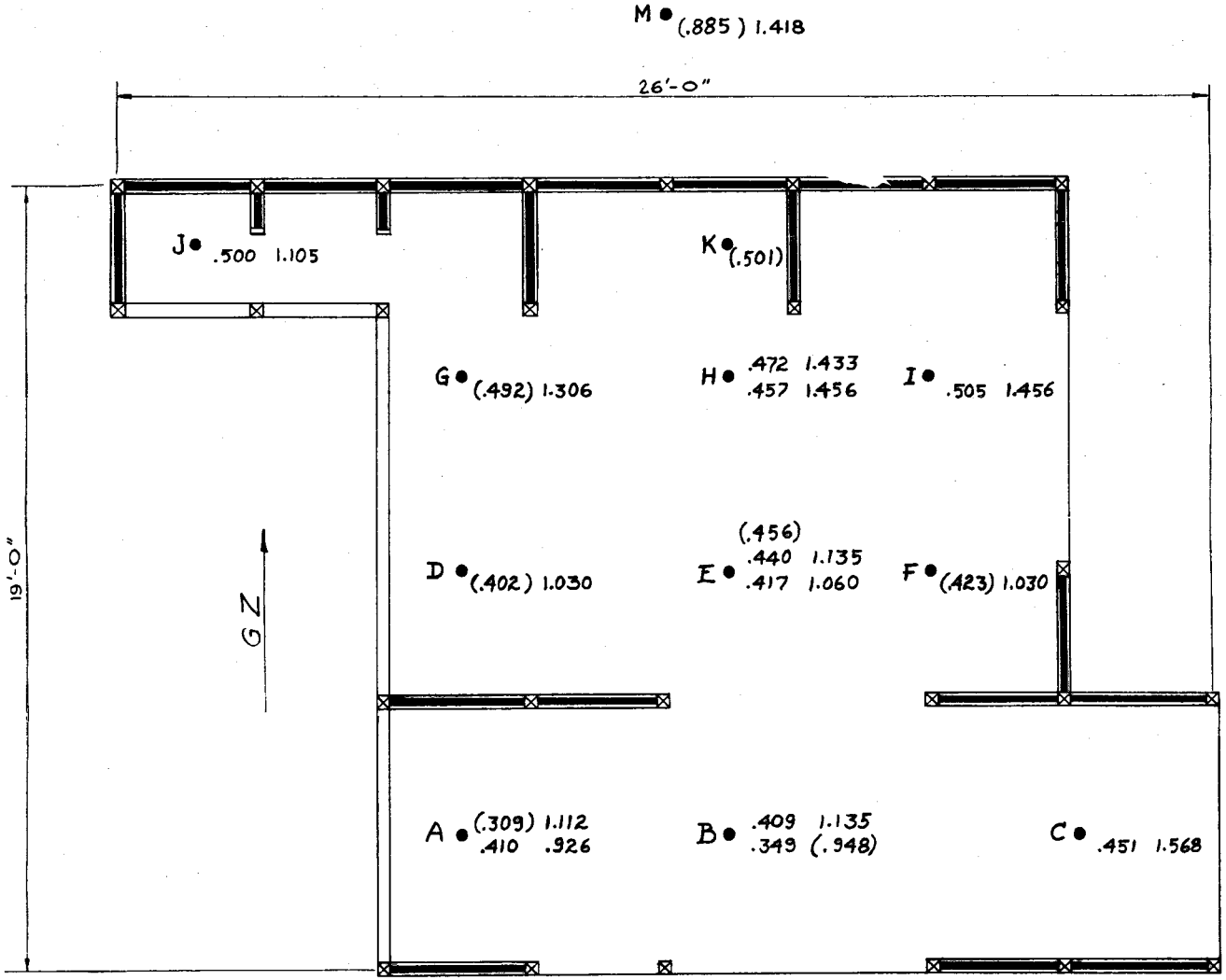

Fig. 4.39—Relative gamma- and neutron-dose distributions in house 4, event Z.

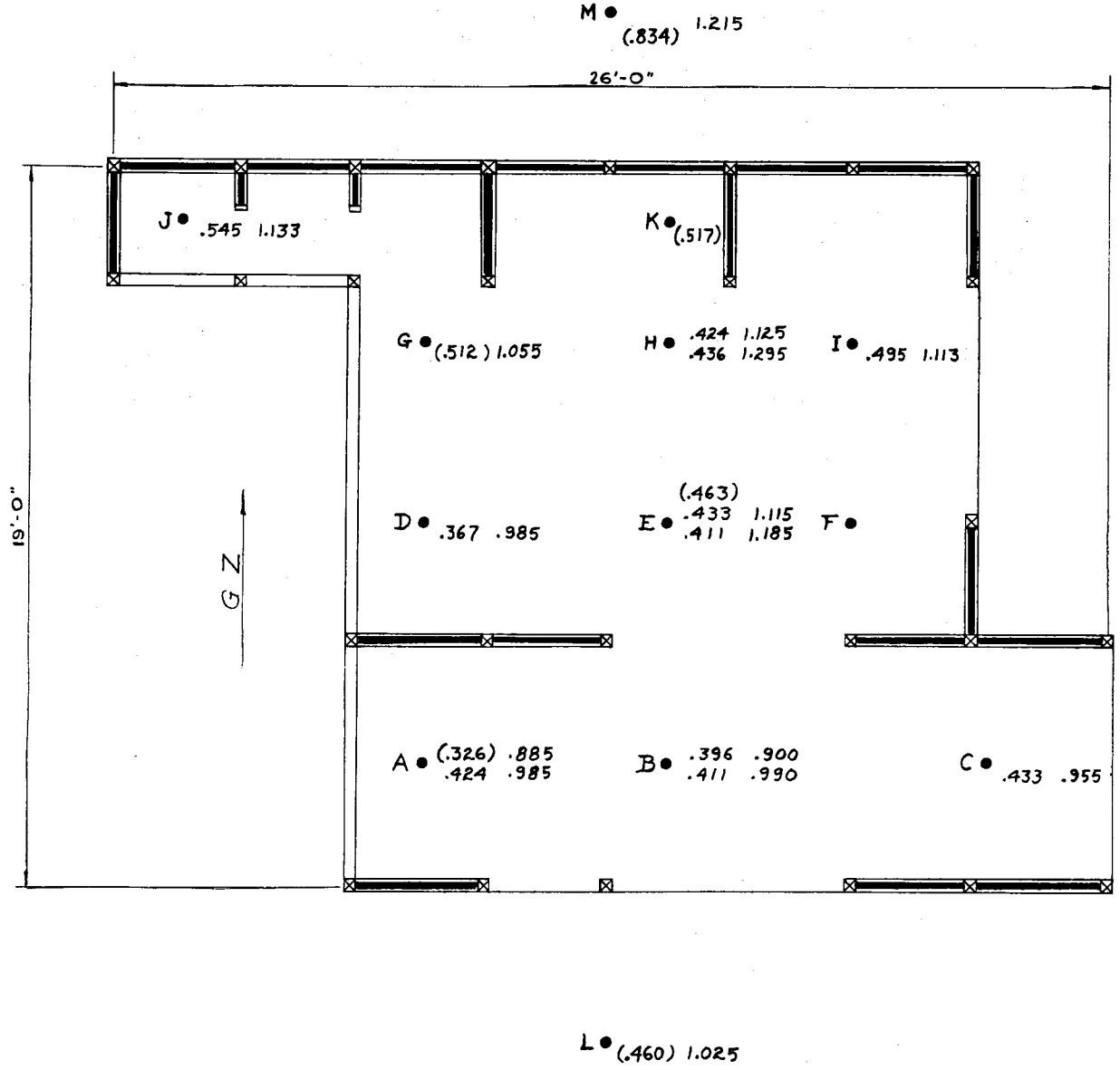

Fig. 4.40—Relative gamma- and neutron-dose distributions in house 5, event Z.

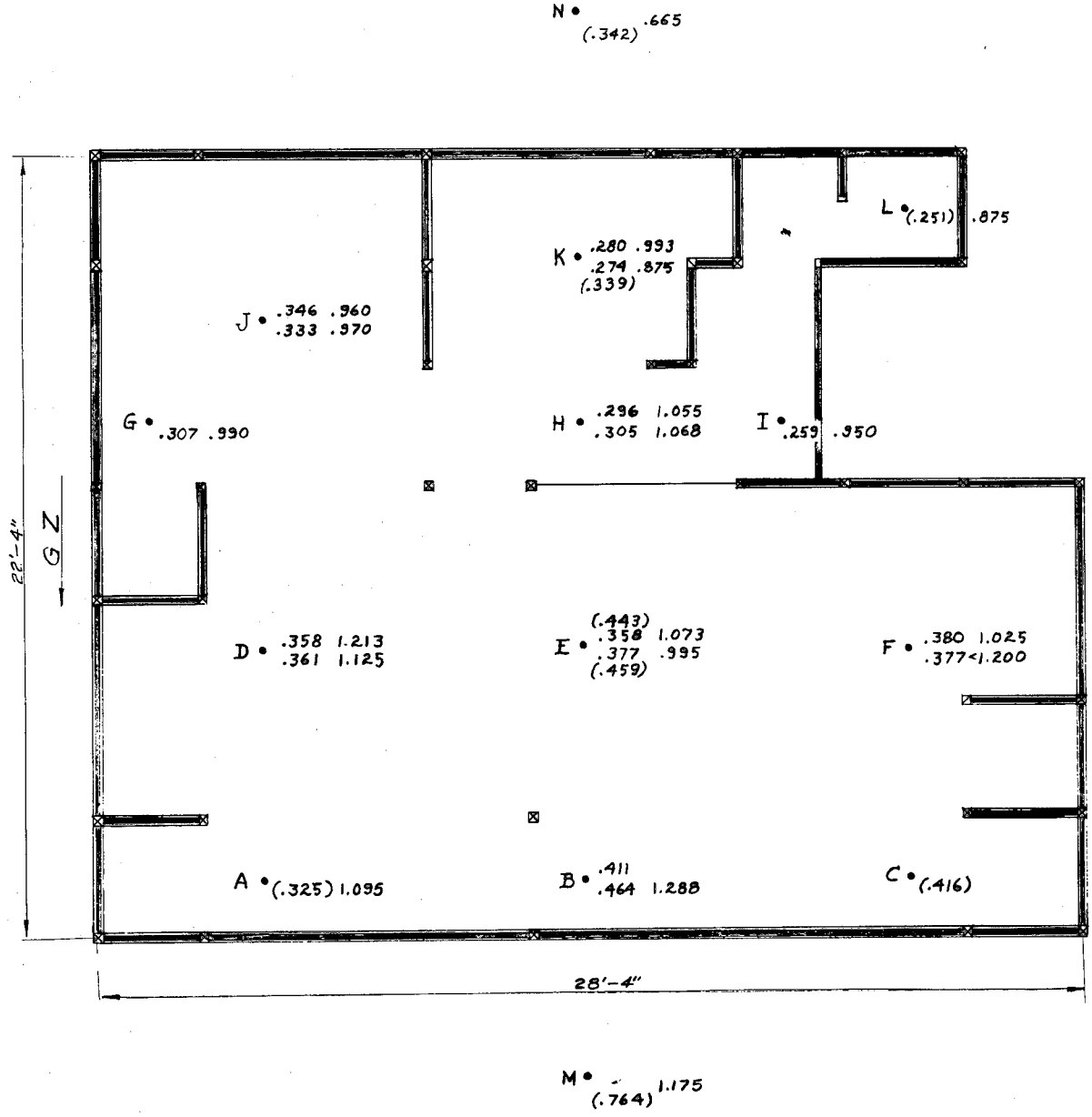

Fig. 4.41—Relative gamma- and neutron-dose distributions in house 6, event Z.

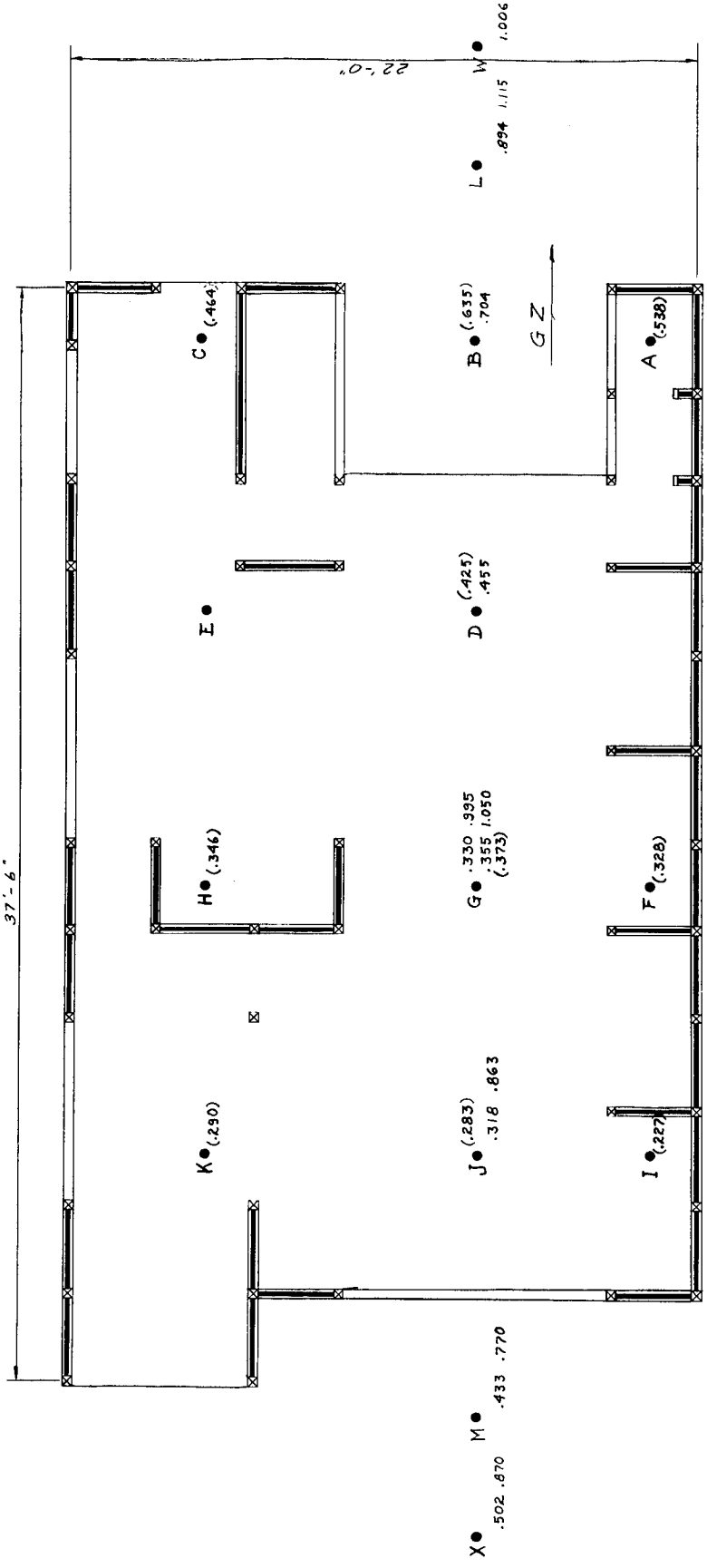

Fig. 4.42—Relative gamma- and neutron-dose distributions in house 7, first floor, event Z.

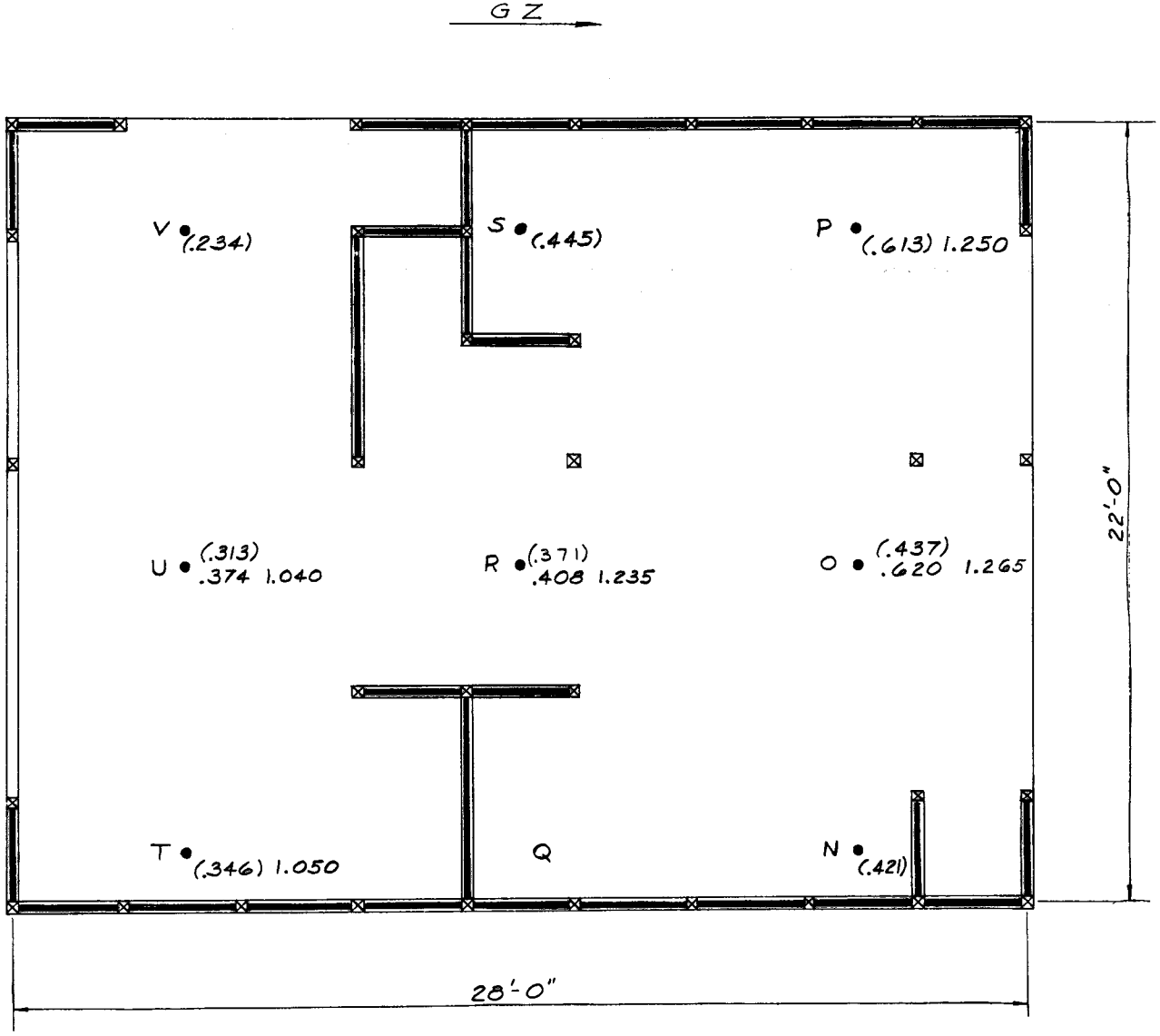

Fig. 4.43—Relative gamma- and neutron-dose distributions in house 7, second floor, event Z.

Chapter 5

ANALYSIS OF DATA

5.1 NEUTRON MEASUREMENTS IN AIR

For the case of nuclear devices detonated above an air-ground interface, it has been shown[1] that the dose-distance relation for gamma rays and fast neutrons can be expressed by

$$D(R) = \frac{Ke^{-R/L}}{R^2}$$

where K is a function of device yield and design, L is the relaxation length for the radiation in question, and R is the slant distance from the burst point to the point of measurement. Under certain conditions this simple relation does not hold, but, for the conditions under which the devices were used in this experiment, the equation is adequate. For a given nuclear detonation, the value of L will depend on air density and, to a lesser extent, on humidity. The value of L as a function of air density can be expressed as

$$L = \frac{\rho_0}{\rho} L_0$$

where ρ_0 and L_0 refer to the values of the quantities for standard conditions, i.e., 1.29 g/liter. The measured values of L for neutrons for the three detonations studied were 275, 283, and 257 yards for events X, Y, and Z, respectively. Correcting for air density, these values become 210, 218, and 205 yards, respectively. The total range of values is approximately 6 per cent of the mean value.

The range of dose values along the arc of 1000-yard radius containing the houses and collimators, approximately 550 yards, was not greater than ±3 per cent of the mean value.

5.2 GAMMA-RADIATION MEASUREMENTS IN AIR

The general discussion in Sec. 5.1 applies also to gamma radiation. However, the accuracy of measurement was less than for the neutrons, as indicated by the greater spread of points about the curves in Fig. 4.4. The measured dose values varied by ±10 per cent along the 550-yard arc of 1000-yard radius.

5.3 ANGULAR DISTRIBUTION OF NEUTRONS AND SLAB PENETRATION BY NEUTRONS

The angular distribution of neutron dose shown in Fig. 4.5 is typical of that measured during both Operation Plumbbob and Operation Hardtack, Phase II. Table 5.1 shows the energy dis-

tribution of neutrons as functions of distance, polar angle, and collimator acceptance angle. Figure 5.1 depicts the smoothed-out distribution of the product of neutron dose and solid angle as a function of polar angle. It is synthesized from measurements of angular distribution made during both Operations Plumbbob and Hardtack. An adjustment was made in the forward direction (small polar angle) to obtain agreement with duplication of house field measurements, described in Sec. 5.5. Table 5.2 shows the integral fraction of neutron dose within the solid angle determined by the rotation of the polar angle about the 0 direction.

The neutron attenuation by slabs of Transite and sand placed over the collimator openings was measured for events Y and Z. Attenuation curves for sand were identical, within the experimental limits of error, with those made during Operation Plumbbob. Transite, which had not been used on Operation Plumbbob, yielded the neutron-attenuation data shown in Fig. 4.6, which agreed well with the measurements made for sand.

5.4 ANGULAR DISTRIBUTION OF GAMMA RAYS AND SLAB PENETRATION BY GAMMA RAYS

Although the angular-distribution data for gamma rays were less reproducible than those for the neutrons, the data obtained agree well with the measurements made during Operation Plumbbob, as shown in Fig. 4.10. However, measurements of the attenuation of gamma rays in Transite did not agree with the measurements for sand when cross sections and density were normalized or with values obtained in the laboratory. The measured values for sand did agree with measurements made during Operation Plumbbob, and the discrepancy between measurements of Transite and sand may be attributed to effects of neutron radiation coexistent with the gamma rays. Correction of the responses of the chemical dosimeter for the response due to thermal-neutron penetration of the protective lithium cans was insufficient to account for the increased response in the collimators behind Transite slabs and in the houses. The fast-neutron response of the chemical detectors had previously been established to be negligible. Therefore, it is assumed that the increased response is due to neutrons at energies greater than thermal and lower than the threshold of the plutonium fission foil contained in B^{10} (~4 kev). This is consonant with the neutron cross section of the materials composing Transite in the so-called epithermal region. In this energy region the response of the chemical dosimeters is unknown, but, even if it were known, there were no measurements made of neutrons in the region between thermal and 4 kev. As a result of these uncertainties, further experimentation is necessary to determine the attenuation of gamma rays by Japanese building materials and Transite. Also, as pointed out in Sec. 5.5, the gamma-dose distribution in Japanese houses should be studied in detail.

5.5 FLUX AND DOSE DISTRIBUTION IN JAPANESE HOUSES

The estimate of the dose at a given point in a structure must be made by means of only a few parameters if such an estimate is to be of practical use in determining the doses received by the survivors of the Hiroshima and Nagasaki bombings. The problem is, then, one of minimizing the number of parameters used while keeping the uncertainty of the estimate reasonably small. A probable error of ±10 per cent was considered acceptable.

The first approach was the use of a single parameter, slant penetration, i.e., the distance, along a line from the burst point to the detector, between the detector and the first house surface intercepting the line. Figure 4.27 illustrates that this treatment is inadequate. The dose values at a given slant-penetration distance were sometimes found to vary by more than a factor of 2.

It was evident that the angular distribution of the radiation and the house configuration were the important parameters. The empirical angular distribution of neutrons shown in Fig. 5.1 was used. In addition, a spherical coordinate projector in the form of a transparent plastic spherical segment was constructed. On the surface of the projector, lines of latitude and longitude

were inscribed at 10° intervals. The axis of the sphere is defined as the line passing through the center and the point at which the longitudinal lines converge. Zones are areas between consecutive parallels, and sections are areas between consecutive longitudinal lines. A small lamp in the center of the sphere made it possible to project the lines. The radiation incident on the point represented by the center of the sphere through each of the projected zones was evaluated from the angular distribution; this included the condition that the radiation incident from above the effective horizon was twice as intense as that from below, as indicated by the angular distribution measurements with collimators. It was further assumed that the effective horizon was 4° below the true horizon.

A scale model of each of the three types of houses used in the test was constructed of clear plastic. The sphere, with its axis pointing in the direction of the burst point, was placed with its center at a point in the model corresponding to a detector station; the latitude and longitude lines were projected on portions of the model house (walls, roof, etc.), and the number of sections of each zone subtended by each portion of the house was counted. Figure 5.2 illustrates this type operation. These data and the angular-distribution data were used to calculate the radiation incident on any given component of the house.

The radiation measurements at stations in a single-story house that has no houses sufficiently near to perturb the radiation field significantly can be closely approximated by making the following assumptions: there is no attenuation of radiation entering through a window or door; 30 per cent of the radiation incident on the roof is transmitted; 50 per cent of the radiation not accounted for by these parameters is transmitted; there are no internal walls. If there are internal walls, say 2 yards from the station, a 20 per cent reduction for a wall in front (between the station and the weapon) of the station and 10 per cent for a lateral wall must be made. Exposure doses calculated with these assumptions agree with the experimental values to within ±10 per cent in most cases. Figure 5.3 illustrates this agreement for a type A house. In this figure the measurements at the 3-ft-level neutron-detector stations are designated by M; the calculated values, by C; and the calculated values corrected for internal walls, by C′. Except for one station, F-3, the deviations greater than 10 per cent all occur at stations where the measured dose is estimated from flux as measured by S only (indicated by parentheses). Table 5.3 shows the comparison of calculated and measured values for a type A house. The ratios of calculated to measured values for all complete neutron-detector stations at 3 ft inside the house average 0.962 ± 0.031. Table 5.4 shows a similar comparison for a type C house. In this case the average of the ratios on complete neutron stations inside the house at 3 ft is 1.005 ± 0.052.

The type B house presents a somewhat different case. The second story may be treated essentially as a single-story house, but the ground-floor shielding is more complex. In addition to the three parameters, window, roof, and wall transmission, which were sufficient to describe the single-story house, one must consider separately the additional attenuation by the second floor. Any radiation entering through this second floor must also have penetrated some portion of the upper story. An average total transmission factor of 0.2 for the radiation incident in areas above the walls of the first floor yielded the best results. Since the floor area in a type B house was large compared to either that of type A or type C, it could not be ignored as it was in the small house. The reflection factor from the floor can be approximated by 0.04. Table 5.5 shows the comparison of this type of calculation with the measured values for corresponding stations in a type B house (lower floor). The ratio of calculated to measured values for complete neutron-detector stations at the 3-ft elevation averages 0.951 ± 0.069.

The next case considered is the shielding of a house by another. This is probably the most important case because it is most representative of the situation in a city. Table 5.6 gives the doses, relative to air dose, of the various neutron-detector stations in type A houses having similar orientations for the different events, except that house 6 for event Y was placed within 4 ft of house 7. House 6 for event X and house 1 for event Z show the reproducibility of measurements. This table shows that the effect of lateral shielding is important only on the side of the house which is nearest the neighboring structure, small along the center line, and negligible on the opposite side. A similar pattern is shown in Table 5.7 for house 7, a type B house. There is no direct comparison for measurement of shielded vs. unshielded values for type C

houses in the same orientation, but on events X and Y, type C houses were similarly oriented behind a type A house (house 2, event X), and behind a type B house with (house 4, event Y) and without (house 4, event X) lateral shielding by another type C house. The results are shown in Table 5.8.

Approximation of measured values in a house shielded by another was tried by the method of calculating the values in the shielded house as if it were in the open, calculating the values in the radiation shadow cast by the shielding house at the station locations, and multiplying the respective values occurring at corresponding station locations. The agreement with measured values was poor.

The models were then set up in the pattern that obtained in the field, and the radiation blocked by each house was determined for each detector station. Under these conditions five parameters were required. In addition to the previous three (window, wall, and roof), the radiation transmitted by the shielding house and that reflected from the floor had to be considered. If 13 per cent is assumed as the transmission factor for the shielding house (and the exterior wall of the house being measured) and 5 per cent is assumed for reflection from the floor, good agreement is found for stations measured in house 4 on events X and Y, except for station J-3, which is in a narrow outlying projection. The results are shown in Tables 5.9 and 5.10.

5.6 GENERAL OBSERVATIONS

The field readings of all the complete neutron-detector stations in each of the houses expressed as decimal fractions of air dose were averaged, and the probable error was calculated. These, together with maximum and minimum readings, appear in Table 5.11. From this table it can be noted that where a side of a house with considerable window area faces GZ, as houses 5, 6, and 7, event X, the average dose increases inversely as the size of the structure and that the upper story of a two-story house behaves much as the medium single-story house (type A). It can also be seen that, if a less-open wall faces GZ, as house 1, event X, compared to houses 6, 3, and 7, event X, and house 5, events X and Z, the average dose and the range of values are both decreased. It also appears that laterally shielded houses have lower average readings but a greater range; whereas, houses shielded from the direction of GZ show a large decrease in both the average dose and the range of doses.

REFERENCE

1. R. H. Ritchie and G. S. Hurst, Penetration of Weapons Radiation: Application to the Hiroshima-Nagasaki Studies, Health Physics, 1: 390 (1959).

TABLE 5.1—NEUTRON-ENERGY DISTRIBUTION WITH RESPECT TO DISTANCE, POLAR ANGLE, AND COLLIMATOR ACCEPTANCE ANGLE

Event	Ground distance, yards	Polar angle, deg	Acceptance angle, deg	ϕ_{Pu}/ϕ_{Pu_0}	ϕ_{Np}/ϕ_{Pu_0}	ϕ_U/ϕ_{Pu_0}	ϕ_S/ϕ_{Pu_0}	ϕ_{n_t}/ϕ_{Pu_0}
Z	750	0	45	1.000	0.704	0.419	0.269	1.183
Z	750	26	45	0.833	0.471	0.232	0.148	1.155
Z	750	34	45	0.511	0.264	0.120	0.0718	1.067
Z	750	35	45	0.657	0.303	0.127	0.0738	1.056
Z	750	70	45	0.439	0.157	0.0571	0.0270	0.913
Z	750	112	45	0.279	0.0949	0.0314	0.0142	0.771
Z	750	0	20	1.000	0.781	0.548	0.350	1.212
Z	1000	0	45	1.000	0.735	0.494	0.324	1.959
Z	1000	0	20	1.000	0.868	0.706	0.487	1.527
Y	1000	0	20	1.000	0.869	0.651	0.384	1.003
Y	1000	79	20	0.302	0.106	0.0599	0.0301	0.720
Y	1000	90	20	0.312	0.101	0.0439	0.0214	0.599

TABLE 5.2—INTEGRAL FRACTION OF NEUTRON DOSE WITHIN SOLID ANGLE OF ROTATION GENERATED BY POLAR ANGLE

Angle, deg	Fraction of dose, %	Angle, deg	Fraction of dose, %
0–15	15.04	0–90	82.6
0–30	30.6	0–105	89.5
0–45	44.6	0–120	94.6
0–60	59.3	0–135	96.7
0–75	71.4	0–150	98.2
		0–180	100.0

TABLE 5.3— COMPARISON OF CALCULATED DOSES WITH FIELD MEASUREMENTS FOR A TYPE A HOUSE*

Station	Radiation incident through: Window	Roof	Other	1.00 × window +0.30 × roof +0.50 × other	Internal-wall correction factor	Corrected value	Field measurement†	Calculated† / Measured
A-3	0.368	0.341	0.291	0.616		0.616	(0.699)	(0.881)
B-3	0.454	0.375	0.171	0.652		0.652	0.692	0.924
B-5	0.161	0.600	0.259	0.471		0.471	0.514	0.916
C-3	0.372	0.333	0.295	0.620		0.620	(0.718)	(0.864)
D-3	0.094	0.496	0.410	0.448		0.448	0.454	0.987
D-5	0.055	0.593	0.352	0.409		0.409	0.422	0.969
E-3	0.148	0.559	0.293	0.462		0.462	0.481	0.960
E-5	0.084	0.645	0.271	0.413		0.413	0.448	0.922
F-3	0.096	0.500	0.404	0.448		0.448	0.523	0.857
F-5	0.047	0.597	0.356	0.404		0.404	0.417	0.969
G-3	0.216	0.431	0.353	0.522	1 front 0.80	0.418	0.438	0.954
H-3	0.103	0.585	0.312	0.435	2/2 lat. 0.90	0.392	0.392	1.000
H-5	0.067	0.660	0.273	0.401	2-2 lat. 0.90	0.361	0.344	1.049
I-3	0.101	0.559	0.340	0.439	1 front 0.80	0.351	0.338	1.038
J-3	0.134	0.551	0.315	0.457	1 lat. 0.90	0.411	0.427	0.963
J-5	0.092	0.608	0.300	0.425	1 lat. 0.90	0.383	0.421	0.910
K-3	0.098	0.596	0.306	0.430	2 lat. 0.80	0.344	0.347	0.991
K-5	0.062	0.644	0.294	0.402	2 lat. 0.80	0.322	0.336	0.958
L-3	0.046	0.489	0.465	0.425	1 front 0.70 1 lat.	0.298	(0.275)	(1.084)

*House 6, event X.
†Parenthetical values are estimated from sulfur flux only.

TABLE 5.4— COMPARISON OF CALCULATED DOSES WITH FIELD MEASUREMENTS FOR A TYPE C HOUSE*

Station	Radiation incident through: Window	Roof	Other	1.00 × window +0.30 × roof +0.50 × other	Internal-wall correction factor	Corrected value	Field measurement†	Calculated† / Measured
A-3	0.253	0.315	0.432	0.564		0.564	0.601	0.938
B-3	0.364	0.286	0.350	0.625		0.625	0.652	0.959
B-5	0.197	0.359	0.444	0.526		0.526	0.546	0.963
C-3	0.114	0.279	0.607	0.502		0.502	0.564	0.890
D-3	0.187	0.483	0.330	0.497	1 front 0.80	0.398	(0.405)	(0.983)
E-3	0.126	0.355	0.519	0.492		0.492	0.455	1.081
E-5	0.078	0.547	0.375	0.430		0.430	0.426	1.009
F-3	0.090	0.367	0.543	0.472	0.5 front 0.90	0.425	(0.477)	(0.951)
G-3	0.204	0.501	0.295	0.502		0.502	(0.397)	(1.264)
H-3	0.099	0.525	0.376	0.445		0.445	0.404	1.101
H-5	0.085	0.622	0.293	0.418		0.418	0.389	1.075
I-3	0.167	0.495	0.338	0.484		0.484	0.435	1.113
J-3	0.262	0.264	0.474	0.578		0.578	0.625	0.925
K-3	0.038	0.451	0.511	0.429	2 lat. 0.80	0.343	(0.369)	(0.930)

*House 5, event X.
†Parenthetical values are estimated from sulfur flux only.

TABLE 5.5— COMPARISON OF CALCULATED DOSES WITH FIELD MEASUREMENTS FOR THE LOWER FLOOR OF A TYPE B HOUSE*

Station	Radiation incident through: Window	Wall	2nd floor	Roof	Radiation reflected from 1st floor	1.00 × window +0.50 × wall +0.20 × 2nd floor +0.30 × roof +0.04 × 1st floor	Internal-wall correction factor		Corrected value	Field measurement†	Calculated† / Measured
B-3	0.366		0.634			0.493			0.493	0.515	0.957
C-3	0.222	0.471	0.092	0.125	0.100	0.517			0.517	0.525	0.985
D-3	0.097	0.356	0.396	0.185	0.139	0.365			0.365	0.323	1.130
E-3	0.070	0.487	0.237	0.066	0.136	0.386			0.386	0.438	0.881
F-3	0.035	0.364	0.445		0.134	0.311	1 lat.	0.90	0.280	(0.260)	(1.077)
G-3	0.040	0.742	0.438		0.171	0.305	1 lat.	0.90	0.275	0.273	1.007
H-3	0.024	0.529	0.280	0.005	0.149	0.352	0.5 front; 1 lat.	0.80	0.282	0.286	0.986
I-3	0.060	0.429	0.382		0.124	0.355	1 lat.	0.90	0.320	(0.303)	(1.019)
J-3	0.073	0.327	0.436	0.006	0.148	0.331			0.331	0.337	0.982
K-3	0.136	0.447	0.268	0.009	0.133	0.421			0.421	0.527	0.799

*House 3, event X.

†Parenthetical values are estimated from sulfur flux only.

TABLE 5.6— TYPE A HOUSE MEASUREMENTS

Station and elevation*	Fraction of air dose (complete stations) House 6, event X	House 6,† event Y	House 1, event Z
D-3	0.454	0.374	0.433
D-5	0.422	0.348	0.383
G-3	0.438	0.249	0.458
J-3	0.427	0.296	0.399
J-5	0.421	0.308	0.386
B-3	0.692	0.616	0.635
B-5	0.514	0.509	0.554
E-3	0.481	0.449	0.449
E-5	0.448	0.434	0.396
H-3	0.392	0.325	0.364
H-5	0.344	0.304	0.315
K-3	0.347	0.330	0.330
K-5	0.336	0.331	0.315
F-3	0.523	0.428	0.427
F-5	0.417	0.380	0.405
I-3	0.338	0.301	0.312

*Stations are grouped in this manner since the first five are on the right side of house 1, the last three are on the left side, and the rest are along the center line.

†Right side of house 6, event Y, was adjacent to house 7.

TABLE 5.7— HOUSE 7 (TYPE B) COMPLETE NEUTRON STATIONS

Station and elevation	Fraction of air dose Event X	Event Y	Event Z
	First floor		
B-3	0.807	0.757	0.704
B-5	0.822	0.810	
C-3	0.707	0.675*	
D-3	0.505	0.452	0.455
E-3	0.424	0.363*	
G-3	0.360	0.326	0.355
J-3	0.294	0.315	0.318
J-5	0.296	0.279	
K-3	0.327	0.235*	
K-5	0.313	0.251	
	Second floor		
O-3	0.613	0.621	0.620
O-5	0.572	0.588	
P-3	0.576	0.546*	
R-3	0.405	0.378	0.408
R-5	0.373	0.350	
S-3	0.390	0.393*	
U-3	0.363	0.360	0.374
U-5	0.357	0.374	
V-3	0.416	0.406*	
V-5	0.406	0.393	

*These stations are on the left side of the house, which was adjacent to house 6.

TABLE 5.8—COMPLETE NEUTRON STATIONS FOR SHIELDED TYPE C HOUSES

Station and elevation	House 2, event X, behind type A	House 4, event X, behind type B	House 4, event Y, behind type B along type C
A-3	0.385	0.364	0.267
B-3	0.369	0.313	0.227
B-5	0.349	0.326	0.217
C-3	0.303	0.254	0.219
E-3	0.307	0.281	0.214
E-5	0.336	0.275	0.253
H-3	0.293	0.274	0.241
H-5	0.330	0.258	0.268
I-3	0.297	0.267	0.226
J-3	0.354	0.341	0.374

TABLE 5.9—COMPARISON OF CALCULATED AND MEASURED VALUES IN HOUSE 4, EVENT X

Station and elevation	Window and door component	Roof component	Wall component	Component blocked by house 3	Component reflected from floor	1.00 × window +0.50 × wall +0.13 × house 3 +0.30 × roof +0.05 × floor	Measured in field	Calculated / Measured
A-3	0.144	0.220	0.224	0.298	0.118	0.366	0.364	1.005
B-3	0.212	0.211	0.183	0.353	0.139	0.329	0.313	1.051
C-3	0.011	0.170	0.182	0.564	0.119	0.232	0.254	0.913
E-3	0.024	0.257	0.189	0.374	0.157	0.252	0.281	0.897
H-3	0.036	0.227	0.290	0.328	0.131	0.298	0.274	1.088
I-3	0.026	0.225	0.199	0.487	0.118	0.262	0.267	0.981
J-3	0.083	0.133	0.541	0.173	0.068	0.419	0.347	1.229
							Av. (except J-3)	0.989

TABLE 5.10—COMPARISON OF CALCULATED AND MEASURED VALUES IN HOUSE 4, EVENT Y

Station and elevation	Window and door component	Roof component	Wall component	Component blocked by houses 3 and 2	Component reflected from floor	1.00 × window +0.30 × roof +0.50 × wall +0.13 × houses 2 and 3 +0.05 × floor	Measured in field	Calculated / Measured
A-3	0.092	0.195	0.095	0.534	0.114	0.275	0.267	1.030
B-3	0.009	0.211	0.094	0.614	0.126	0.205	0.227	0.903
C-3	0.002	0.142	0.144	0.712	0.087	0.213	0.219	0.973
E-3	0.009	0.244	0.112	0.481	0.176	0.210	0.214	0.981
H-3	0.013	0.214	0.224	0.409	0.146	0.250	0.241	1.037
I-3	0.002	0.210	0.188	0.453	0.153	0.225	0.226	0.996
							Av.	0.987

TABLE 5.11— HOUSE SHIELDING SUMMARY

Event and house	House type	Orientation	External shielding	Distance from GZ, yards	Average readings	Maximum readings	Minimum readings	P.E.*	Per cent P.E.
X-1	A	E		1000	0.378	0.478	0.302	0.036	9.52
X-6	A	S		1000	0.437	0.692	0.336	0.048	10.98
Y-1	A	NE		1000	0.379	0.463	0.312	0.032	8.44
Y-6	A	S	Lat. B	1000	0.374	0.616	0.249	0.052	13.90
Z-1	A	S		1000	0.405	0.635	0.312	0.059	14.57
Z-6	A	S	Shell	1000	0.343	0.464	0.259	0.076	10.50
X-3, 1st floor	B	E	Rear C	1000	0.387	0.527	0.273	0.065	16.76
2nd floor					0.461	0.653	0.327	0.069	15.07
X-7, 1st floor	B	S		1000	0.407	0.707	0.294	0.090	22.31
2nd floor					0.447	0.613	0.357	0.064	14.24
Y-3, 1st floor	B	E	Rear C	1000	0.388	0.550	0.276	0.070	18.04
2nd floor					0.448	0.617	0.314	0.069	15.40
Y-7, 1st floor	B	S	Lat. A	1000	0.351	0.675	0.235	0.090	25.64
2nd floor					0.431	0.621	0.350	0.066	15.27
Z-7, 1st floor	B	S		1000	0.365	0.455	0.318	0.036	9.86
2nd floor					0.468	0.620	0.374	0.073	15.60
X-2	C	E	Front A	1010	0.332	0.385	0.293	0.021	6.33
X-4	C	E	Front B	1010	0.295	0.364	0.254	0.024	8.14
X-5	C	S		1000	0.510	0.652	0.389	0.063	12.35
Y-2	C	E	Front B; lat. C†	1010	0.389	0.596	0.323	0.051	13.11
Y-4	C	E	Front B; lat. C	1010	0.251	0.374	0.217	0.010	3.82
Y-5	C	S		1000	0.500	0.639	0.413	0.054	10.80
Z-2	C	N		1500	0.421	0.496	0.376	0.021	4.99
Z-4	C	N		1250	0.441	0.505	0.349	0.030	6.80
Z-5	C	N		1000	0.434	0.545	0.367	0.031	7.14

*Probable error.

†The front was only partially shielded by B.

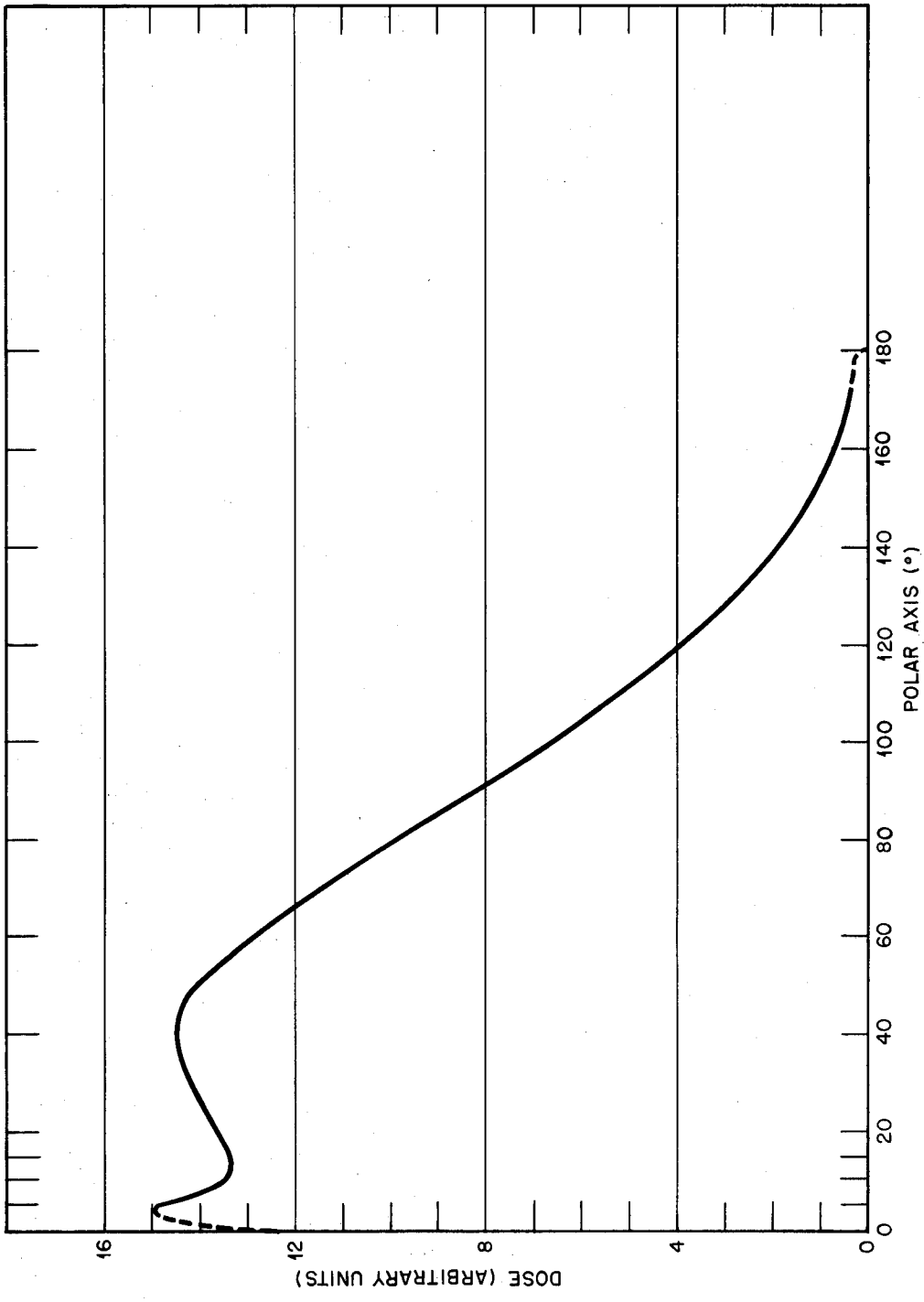

Fig. 5.1—Fast-neutron angular-distribution function.

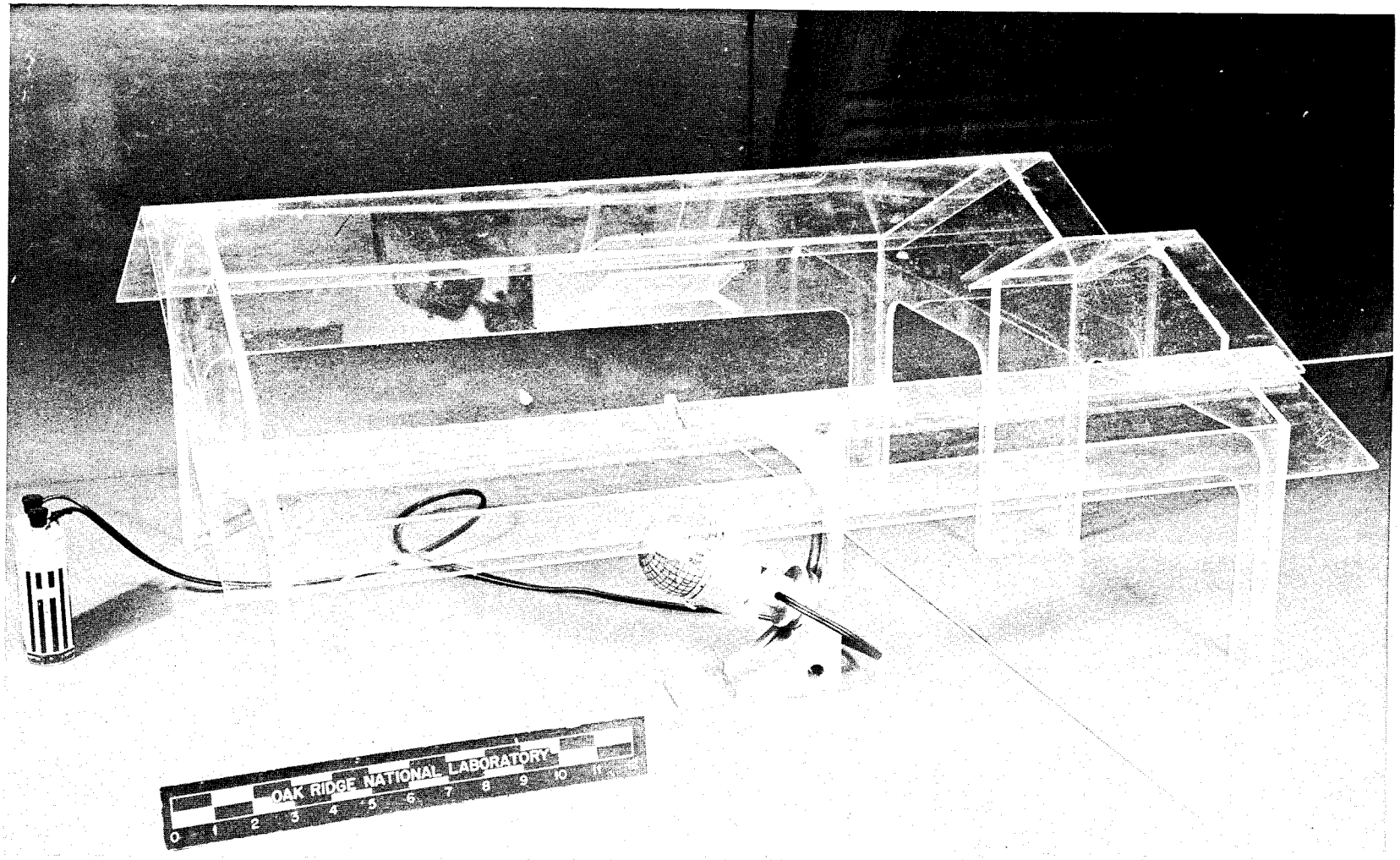

Fig. 5.2—Spherical-coordinate projector in a model of a type A house.

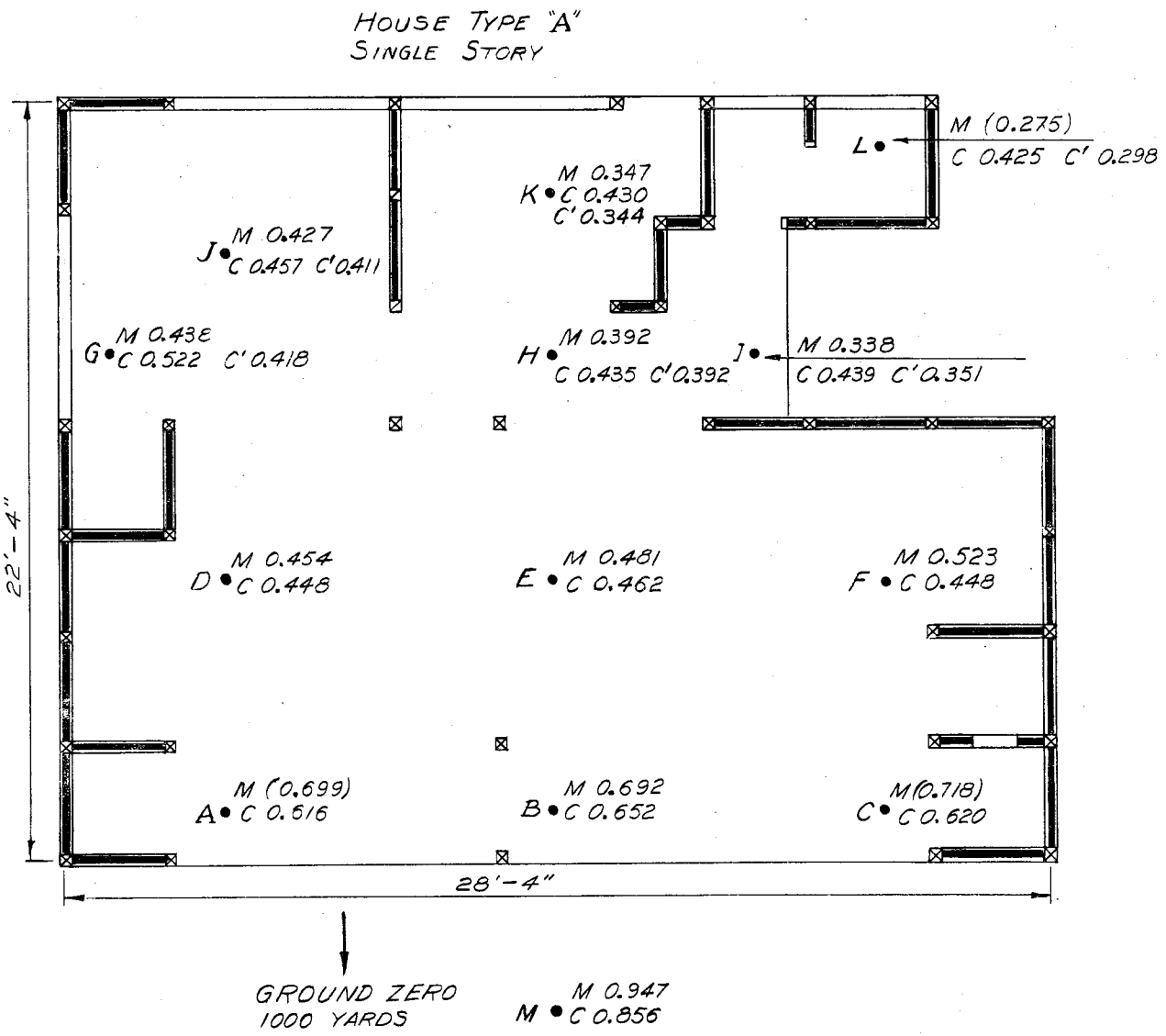

Fig. 5.3—Calculated and measured neutron-dose distribution in a type A house standing alone.

Appendix A

Events X, Y, and Z designate Mora, Lea, and Socorro, respectively; the yields were 2.0 ± 0.1, 1.4 ± 0.14, and 5.7 ± 0.6 kt, respectively. All detonations occurred at the balloon site in Area 7.

Table A-1 shows the scaling factors for reducing the ordinates of the normalized data plots to actual values (Figs. 4.1 through 4.4).

TABLE A-1—SCALE FACTORS (MULTIPLICATIVE) TO REDUCE THE ORDINATES OF NORMALIZED DATA PLOTS TO ACTUAL VALUES

	Mora		Lea		Socorro	
Figure	Neutron	Gamma	Neutron	Gamma	Neutron	Gamma
4.1	0.95					
4.2			1.21			
4.3					0.314	
4.4		0.81		0.291		0.499
4.4 (glass)		1.62				

DISTRIBUTION

Military Distribution Category 28

ARMY ACTIVITIES

1 Deputy Chief of Staff for Military Operations, D/A, Washington 25, D.C. ATTN: Dir. of SW&R
2 Chief of Research and Development, D/A, Washington 25, D.C. ATTN: Atomic Div.
3 Assistant Chief of Staff, Intelligence, D/A, Washington 25, D.C.
4- 5 The Quartermaster General, D/A, Washington 25, D.C. ATTN: Research and Dev.
6- 7 Chief Chemical Officer, D/A, Washington 25, D.C.
8 Chief of Engineers, D/A, Washington 25, D.C. ATTN: ENGNB
9 Chief of Engineers, D/A, Washington 25, D.C. ATTN: ENGEB
10 Chief of Engineers, D/A, Washington 25, D.C. ATTN: ENGTB
11- 12 Office, Chief of Ordnance, D/A, Washington 25, D.C. ATTN: ORDTN
13 Chief Signal Officer, D/A, Research and Development Div., Washington 25, D.C. ATTN: SIGRD-4
14 Chief of Transportation, D/A, Office of Planning and Int., Washington 25, D.C.
15- 16 The Surgeon General, D/A, Washington 25, D.C. ATTN: MEDNE
17- 19 Commanding General, U.S. Continental Army Command, Ft. Monroe, Va.
20 Director of Special Weapons Development Office, Headquarters CONARC, Ft. Bliss, Tex. ATTN: Capt. Chester I. Peterson
21 President, U.S. Army Artillery Board, Ft. Sill, Okla.
22 President, U.S. Army Infantry Board, Ft. Benning, Ga.
23 President, U.S. Army Air Defense Board, Ft. Bliss, Tex.
24 President, U.S. Army Aviation Board, Ft. Rucker, Ala. ATTN: ATBG-DG
25 Commanding General, First United States Army, Governor's Island, New York 4, N.Y.
26 Commanding General, Second U.S. Army, Ft. George G. Meade, Md.
27 Commanding General, Third United States Army, Ft. McPherson, Ga. ATTN: ACofS G-3
28 Commanding General, Fourth United States Army, Ft. Sam Houston, Tex. ATTN: G-3 Section
29 Commanding General, Fifth United States Army, 1660 E. Hyde Park Blvd., Chicago 15, Ill.
30 Commanding General, Sixth United States Army, Presidio of San Francisco, San Francisco, Calif. ATTN: AMGCT-4
31 Commandant, U.S. Army Command & General Staff College, Ft. Leavenworth, Kansas. ATTN: ARCHIVES
32 Commandant, U.S. Army Air Defense School, Ft. Bliss, Tex. ATTN: Command & Staff Dept.
33 Commandant, U.S. Army Armored School, Ft. Knox, Ky.
34 Commandant, U.S. Army Artillery and Missile School, Ft. Sill, Okla. ATTN: Combat Development Department
35 Commandant, U.S. Army Infantry School, Ft. Benning, Ga. ATTN: C.D.S.
36 The Superintendent, U.S. Military Academy, West Point, N.Y. ATTN: Prof. of Ordnance
37 Commandant, The Quartermaster School, U.S. Army, Ft. Lee, Va. ATTN: Chief, QM Library
38 Commanding General, Chemical Corps Training Comd., Ft. McClellan, Ala.
39 Commandant, USA Signal School, Ft. Monmouth, N.J.
40 Commandant, USA Transport School, Ft. Eustis, Va. ATTN: Security and Info. Off.
41 Commanding General, The Engineer Center, Ft. Belvoir, Va. ATTN: Asst. Cmdt, Engr. School
42 Commanding General, Army Medical Service School, Brooke Army Medical Center, Ft. Sam Houston, Tex.
43 Director, Armed Forces Institute of Pathology, Walter Reed Army Med. Center, 625 16th St., NW, Washington 25, D.C.
44 Commanding Officer, U.S. Army Research Lab., Ft. Knox, Ky.
45 Commandant, Walter Reed Army Inst. of Res., Walter Reed Army Medical Center, Washington 25, D.C.
46- 47 Commanding General, Qm R&D Comd., QM R&D Cntr., Natick, Mass. ATTN: CBR Liaison Officer
48- 49 Commanding General, Qm. Research and Engr. Comd., USA, Natick, Mass.
50- 51 Commanding General, U.S. Army Chemical Corps, Research and Development Comd., Washington 25, D.C.
52- 53 Commanding Officer, Chemical Warfare Lab., Army Chemical Center, Md. ATTN: Tech. Library
54 Commanding General, Engineer Research and Dev. Lab., Ft. Belvoir, Va. ATTN: Chief, Tech. Support Branch
55 Director, Waterways Experiment Station, P.O. Box 631, Vicksburg, Miss. ATTN: Library
56 Commanding Officer, Diamond Ord. Fuze Labs., Washington 25, D.C. ATTN: Chief, Nuclear Vulnerability Br. (230)
57 Commanding General, Aberdeen Proving Grounds, Md. ATTN: Director, Ballistics Research Laboratory
58 Commanding Officer, Ord. Materials Research Off., Watertown Arsenal, Watertown 72, Mass. ATTN: Dr. Foster
59 Commanding General, Ordnance Tank Automotive Command, Detroit Arsenal, Centerline, Mich. ATTN: ORDMC-RO
60 Commanding General, Ordnance Ammunition Command, Joliet, Ill.
61 Commanding Officer, USA Signal R&D Laboratory, Ft. Monmouth, N.J.
62 Commanding General, U.S. Army Electronic Proving Ground, Ft. Huachuca, Ariz. ATTN: Tech. Library
63 Commanding General, USA Combat Surveillance Agency, 1124 N. Highland St., Arlington, Va.
64 Commanding Officer, USA, Signal R&D Laboratory, Ft. Monmouth, N.J. ATTN: Tech. Doc. Ctr., Evans Area
65 Commanding Officer, USA Transportation Research Command, Ft. Eustis, Va. ATTN: Chief, Tech. Info. Div.
66 Commanding Officer, USA Transportation Combat Development Group, Ft. Eustis, Va.
67 Director, Operations Research Office, Johns Hopkins University, 6935 Arlington Rd., Bethesda 14, Md.
68 Commandant, U.S. Army Chemical Corps, CBR Weapons School, Dugway Proving Ground, Dugway, Utah.
69 Commanding General, Southern European Task Force, APO 168, New York, N.Y. ATTN: ACofS G-3
70 Commanding General, Eighth U.S. Army, APO 301, San Francisco, Calif. ATTN: ACofS G-3
71 Commanding General, U.S. Army Alaska, APO 949, Seattle, Washington
72 Commanding General, U.S. Army Caribbean, Ft. Amador, Canal Zone. ATTN: Cml Office
73 Commander-in-Chief, U.S. Army Pacific, APO 958, San Francisco, Calif. ATTN: Ordnance Officer
74 Commanding General, USARFANT & MDPR, Ft. Brooke, Puerto Rico
75 Commanding Officer, 9th Hospital Center, APO 180, New York, N.Y. ATTN: CO, US Army Nuclear Medicine Research Detachment, Europe

NAVY ACTIVITIES

76- 77 Chief of Naval Operations, D/N, Washington 25, D.C. ATTN: OP-03EG
78 Chief of Naval Operations, D/N, Washington 25, D.C. ATTN: OP-75
79 Chief of Naval Operations, D/N, Washington 25, D.C. ATTN: OP-922G2
80 Chief of Naval Personnel, D/N, Washington 25, D.C.
81- 82 Chief of Naval Research, D/N, Washington 25, D.C. ATTN: Code 811
83 Chief, Bureau of Naval Weapons, D/N, Washington 25, D.C. ATTN: DLI-3
84 Chief, Bureau of Medicine and Surgery, D/N, Washington 25, D.C. ATTN: Special Wpns. Def. Div.
85 Chief, Bureau of Ordnance, D/N, Washington 25, D.C.

86 Chief, Bureau of Ships, D/N, Washington 25, D.C. ATTN: Code 423
87 Chief, Bureau of Yards and Docks, D/N, Washington 25, D.C. ATTN: D-440
88 Director, U.S. Naval Research Laboratory, Washington 25, D.C. ATTN: Mrs. Katherine H. Cass
89- 90 Commander, U.S. Naval Ordnance Laboratory, White Oak, Silver Spring 19, Md.
91 Director, Material Lab. (Code 900), New York Naval Shipyard, Brooklyn 1, N.Y.
92- 95 Commanding Officer, U.S. Naval Radiological Defense Laboratory, San Francisco, Calif. ATTN: Tech. Info. Div.
96- 97 Commanding Officer and Director, U.S. Naval Civil Engineering Laboratory, Port Hueneme, Calif. ATTN: Code L31
98 Superintendent, U.S. Naval Academy, Annapolis, Md.
99 Commanding Officer, U.S. Naval Schools Command, U.S. Naval Station, Treasure Island, San Francisco, Calif.
100 Superintendent, U.S. Naval Postgraduate School, Monterey, Calif.
101 Officer-in-Charge, U.S. Naval School, CEC Officers, U.S. Naval Construction Bn. Center, Port Hueneme, Calif.
102 Commanding Officer, Nuclear Weapons Training Center, Atlantic, U.S. Naval Base, Norfolk 11, Va. ATTN: Nuclear Warfare Dept.
103 Commanding Officer, Nuclear Weapons Training Center, Pacific, Naval Station, San Diego, Calif.
104 Commanding Officer, U.S. Naval Damage Control Tng. Center, Naval Base, Philadelphia 12, Pa. ATTN: ABC Defense Course
105 Commanding Officer, U.S. Naval Air Development Center, Johnsville, Pa. ATTN: NAS, Librarian
106 Commanding Officer, U.S. Naval Medical Research Institute, National Naval Medical Center, Bethesda, Md.
107 Commanding Officer and Director, David W. Taylor Model Basin, Washington 7, D.C. ATTN: Library
108 Officer-in-Charge, U.S. Naval Supply Research and Development Facility, Naval Supply Center, Bayonne, N.J.
109 Commander-in-Chief, U.S. Atlantic Fleet, U.S. Naval Base, Norfolk 11, Va.
110 Commandant, U.S. Marine Corps, Washington 25, D.C. ATTN: Code A03H
111 Director, Marine Corps Landing Force, Development Center, MCS, Quantico, Va.
112 Chief, Bureau of Ships, D/N, Washington 25, D.C. ATTN: Code 372
113 Commanding Officer, U.S. Naval CIC School, U.S. Naval Air Station, Glynco, Brunswick, Ga.
114 Chief of Naval Operations, Department of the Navy, Washington 25, D.C. ATTN: OP-09B5
115 Chief, Bureau of Naval Weapons, Navy Department, Washington 25, D.C. ATTN: RR12
116 Commander-in-Chief, U.S. Pacific Fleet, Fleet Post Office, San Francisco, Calif.

AIR FORCE ACTIVITIES

117 Air Force Technical Application Center, HQ. USAF, Washington 25, D.C.
118 Deputy Chief of Staff, Operations, HQ. USAF, Washington 25, D.C. ATTN: AFOOP
119 Hq. USAF, ATTN: Operations Analysis Office, Office, Vice Chief of Staff, Washington 25, D. C.
120 Director of Civil Engineering, HQ. USAF, Washington 25, D.C. ATTN: AFOCE
121-131 HQ. USAF, Washington 25, D.C. ATTN: AFCIN-3D1
132 Director of Research and Development, DCS/D, HQ. USAF, Washington 25, D.C. ATTN: Guidance and Weapons Div.
133 The Surgeon General, HQ. USAF, Washington 25, D.C. ATTN: Bio.-Def. Pre. Med. Division
134 Commander, Tactical Air Command, Langley AFB, Va. ATTN: Doc. Security Branch
135 Commander, Air Defense Command, Ent AFB, Colorado. ATTN: Operations Analysis Section, ADOOA
136 Commander, Hq. Air Research and Development Command, Andrews AFB, Washington 25, D.C. ATTN: RDRWA
137 Commander, Air Force Ballistic Missile Div. HQ. ARDC, Air Force Unit Post Office, Los Angeles 45, Calif. ATTN: WDSOT
138 Commander, Second Air Force, Barksdale AFB, La. ATTN: Operations Analysis Office
139-140 Commander, AF Cambridge Research Center, L. G. Hanscom Field, Bedford, Mass. ATTN: CRQST-2
141-145 Commander, Air Force Special Weapons Center, Kirtland AFB, Albuquerque, N. Mex. ATTN: Tech. Info. & Intel. Div.
146-147 Director, Air University Library, Maxwell AFB, Ala.
148 Commander, Lowry Technical Training Center (TW), Lowry AFB, Denver, Colorado.
149 Commandant, School of Aviation Medicine, USAF Aerospace Medical Center (ATC), Brooks Air Force Base, Tex. ATTN: Col. G. L. Hekhuis
150 Commander, 1009th Sp. Wpns. Squadron, HQ. USAF, Washington 25, D.C.
151-153 Commander, Wright Air Development Center, Wright-Patterson AFB, Dayton, Ohio. ATTN: WCACT (For WCOSI)
154-155 Director, USAF Project RAND, VIA: USAF Liaison Office, The RAND Corp., 1700 Main St., Santa Monica, Calif.
156 Commander, Air Technical Intelligence Center, USAF, Wright-Patterson AFB, Ohio. ATTN: AFCIN-4Bla, Library
157 Assistant Chief of Staff, Intelligence, HQ. USAFE, APO 633, New York, N.Y. ATTN: Directorate of Air Targets
158 Commander, Alaskan Air Command, APO 942, Seattle, Washington. ATTN: AAOTN
159 Commander-in-Chief, Pacific Air Forces, APO 953, San Francisco, Calif. ATTN: PFCIE-MB, Base Recovery

OTHER DEPARTMENT OF DEFENSE ACTIVITIES

160 Director of Defense Research and Engineering, Washington 25, D.C. ATTN: Tech. Library
161 Director, Weapons Systems Evaluation Group, Room 1E880, The Pentagon, Washington 25, D.C.
162 Commandant, The Industrial College of The Armed Forces, Ft. McNair, Washington 25, D.C.
163 Commandant, Armed Forces Staff College, Norfolk 11, Va. ATTN: Library
164-167 Chief, Defense Atomic Support Agency, Washington 25, D.C. ATTN: Document Library
168 Commander, Field Command, DASA, Sandia Base, Albuquerque, N. Mex.
169 Commander, Field Command, DASA, Sandia Base, Albuquerque, N. Mex. ATTN: FCTG
170-171 Commander, Field Command, DASA, Sandia Base, Albuquerque, N. Mex. ATTN: FCWT
172 Commander-in-Chief, Strategic Air Command, Offutt AFB, Neb. ATTN: OAWS
173 Commandant, US Coast Guard, 1300 E. St., N.W., Washington 25, D.C. ATTN: Cdr. B. E. Koikhorst
174 Commander-in-Chief, EUCOM, APO 128, New York, N.Y.
175 Commander-in-Chief, Pacific, c/o Fleet Post Office, San Francisco, Calif.
176 U.S. Documents Officer, Office of the United States National Military Representative - SHAPE, APO 55, New York, N.Y.
177 SAC (SUP3.1), Offutt AFB, Neb.

ATOMIC ENERGY COMMISSION ACTIVITIES

178-180 U.S. Atomic Energy Commission, Technical Library, Washington 25, D.C. ATTN: For DMA
181-185 U.S. Atomic Energy Commission, Technical Library, Washington 25, D.C. ATTN: For DBM
186-189 U.S. Atomic Energy Commission, Technical Library, Washington 25, D.C. ATTN: For R. L. Corsbie, CETG
190-191 Los Alamos Scientific Laboratory, Report Library, P.O. Box 1663, Los Alamos, N. Mex. ATTN: Helen Redman
192-196 Sandia Corporation, Classified Document Division, Sandia Base, Albuquerque, N. Mex. ATTN: H. J. Smyth, Jr.
197-206 University of California Lawrence Radiation Laboratory, P.O. Box 808, Livermore, Calif. ATTN: Clovis G. Craig
207 Office of Technical Information Extension, Oak Ridge, Tenn. (Master)
208-240 Office of Technical Information Extension, Oak Ridge, Tenn. (Surplus)